A satellite-style map of the African continent, showing topography and vegetation. The map is centered on the continent, with the Atlantic Ocean to the west, the Indian Ocean to the east, and the Mediterranean Sea to the north. The text is overlaid on the central part of the continent.

A Review of the Structure and Variability of African Easterly Waves including their relationship with Tropical Cyclones

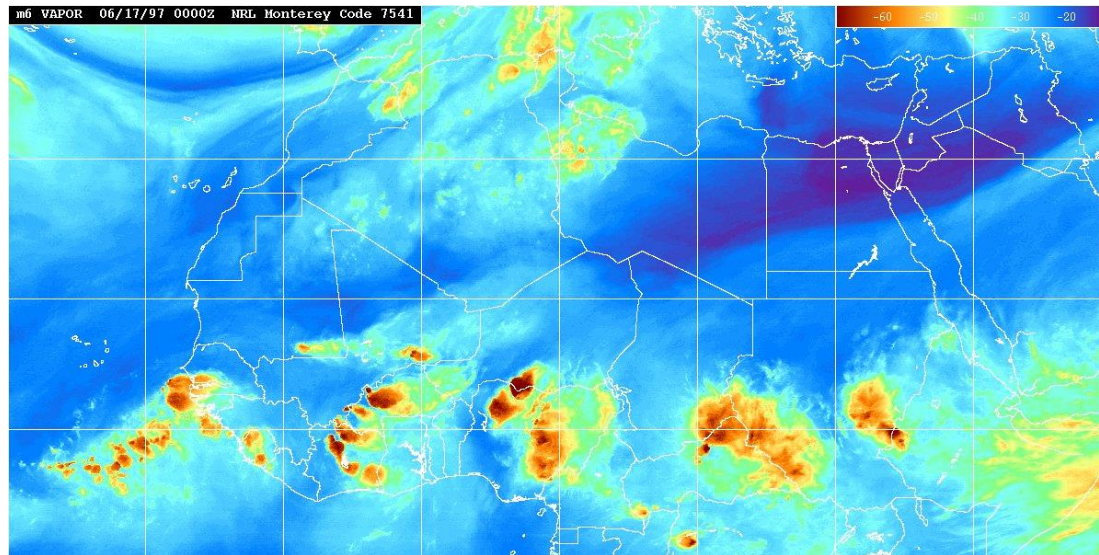
Chris Thorncroft
Department of Atmospheric and Environmental Sciences
University at Albany

Special Acknowledgements to:
Yuan Ming Chen (UAlbany), Alan Brammer (ClimaCell),
Matt Janiga (NRL) and George Kiladis (NOAA)

Funded by: NSF and NASA

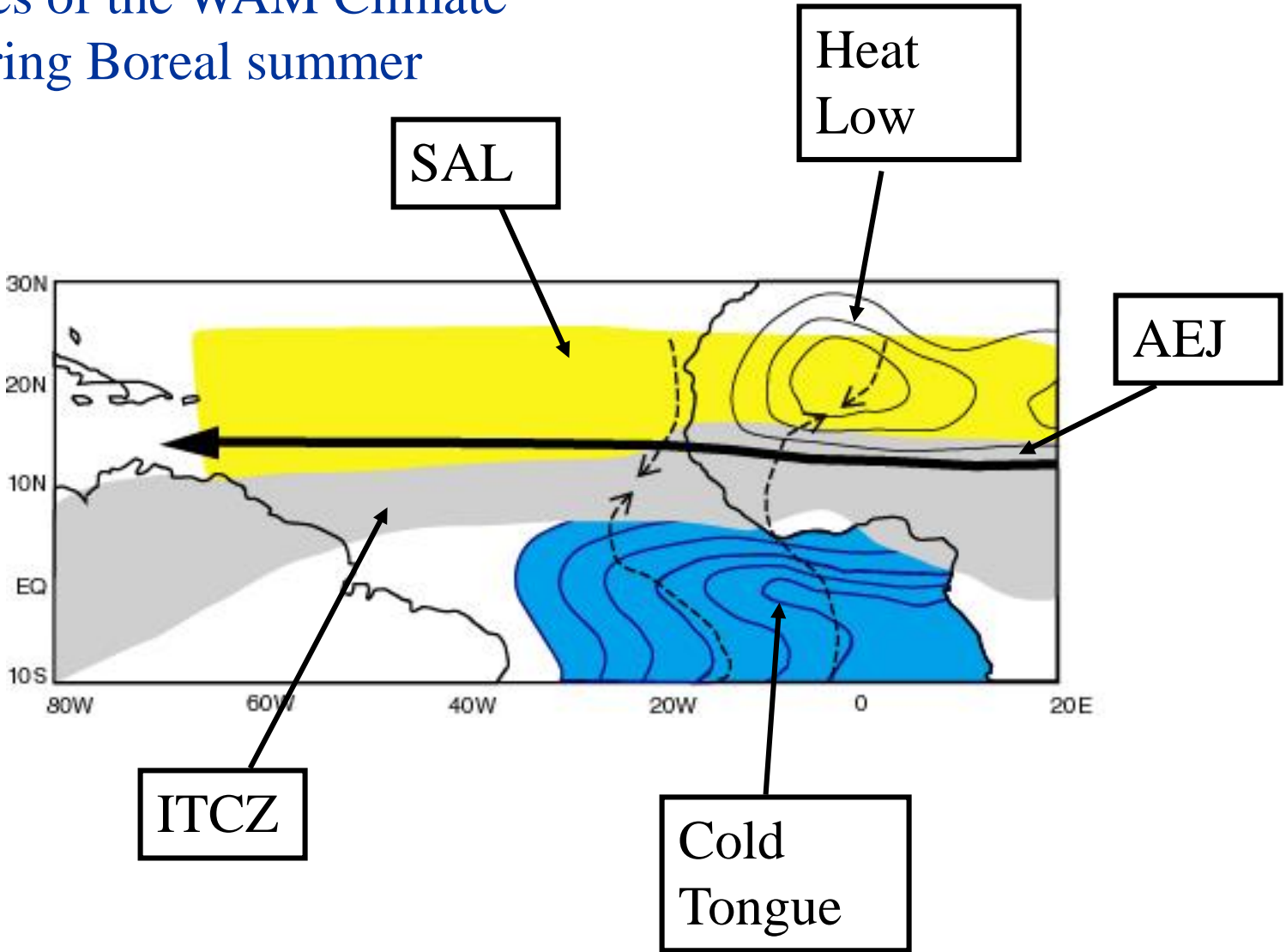
Introduction

- (1) Background
- (2) Two types of AEW behaviour
- (3) Recent work on AEW-TC relationships
- (4) Summary



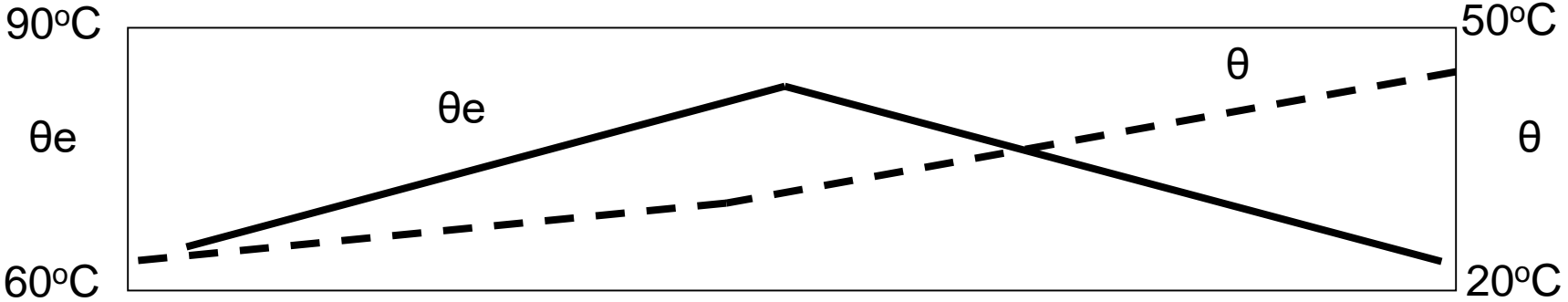
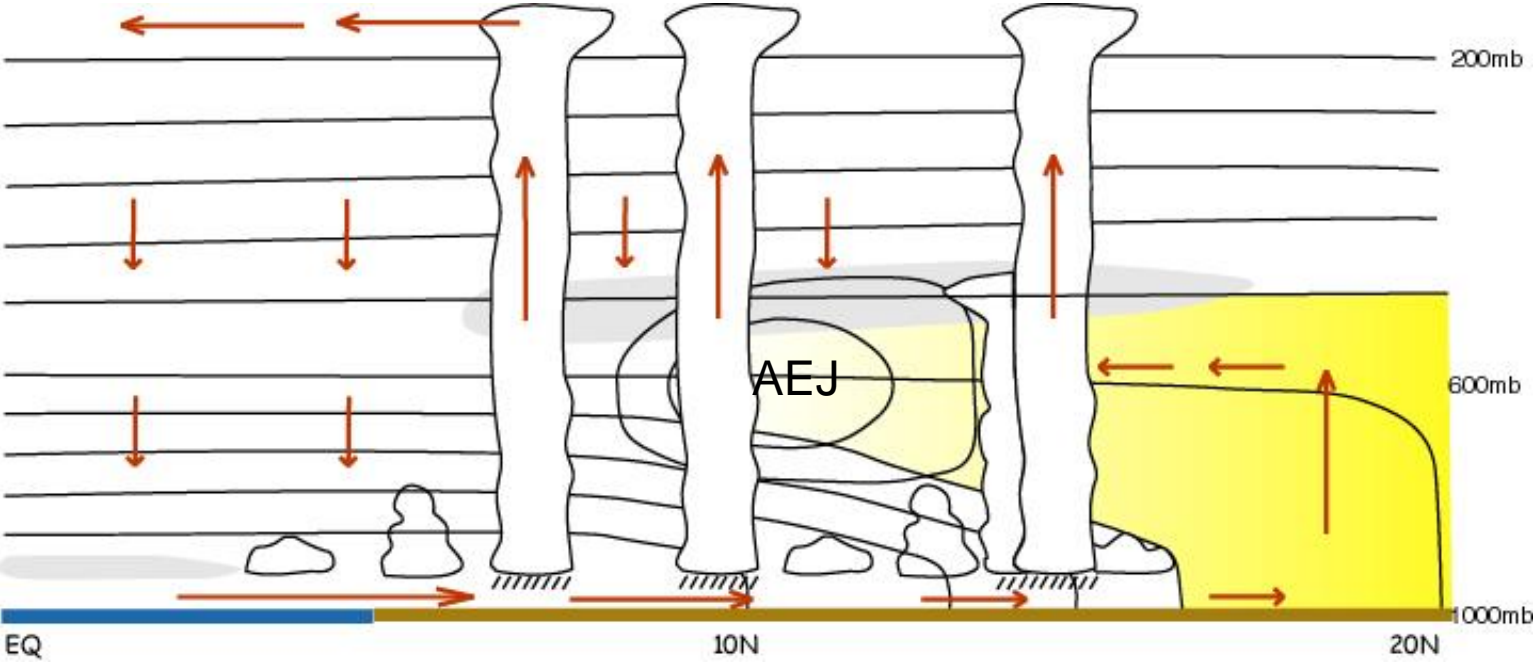
1. Background

Key features of the WAM Climate System during Boreal summer



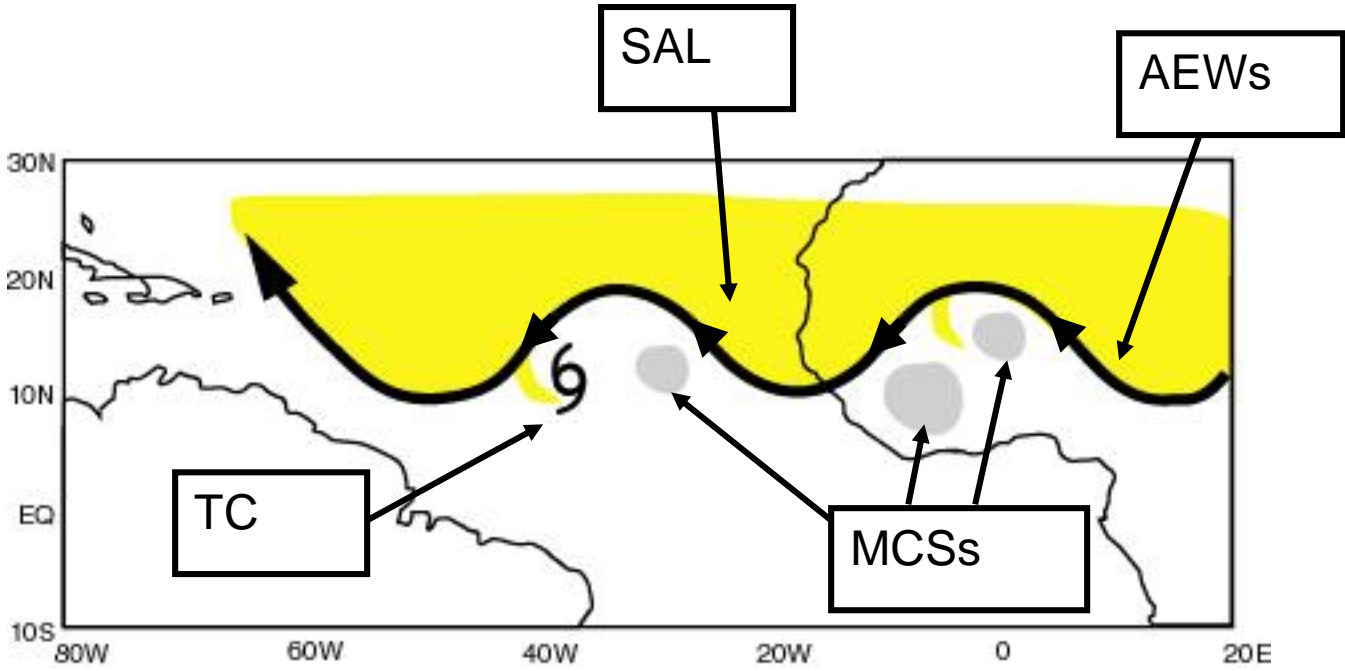
1. Background

North-South Section along the Greenwich Meridian

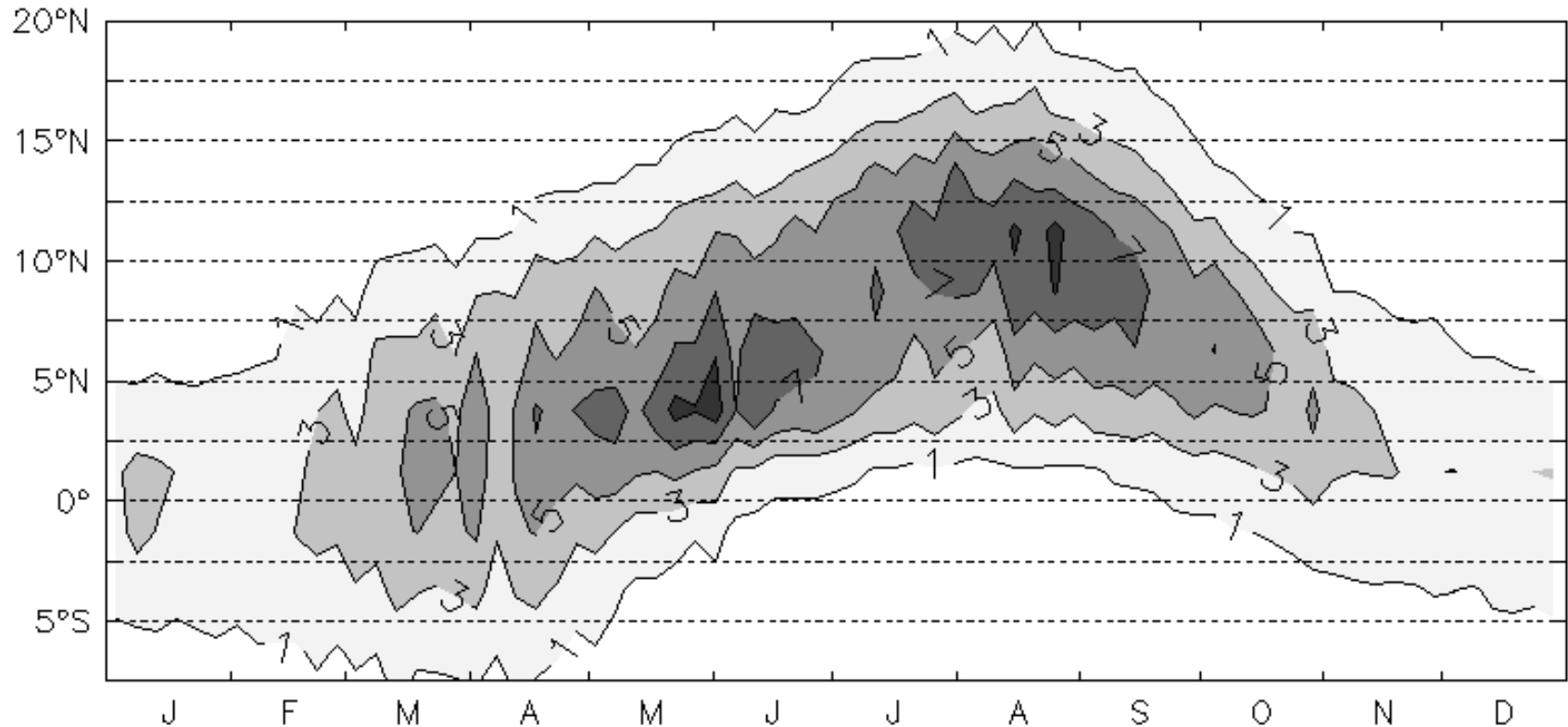


1. Background

West African and Tropical Atlantic Weather Systems

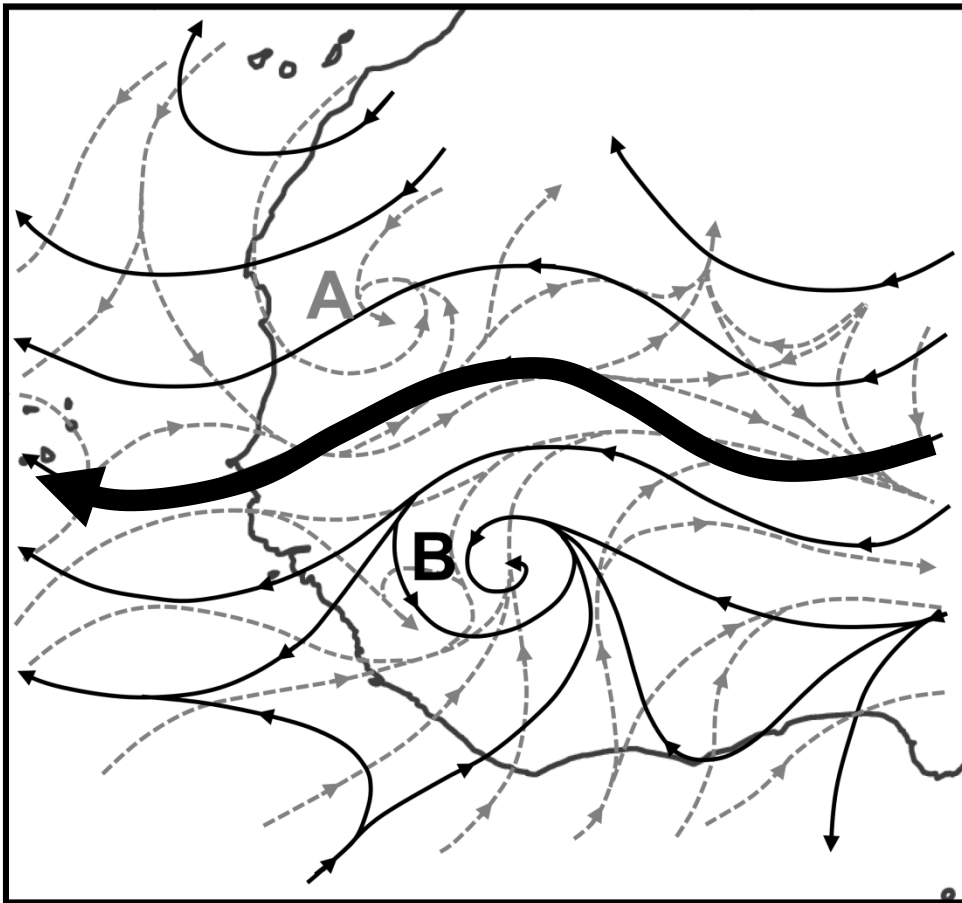


1. Background (Annual Cycle of Rainfall)

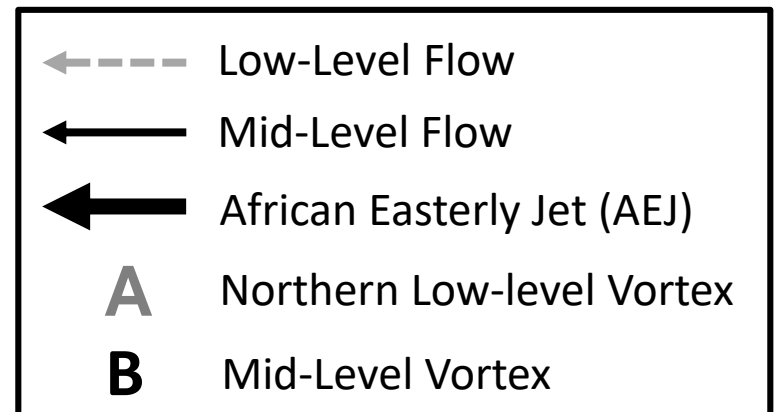


Data: GPCP (Global Precipitation Climatological Project).
Resolution: pentad on a 2.5° grid.
Averaged from 10°W to 10°E over 23 years (1979-2001).
c.f. Gu and Adler (2004)

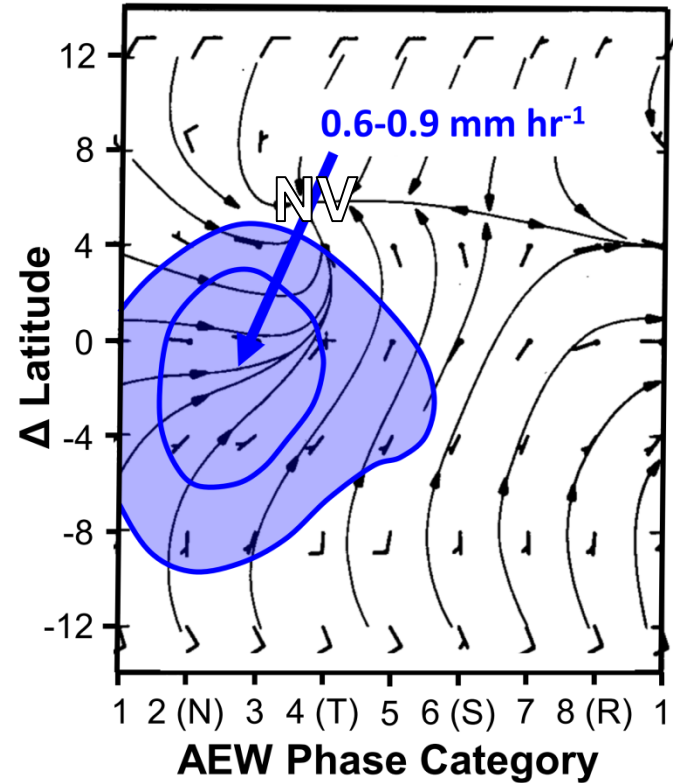
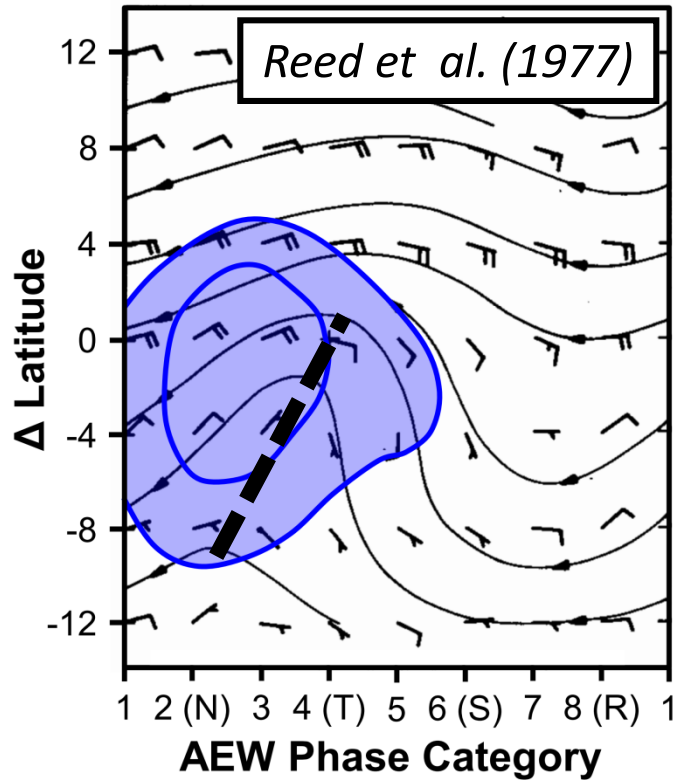
1. Background (Previous Work)



- *Carlson (1969)* was the first study to document the tilted structure of AEWs over the continent.
- *Burpee (1972)* described how this was related to the instability of the basic state.

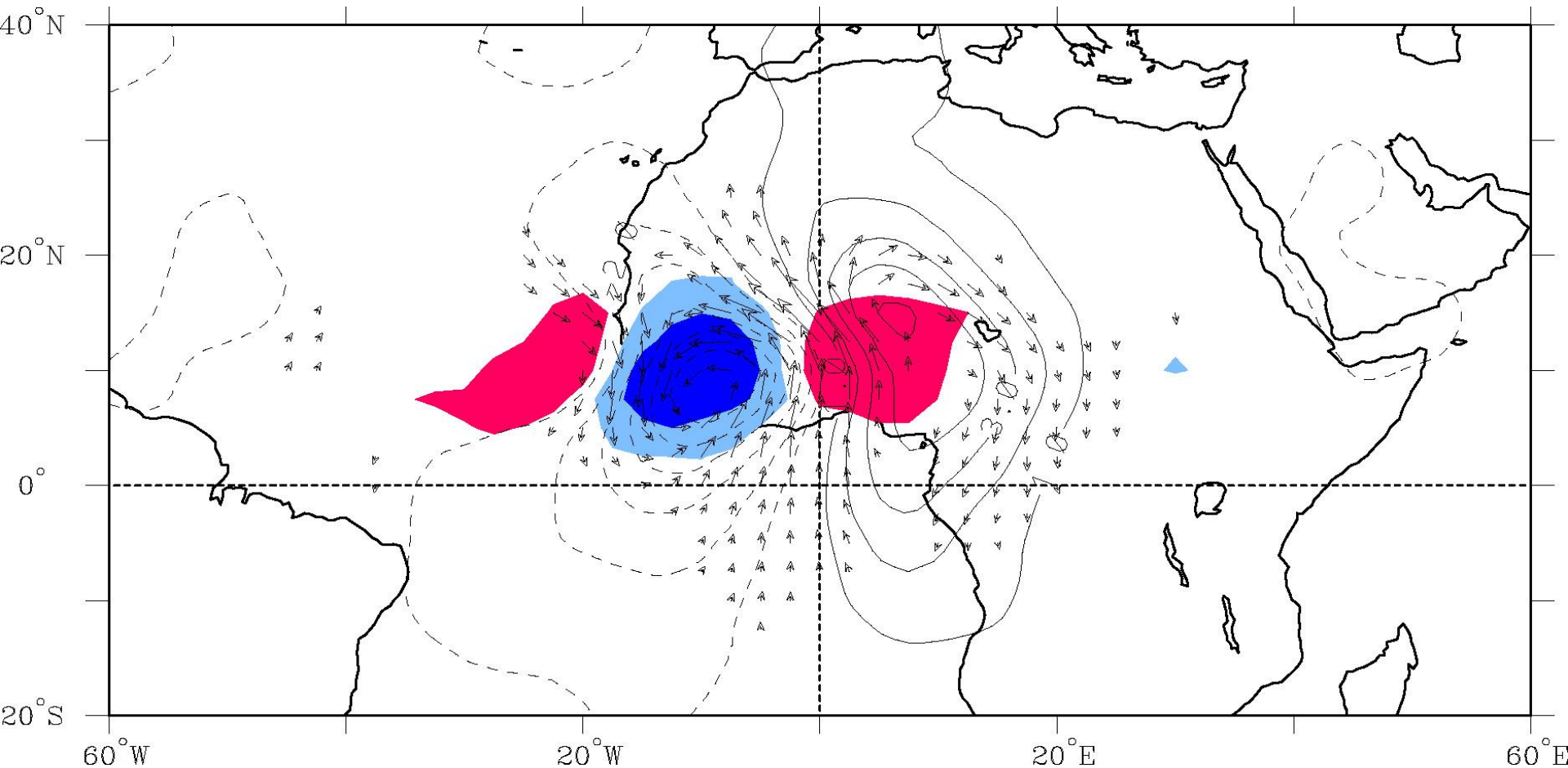


1. Background (Previous Work)



The GATE Experiment (1974) provided additional details on the structure of AEWs, their relationship with rainfall, and their energetics (Norquist et al. 1977; Reed et al. 1977; Thompson et al. 1979).

OLR and 850 hPa Flow Regressed against TD-filtered OLR (scaled -20 W m^2) at 10°N , 10°W for June-September 1979-1993



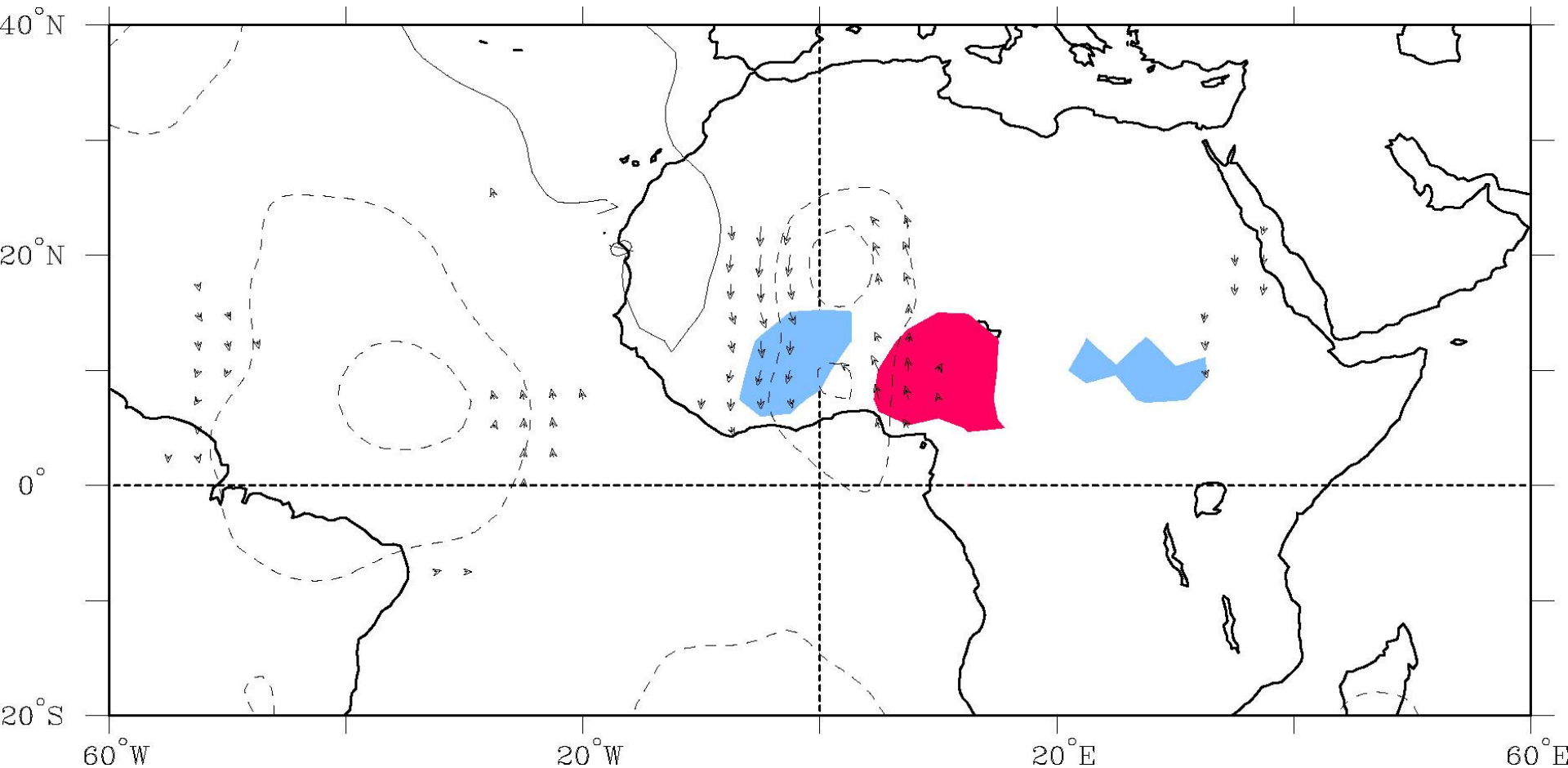
Day 0

Streamfunction (contours $1 \times 10^5 \text{ m}^2 \text{ s}^{-1}$)

Wind (vectors, largest around 2 m s^{-1})

OLR (shading starts at $\pm 6 \text{ W s}^{-2}$), negative blue

OLR and 850 hPa Flow Regressed against TD-filtered OLR (scaled -20 W m^2) at 10°N , 10°W for June-September 1979-1993



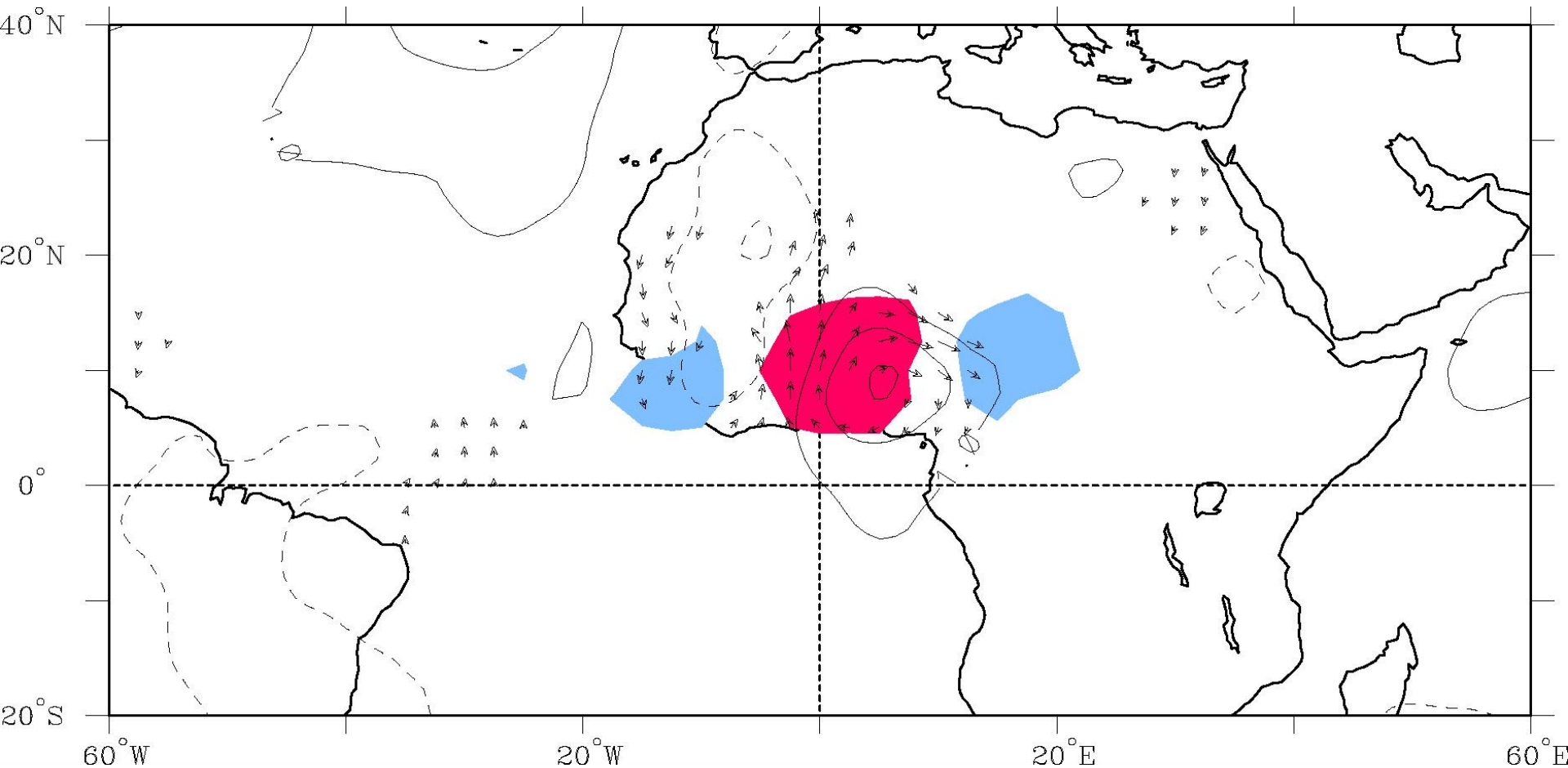
Day-4

Streamfunction (contours $1 \times 10^5 \text{ m}^2 \text{ s}^{-1}$)

Wind (vectors, largest around 2 m s^{-1})

OLR (shading starts at $\pm 6 \text{ W s}^{-2}$), negative blue

OLR and 850 hPa Flow Regressed against TD-filtered OLR (scaled -20 W m^2) at 10°N ,
 10°W for June-September 1979-1993



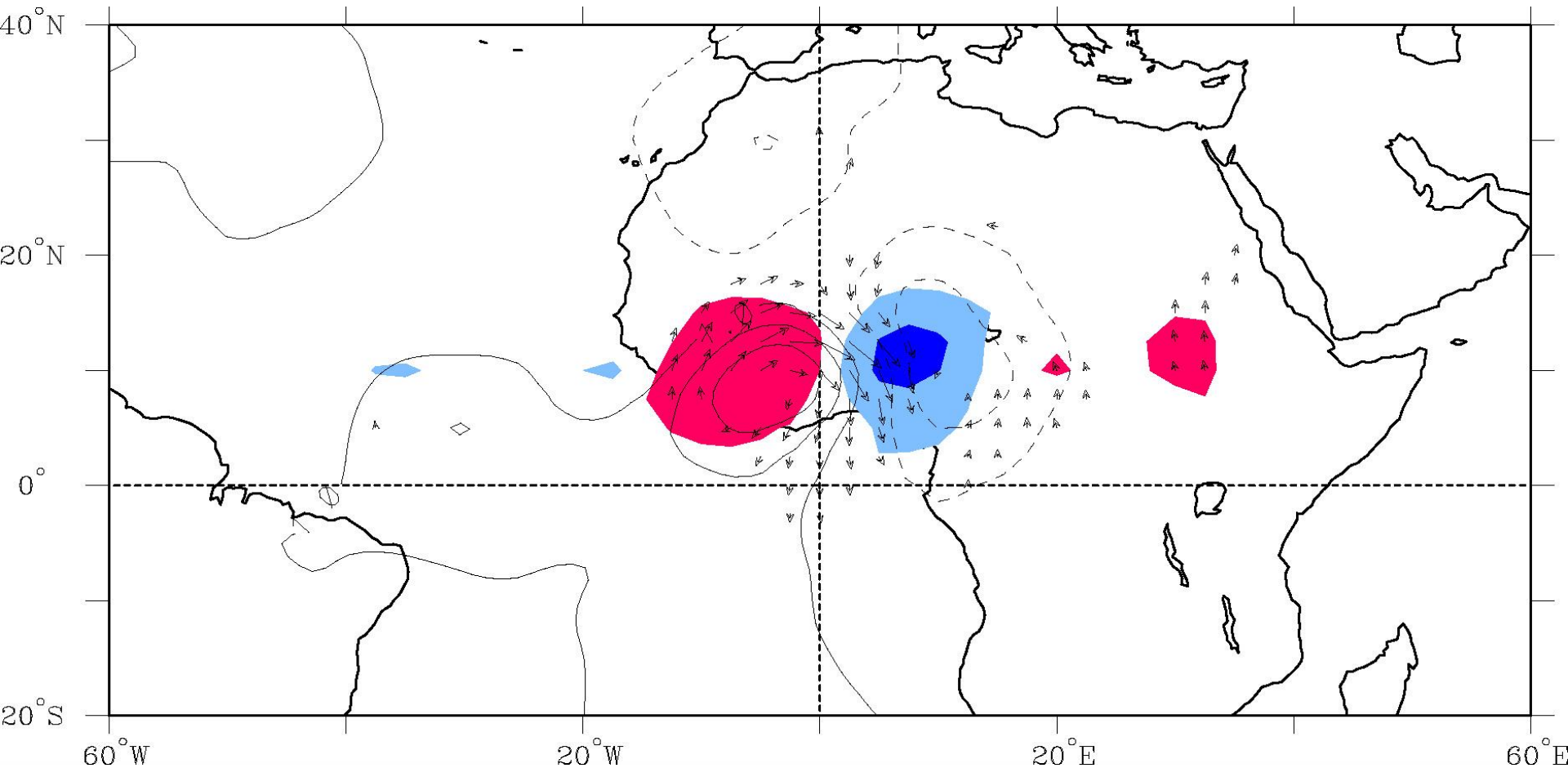
Day-3

Streamfunction (contours $1 \times 10^5 \text{ m}^2 \text{ s}^{-1}$)

Wind (vectors, largest around 2 m s^{-1})

OLR (shading starts at $\pm 6 \text{ W s}^{-2}$), negative blue

OLR and 850 hPa Flow Regressed against TD-filtered OLR (scaled -20 W m^2) at 10°N , 10°W for June-September 1979-1993



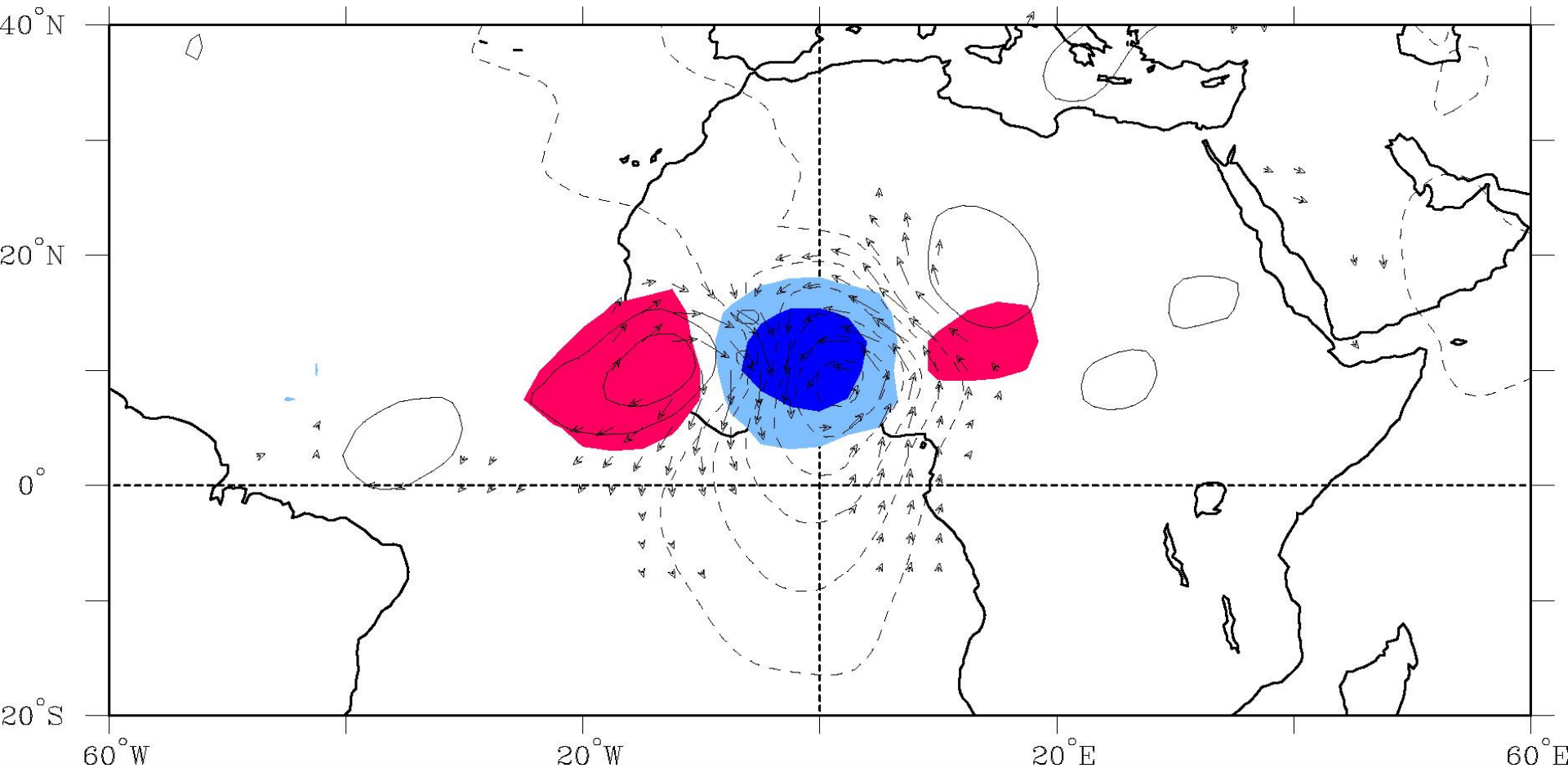
Day-2

Streamfunction (contours $1 \times 10^5 \text{ m}^2 \text{ s}^{-1}$)

Wind (vectors, largest around 2 m s^{-1})

OLR (shading starts at $\pm 6 \text{ W s}^{-2}$), negative blue

OLR and 850 hPa Flow Regressed against TD-filtered OLR (scaled -20 W m^2) at 10°N ,
 10°W for June-September 1979-1993



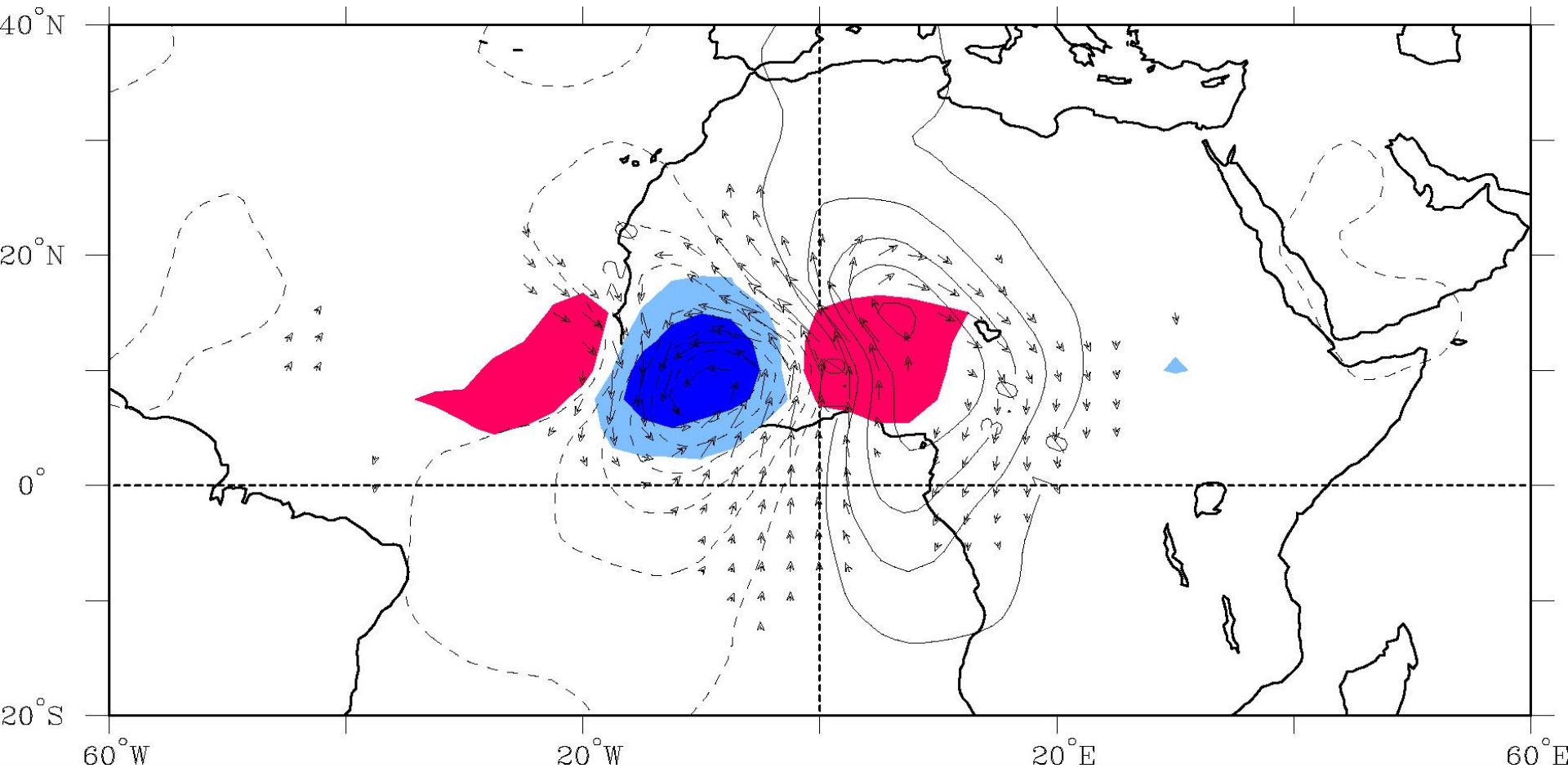
Day-1

Streamfunction (contours $1 \times 10^5 \text{ m}^2 \text{ s}^{-1}$)

Wind (vectors, largest around 2 m s^{-1})

OLR (shading starts at $\pm 6 \text{ W s}^{-2}$), negative blue

OLR and 850 hPa Flow Regressed against TD-filtered OLR (scaled -20 W m^2) at 10°N , 10°W for June-September 1979-1993



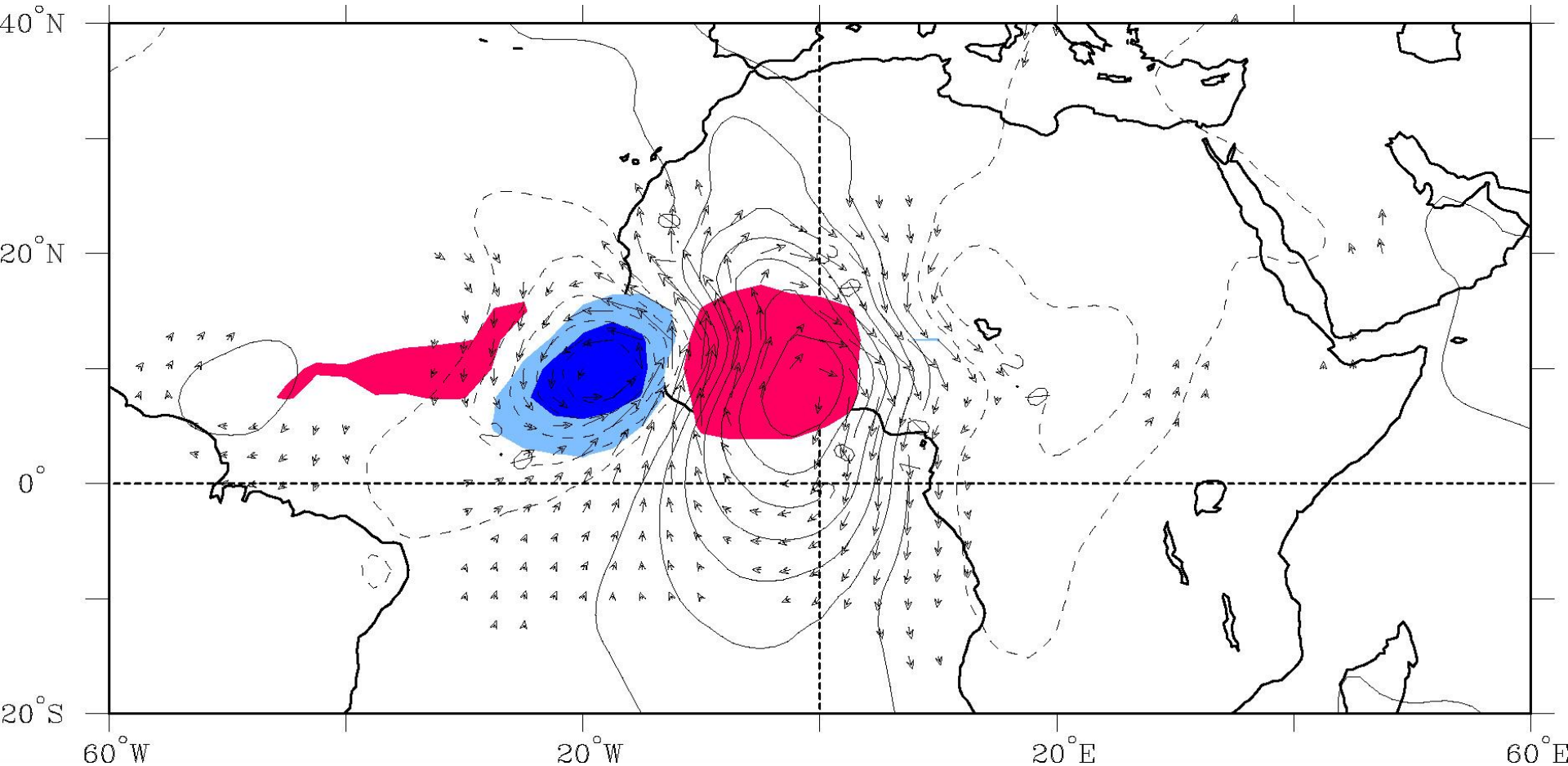
Day 0

Streamfunction (contours $1 \times 10^5 \text{ m}^2 \text{ s}^{-1}$)

Wind (vectors, largest around 2 m s^{-1})

OLR (shading starts at $\pm 6 \text{ W s}^{-2}$), negative blue

OLR and 850 hPa Flow Regressed against TD-filtered OLR (scaled -20 W m^2) at 10°N , 10°W for June-September 1979-1993



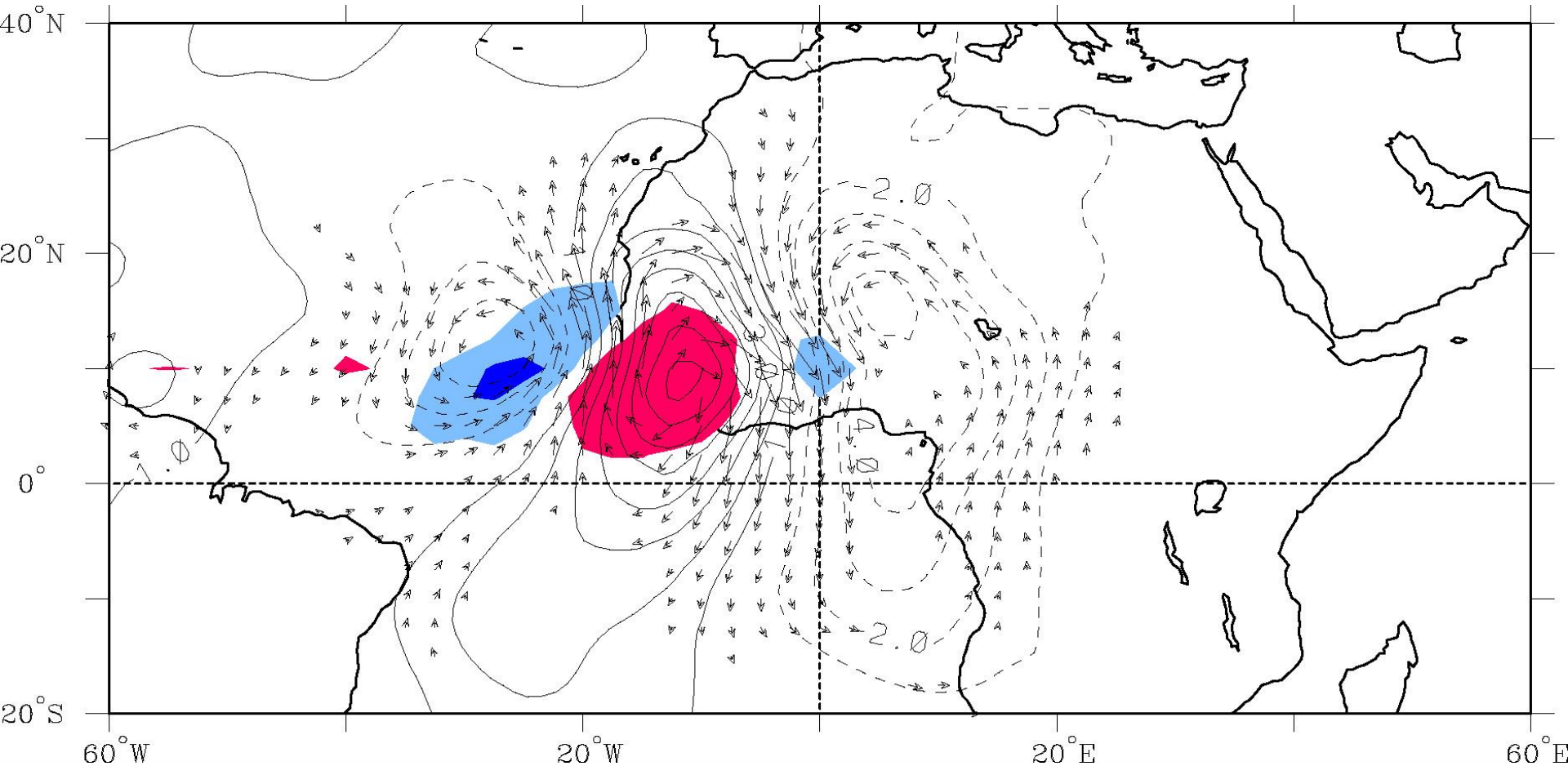
Day+1

Streamfunction (contours $1 \times 10^5 \text{ m}^2 \text{ s}^{-1}$)

Wind (vectors, largest around 2 m s^{-1})

OLR (shading starts at $\pm 6 \text{ W s}^{-2}$), negative blue

OLR and 850 hPa Flow Regressed against TD-filtered OLR (scaled -20 W m^2) at 10°N , 10°W for June-September 1979-1993



Day+2

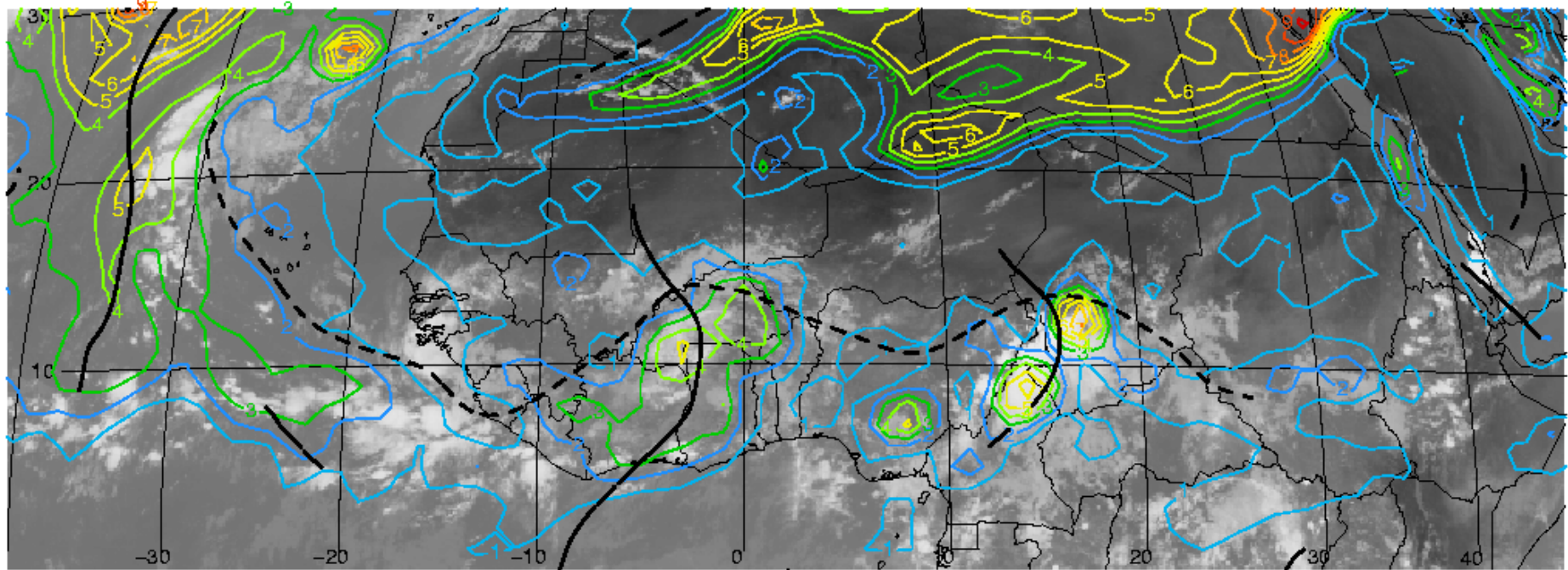
Streamfunction (contours $1 \times 10^5 \text{ m}^2 \text{ s}^{-1}$)

Wind (vectors, largest around 2 m s^{-1})

OLR (shading starts at $\pm 6 \text{ W s}^{-2}$), negative blue

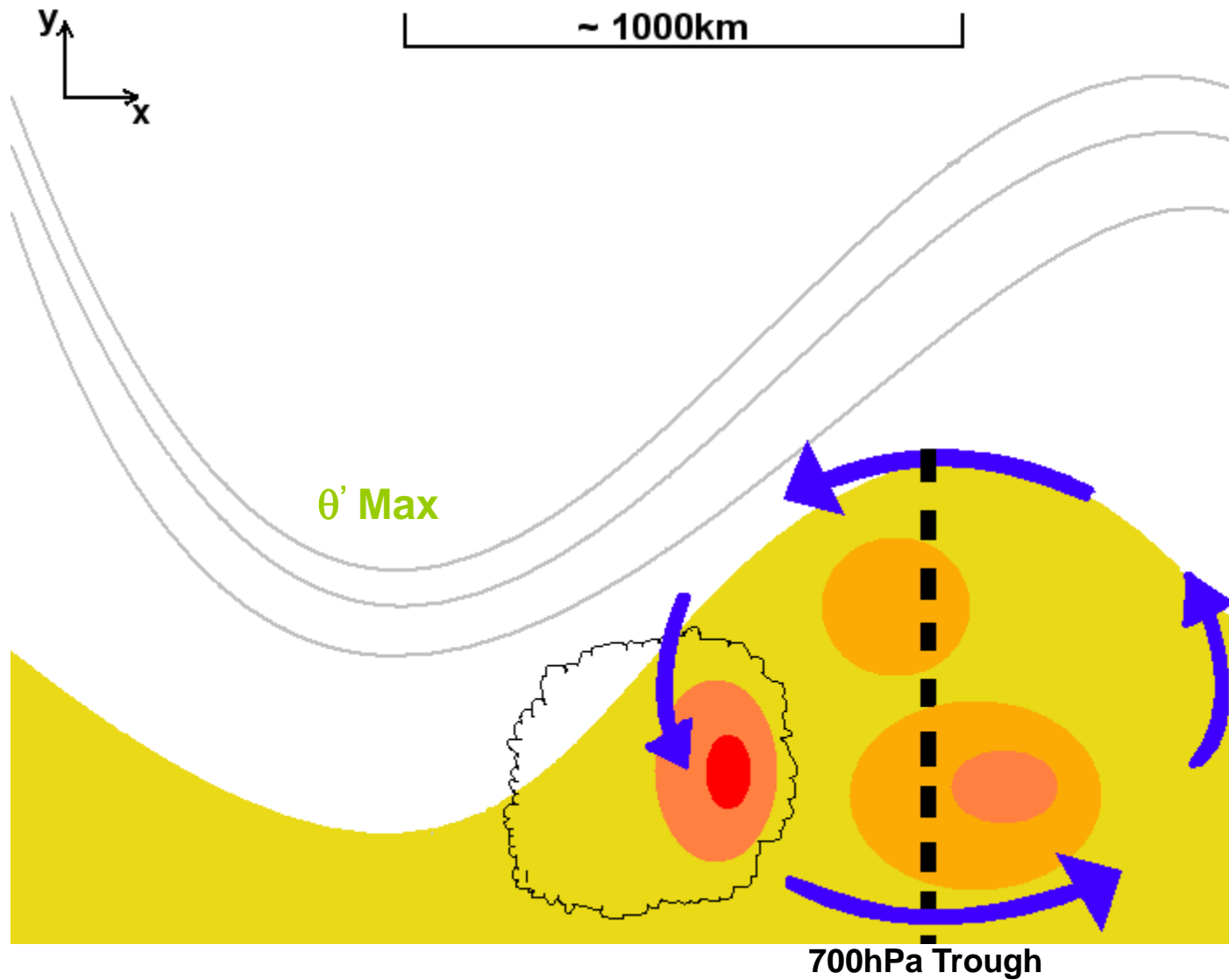
1. Background

Objectively diagnosed troughs (solid lines), African Easterly Jet (dashed), with PV (315K) and IR from METEOSAT

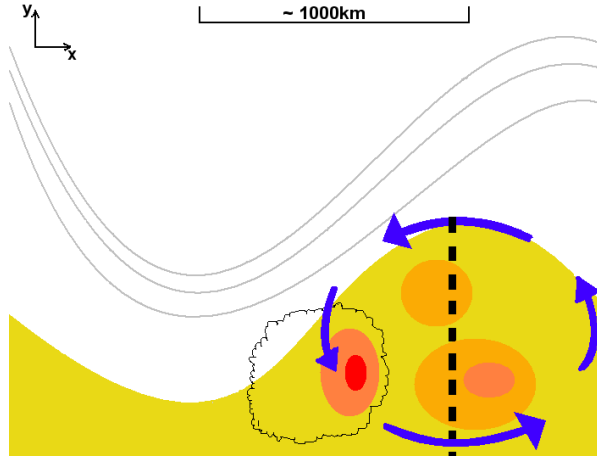


04.0912/1200F000

Conceptual framework for Baroclinic growth.

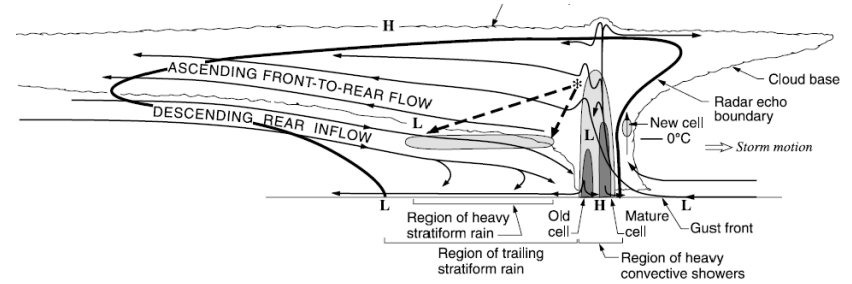
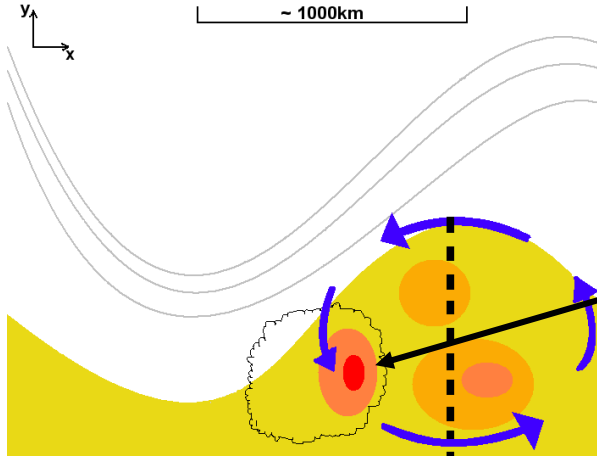


PV-theta analysis of AEWs – Scale Interactions



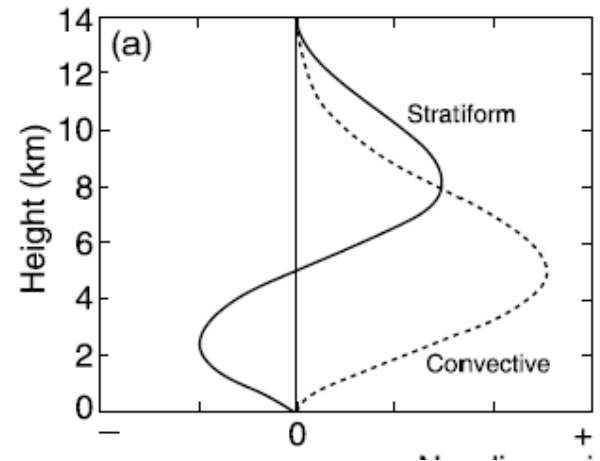
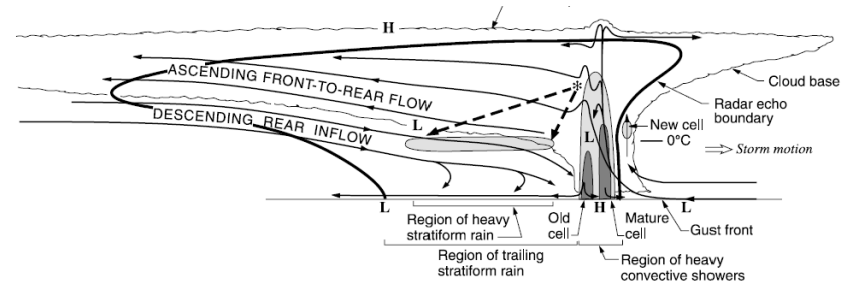
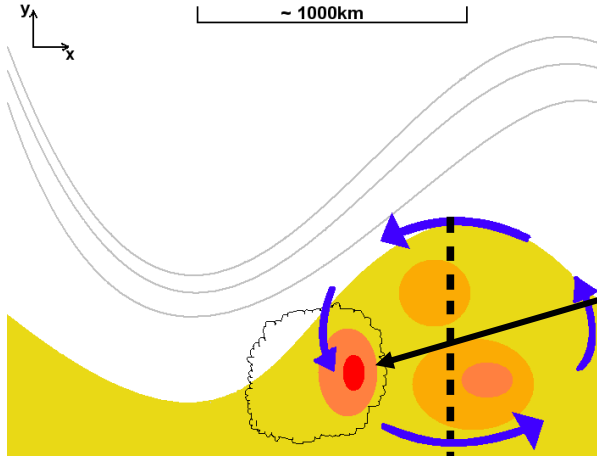
Synoptic-Mesoscale Interactions

PV- θ analysis of AEWs – Scale Interactions



Synoptic-Mesoscale Interactions

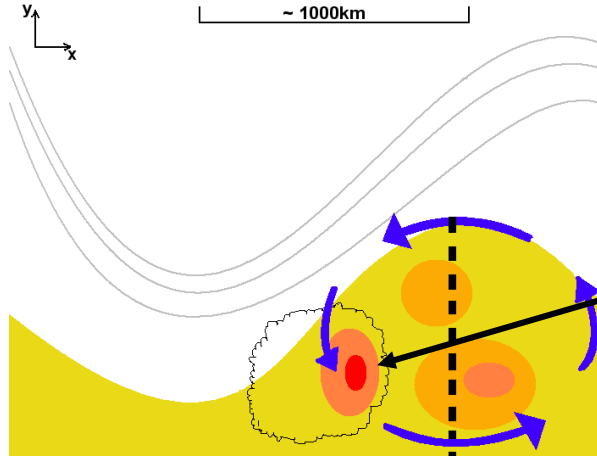
PV-theta analysis of AEWs – Scale Interactions



Synoptic-Mesoscale Interactions

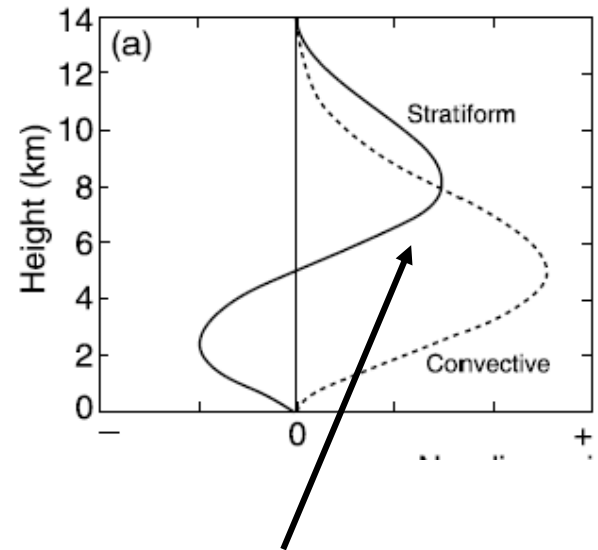
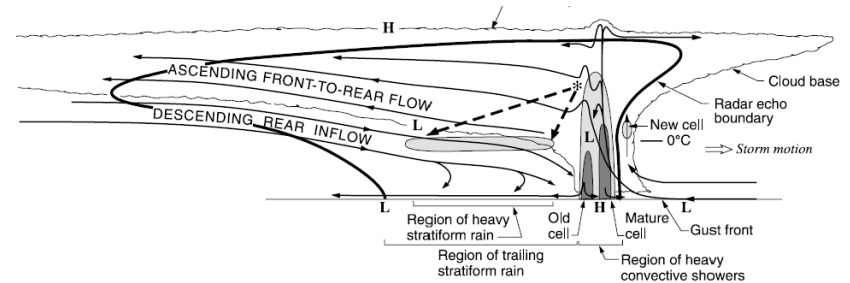
From a PV- θ perspective, the heating rate profiles are crucial to know and understand.

PV- θ analysis of AEWs – Scale Interactions



Synoptic-Mesoscale Interactions

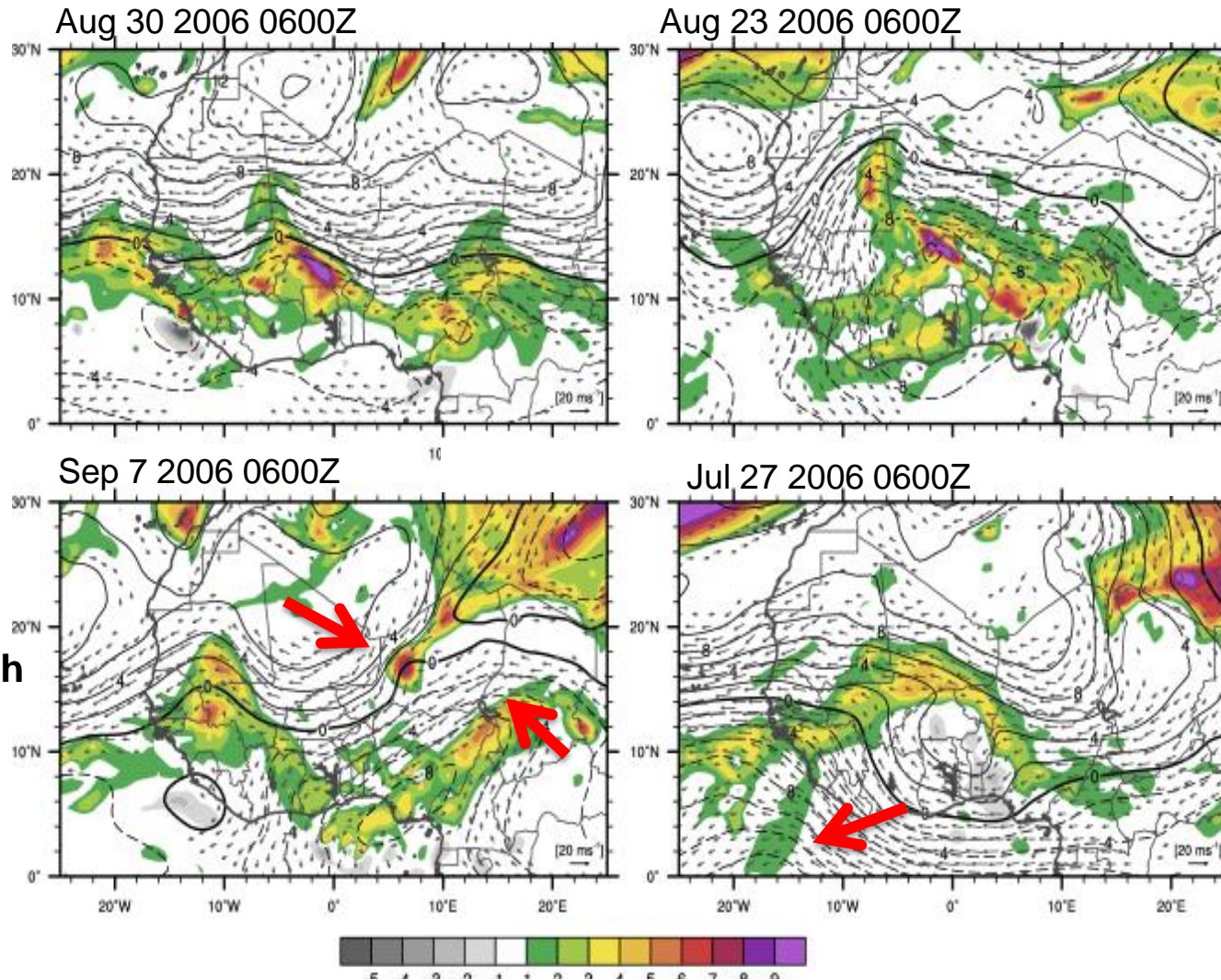
From a PV- θ perspective, the heating rate profiles are crucial to know and understand.



Mesoscale-Microscale Interactions

Ultimately these profiles are influenced by the nature of the microphysics!

2. Two Types of AEW Behavior (Cheng et al, 2019)



We know little about variability of the AEWs

Methodology

- Empirical Orthogonal Functions (EOFs)
 - highlight the dominant wave structure

Methodology

- Empirical Orthogonal Functions (EOFs)
 - highlight the dominant wave structure

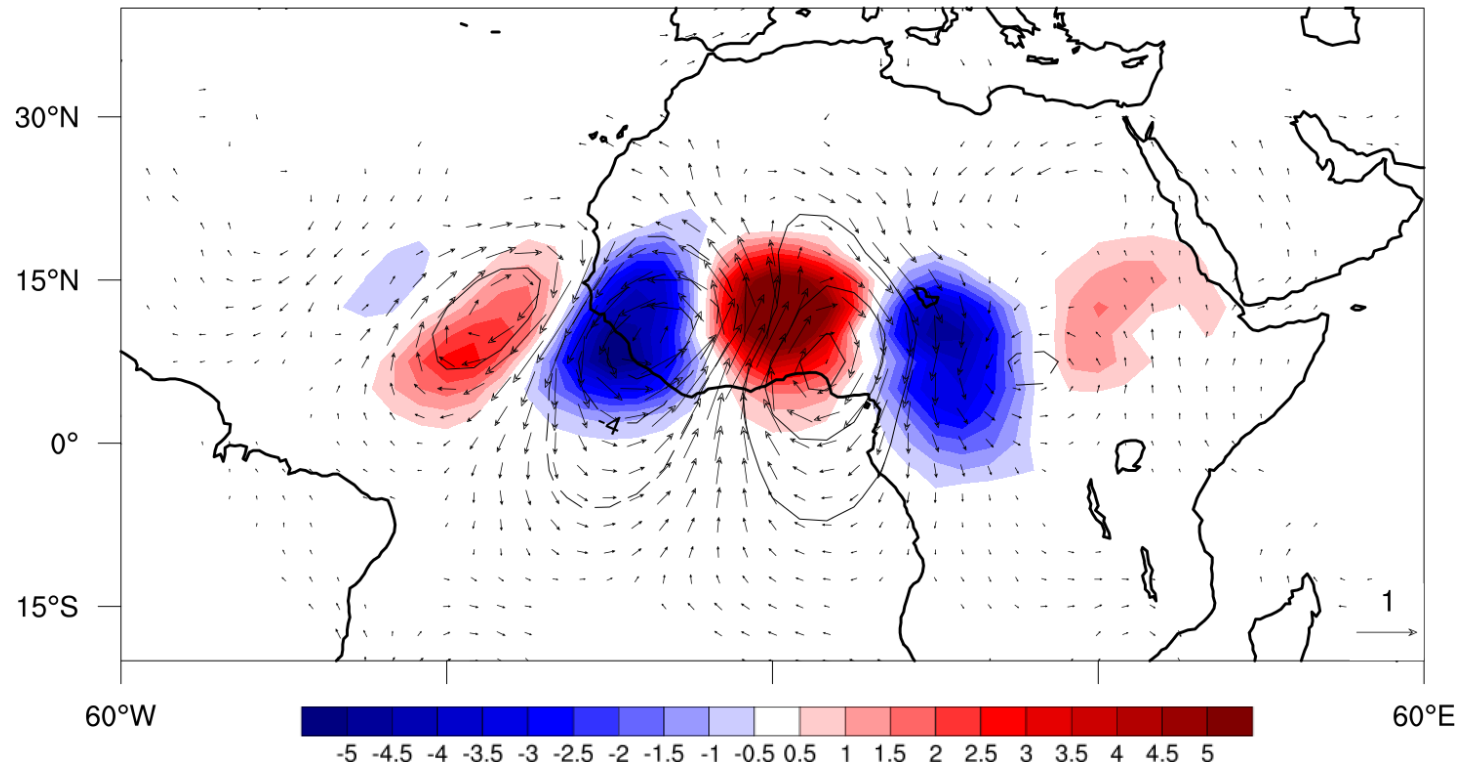
	ECMWF Interim	Claus Brightness Temperature (T_b)
Spatial resolution	2.5 × 2.5	
Temporal resolution	6 hour	
Period	JAS of 1984-2013	

Three Kinds of EOFs

EOF Name	Variable	Domain
T_b EOF	2-6-day-westward-filtered brightness temperature (T_b)	15S-30N, 40W-40E
v700 EOF	2-6-day-filtered meridional wind at 700 hPa	15S-30N, 40W-40E
v200 EOF	2-6-day-filtered meridional wind at 200 hPa	5S-5N, 40W-40E

T_b EOF Structure

Day 0

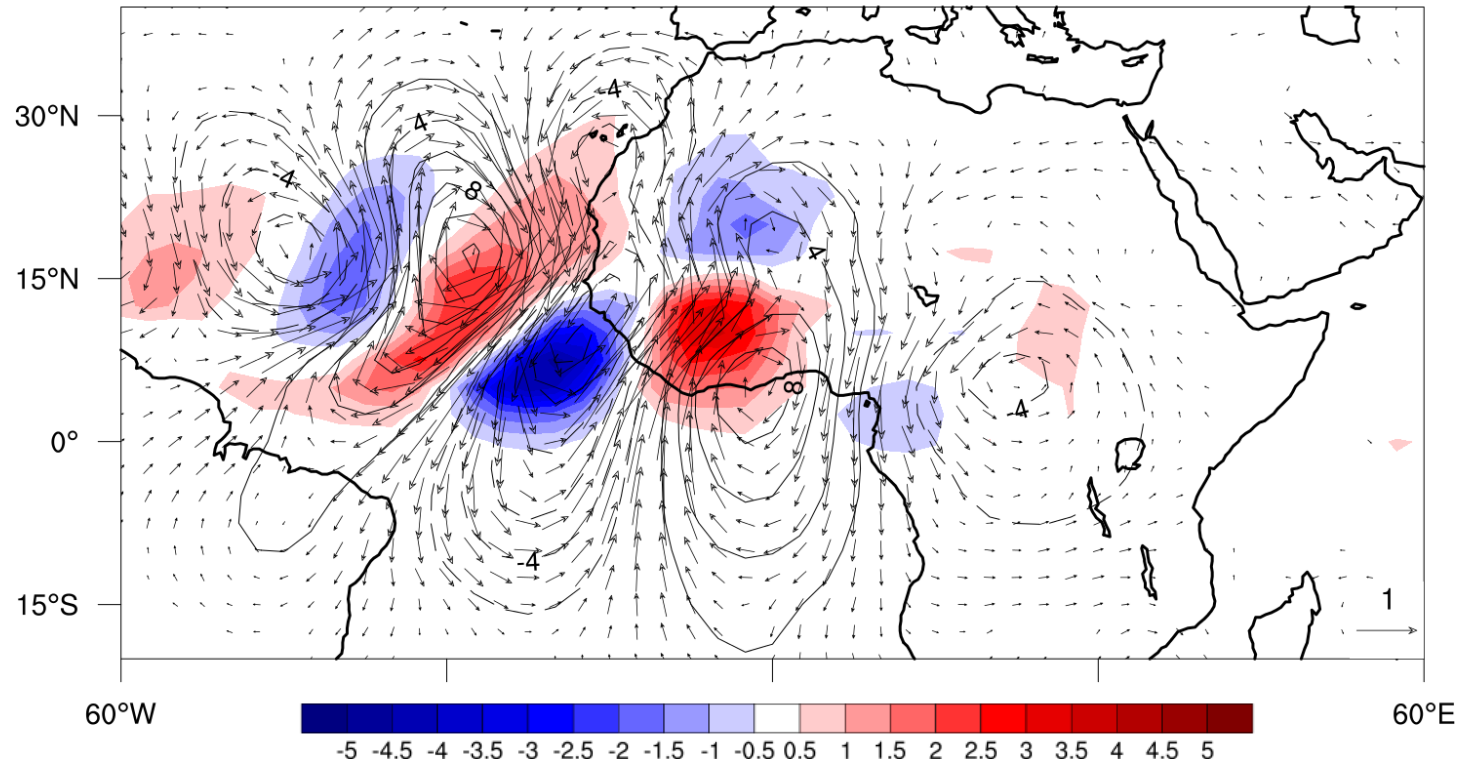


T_b (shadings, K), 700-hPa wind (m s⁻¹) and streamfunction (contours, 2×10^5 m² s⁻²)

- The first pair of EOFs explains 20% of the variance
- T_b EOF captures a typical AEW evolution closely coupled with convection
- Convection and circulation centered and confined around the ITCZ

v700 EOF Structure

Day 0

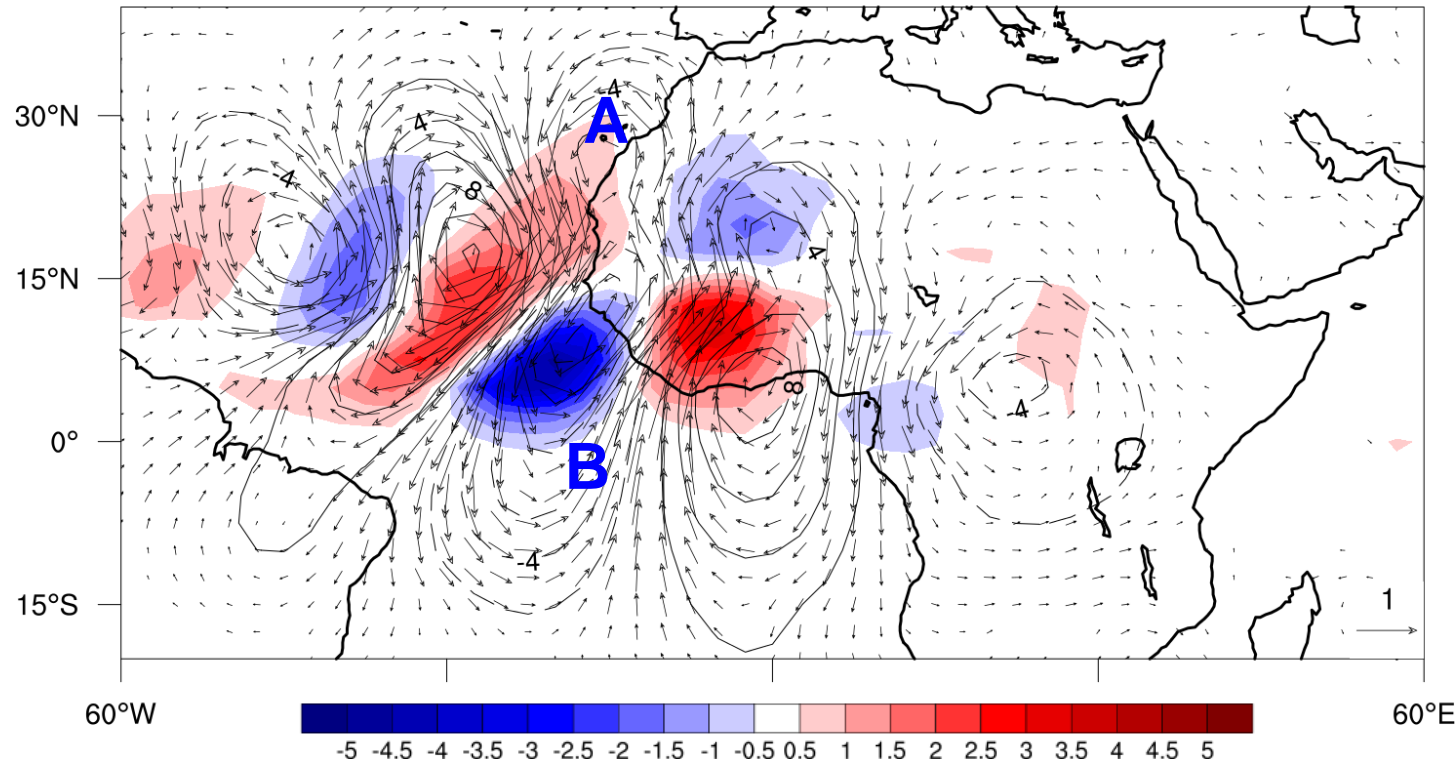


T_b (shadings, K), 700-hPa wind (m s^{-1}) and streamfunction (contours, $2 \times 10^5 \text{ m}^2 \text{ s}^{-2}$)

- The first pair of EOFs explains 16% of the variance
- v700 EOF shows the interaction of AEWs with extratropical waves and equatorial modes.

v700 EOF Structure

Day 0



T_b (shadings, K), 700-hPa wind (m s^{-1}) and streamfunction (contours, $2 \times 10^5 \text{ m}^2 \text{ s}^{-2}$)

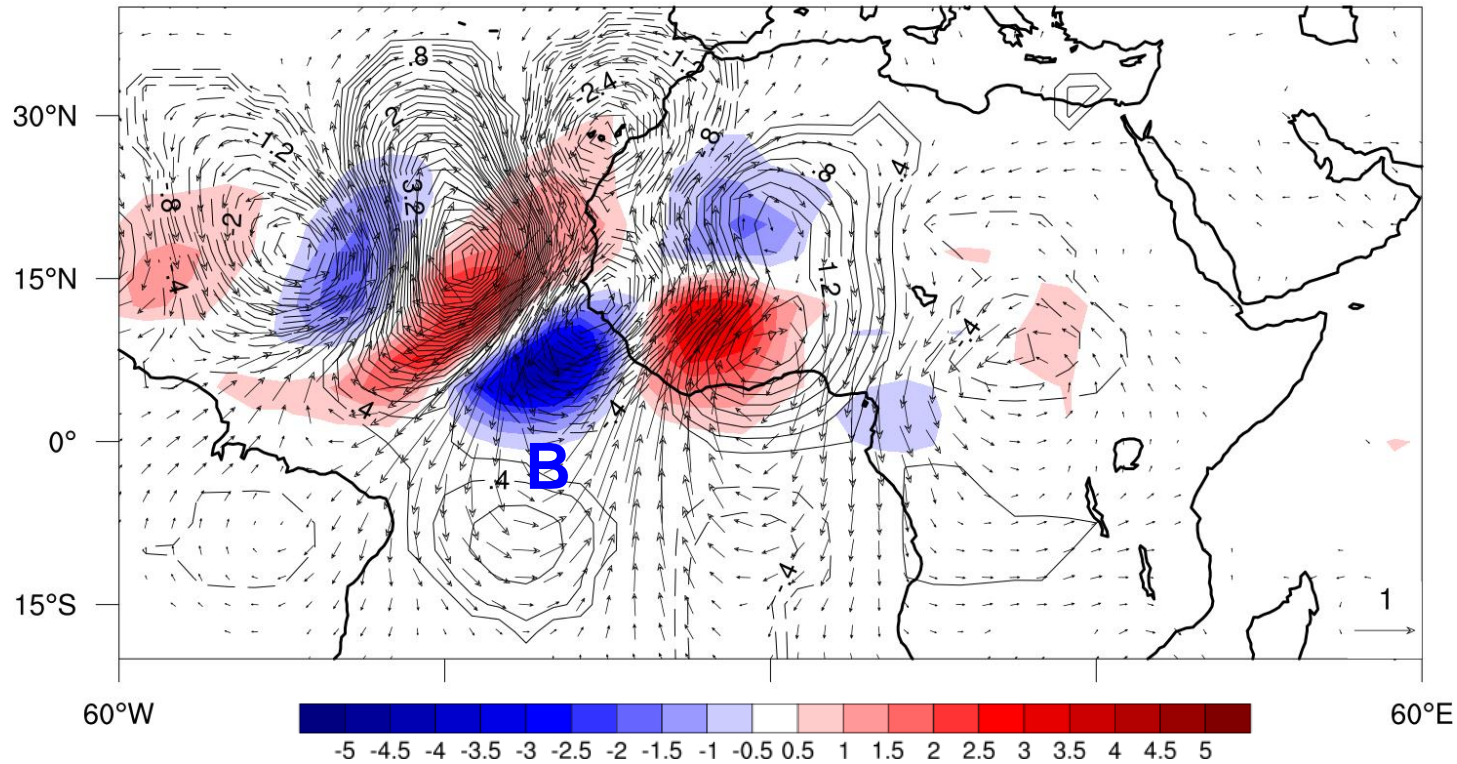
- v700 EOF shows the interaction of AEWs with extratropical waves and equatorial modes.

A Moroccan Vortex

B Mixed Rossby Gravity wave (MRG)

Interaction with the MRG

Day 0

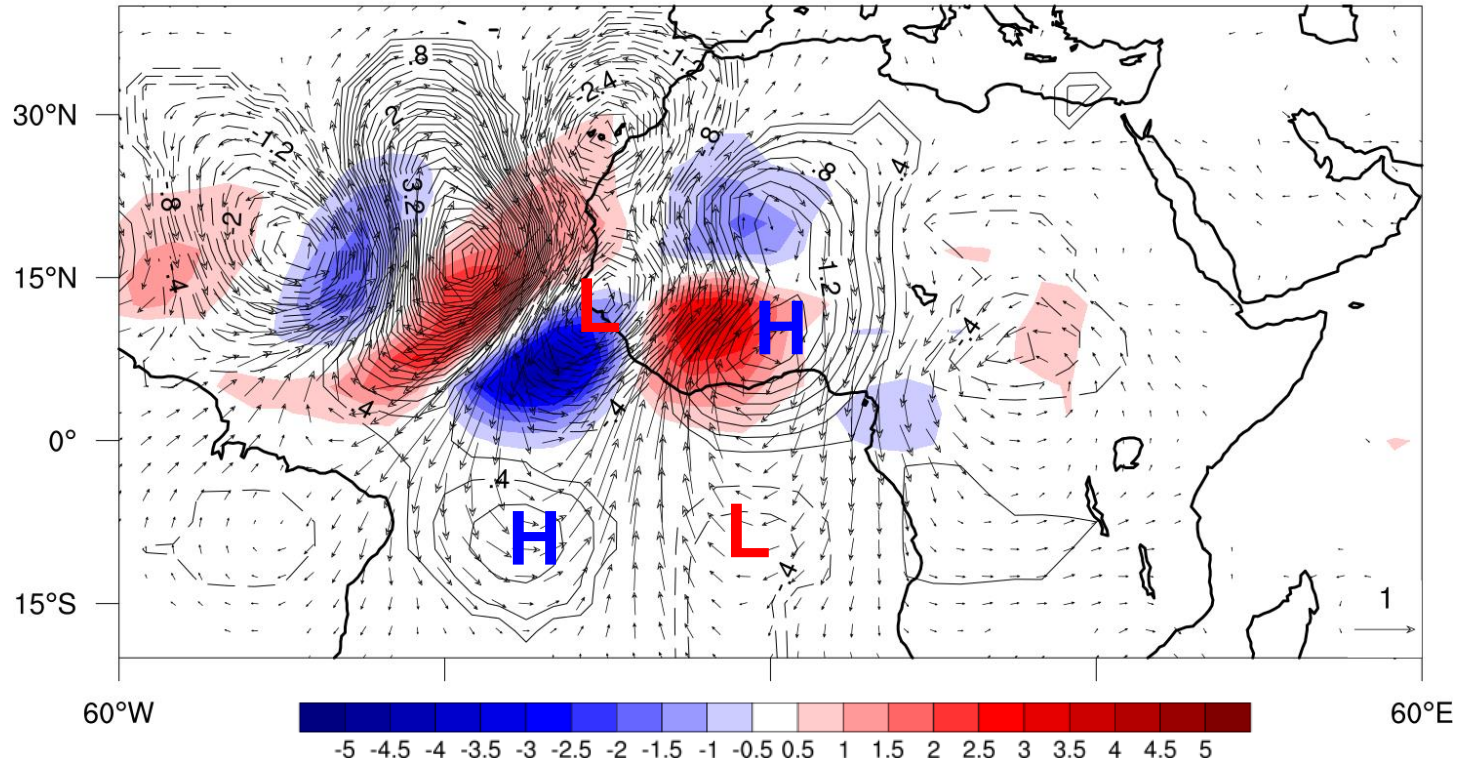


T_b (shadings, K), 700-hPa wind (m s^{-1}) and geopotential height (contours, 0.2 m)

- Prominent cross-equatorial meridional flow

Interaction with the MRG

Day 0

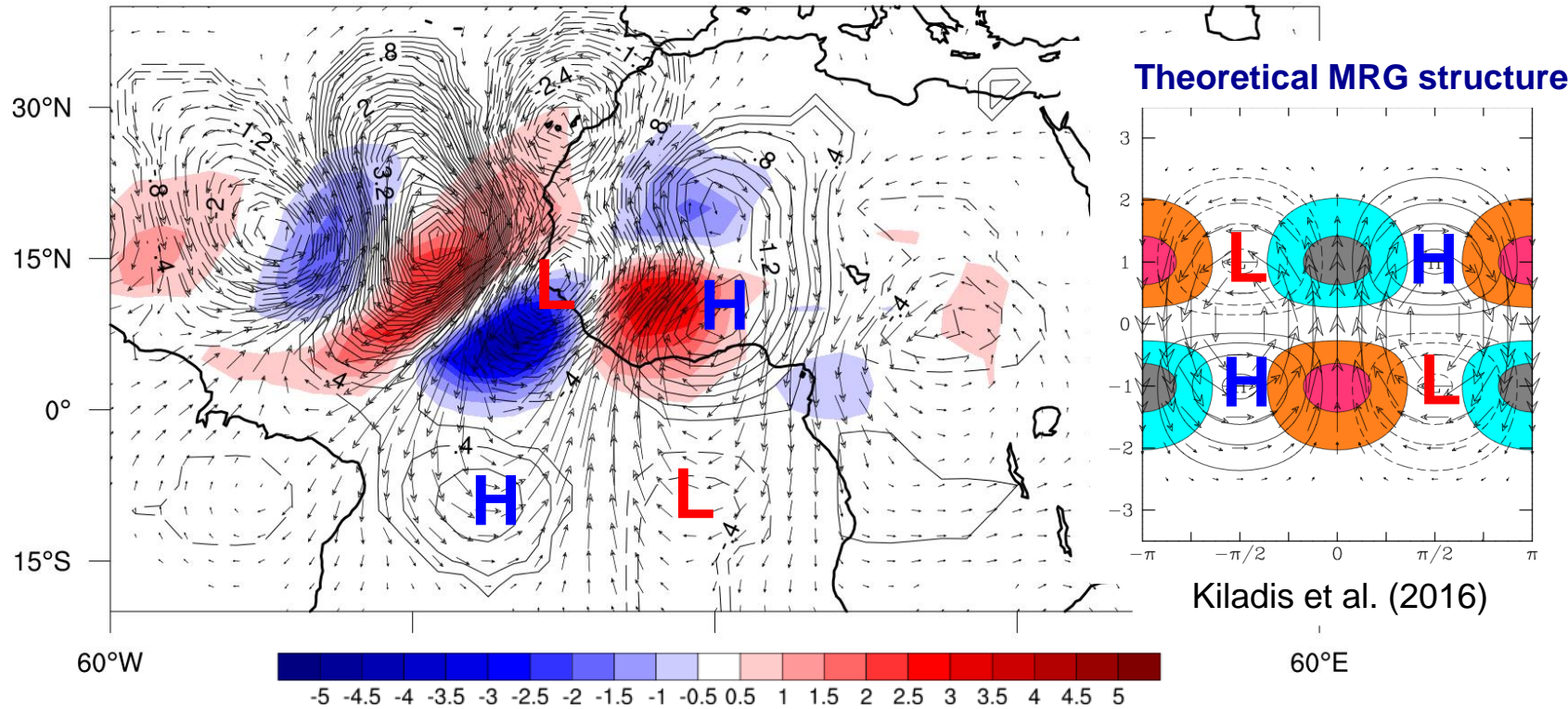


T_b (shadings, K), 700-hPa wind (m s^{-1}) and geopotential height (contours, 0.2 m)

- Prominent cross-equatorial meridional flow
- Antisymmetric geopotential height

Interaction with the MRG

Day 0

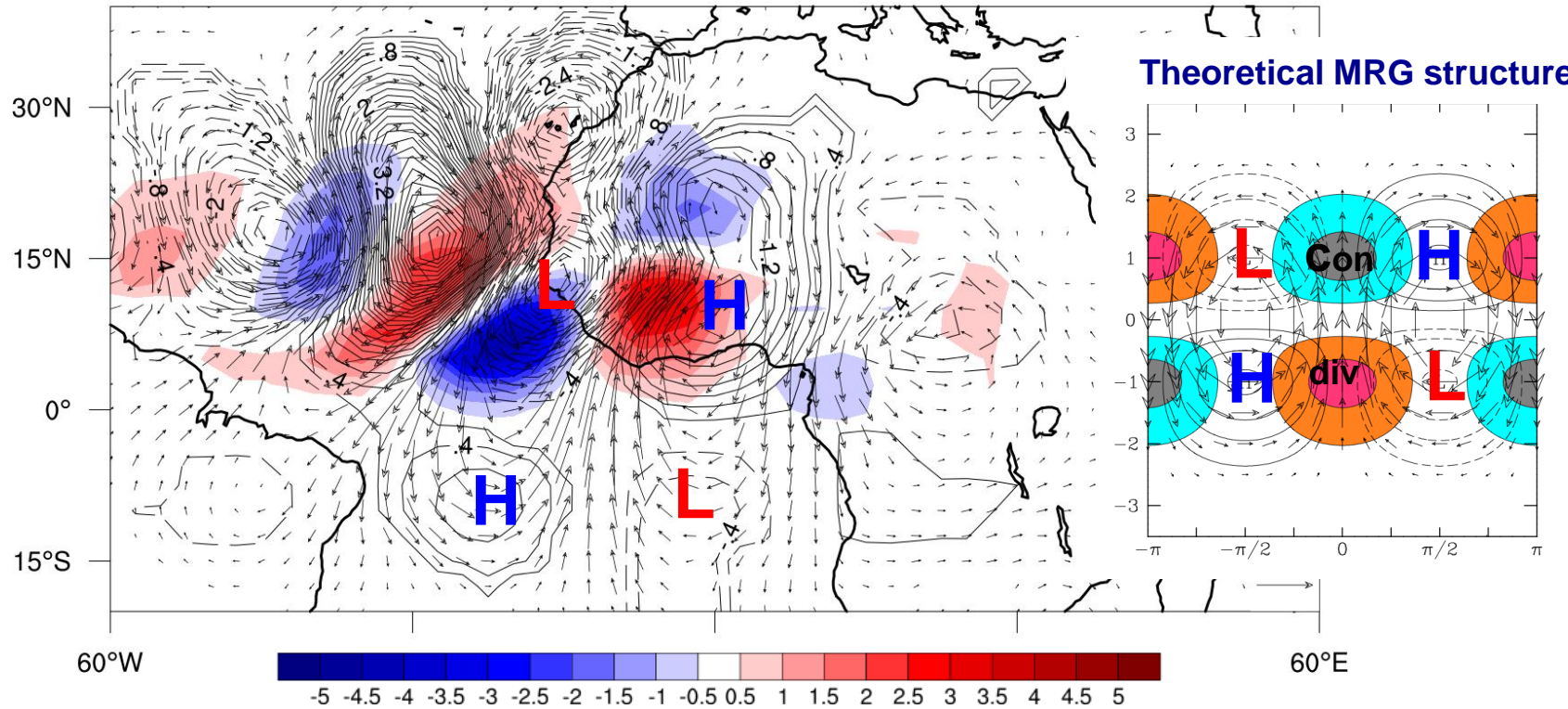


T_b (shadings, K), 700-hPa wind (m s^{-1}) and geopotential height (contours, 0.2 m)

- Prominent cross-equatorial meridional flow
- Antisymmetric geopotential height

Interaction with the MRG

Day 0

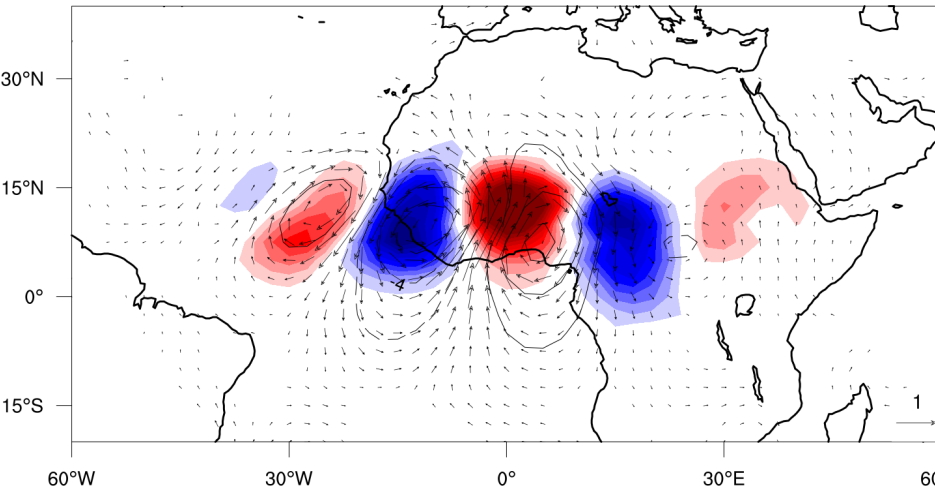


T_b (shadings, K), 700-hPa wind (m s^{-1}) and geopotential height (contours, 0.2 m)

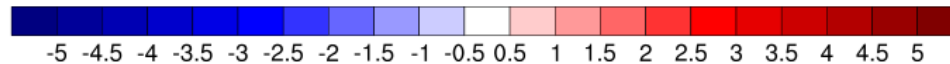
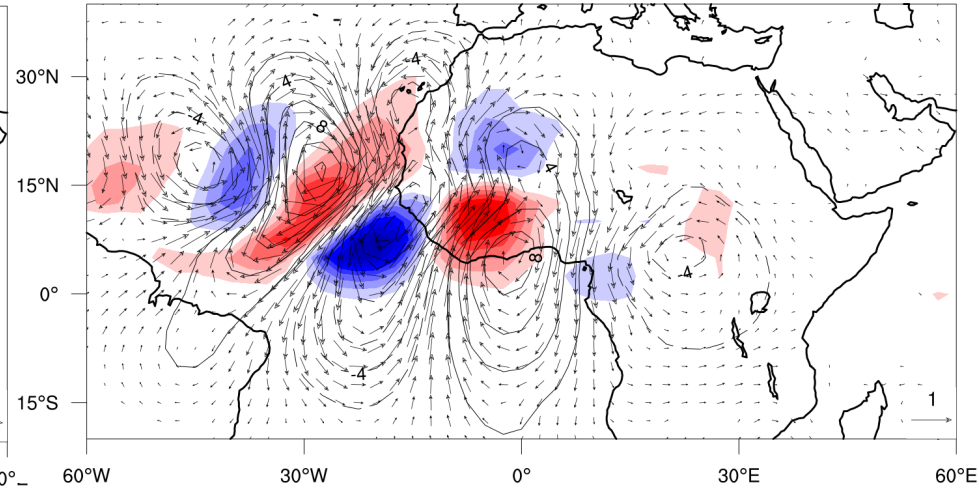
- Prominent cross-equatorial meridional flow
- Antisymmetric geopotential height
- “AEW-MRG hybrid” Convection more “AEW-like”

Two AEW Behaviors

T_b EOF



v700 EOF

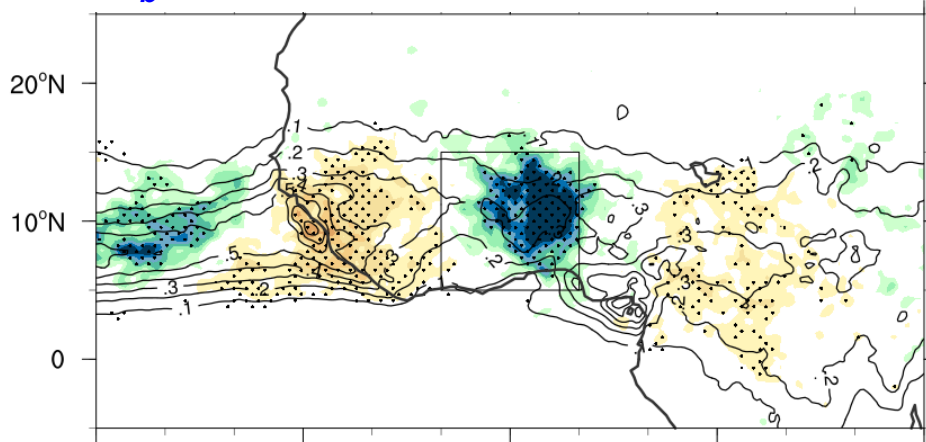


T_b (shadings, K), 700-hPa wind (m s^{-1}) and geopotential height (contours, 0.2 m)

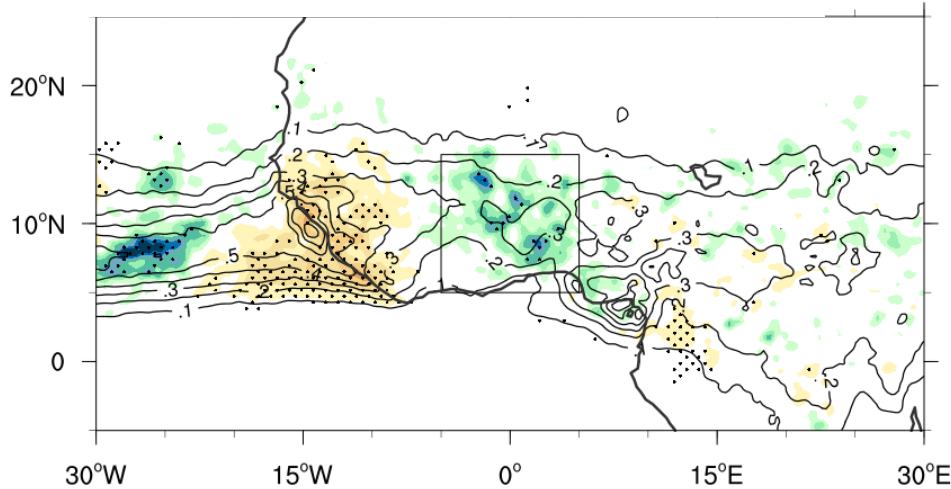
- **Two different behaviors of AEWs:**
 - Circulation and convection closely coupled and centered around the ITCZ
 - AEW-MRG hybrid and interaction with the subtropics

Impact of Different AEW Behaviors on PPN

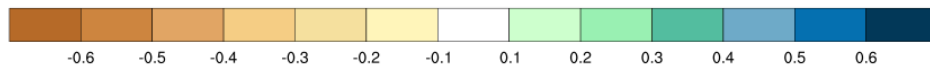
T_b EOF: 157 counts



v700 EOF: 140 counts



Rainfall more likely for T_b EOF
and more frequent intense
rainfall



Rain rate anomalies (shadings, mm hr⁻¹) and
climatological rain rate (contours, mm hr⁻¹)

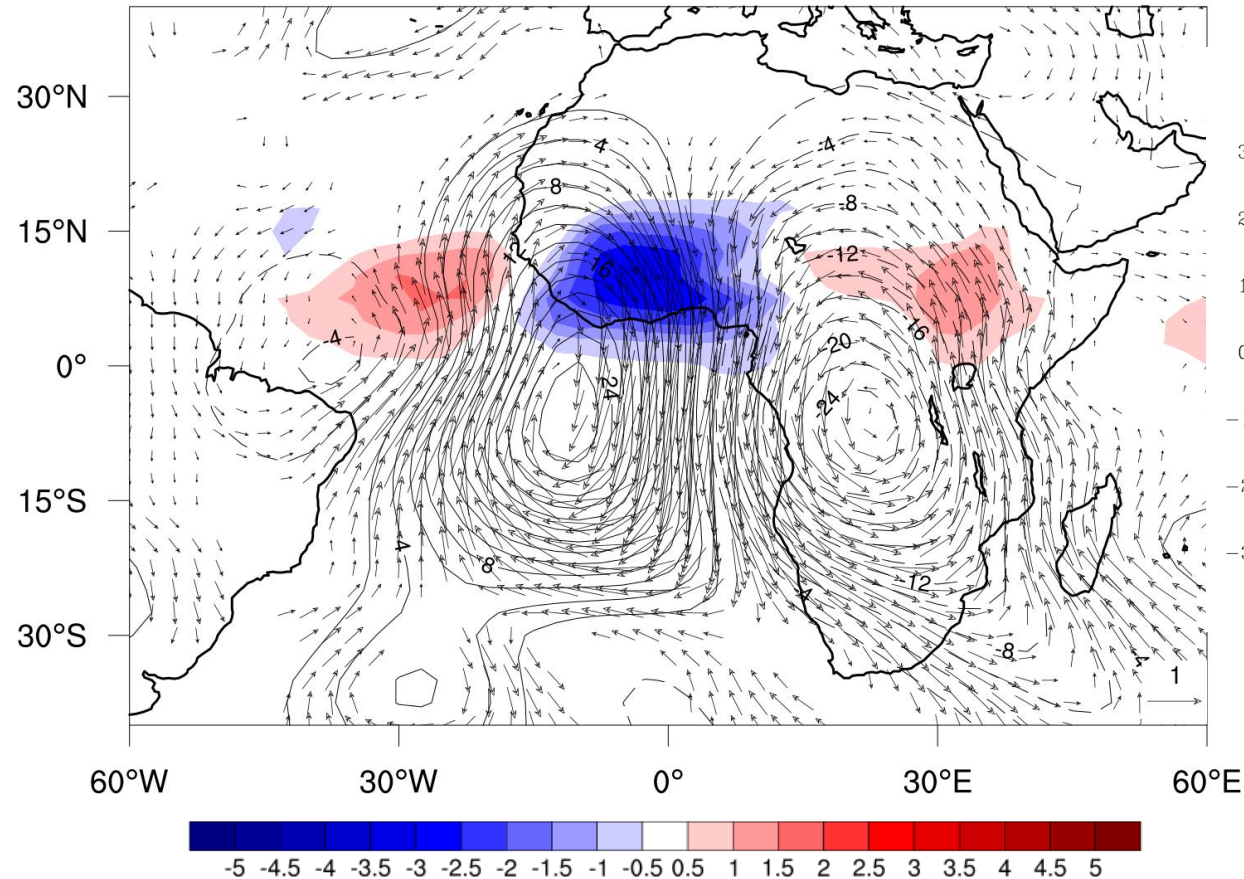
v200 EOF

2-6-day-filtered meridional wind at 200 hPa

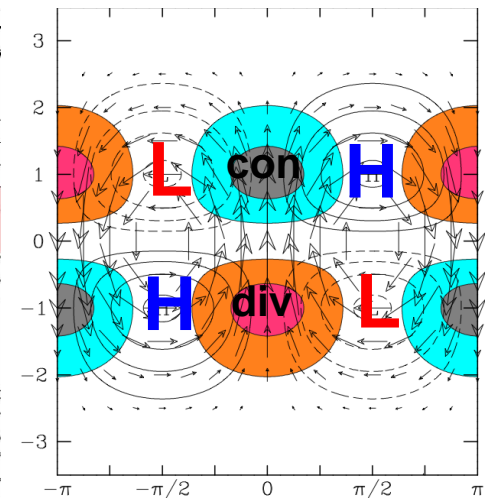
Domain: 5S-5N, 40W-40E

v200 EOF Structure

Day 0



Theoretical MRG structure

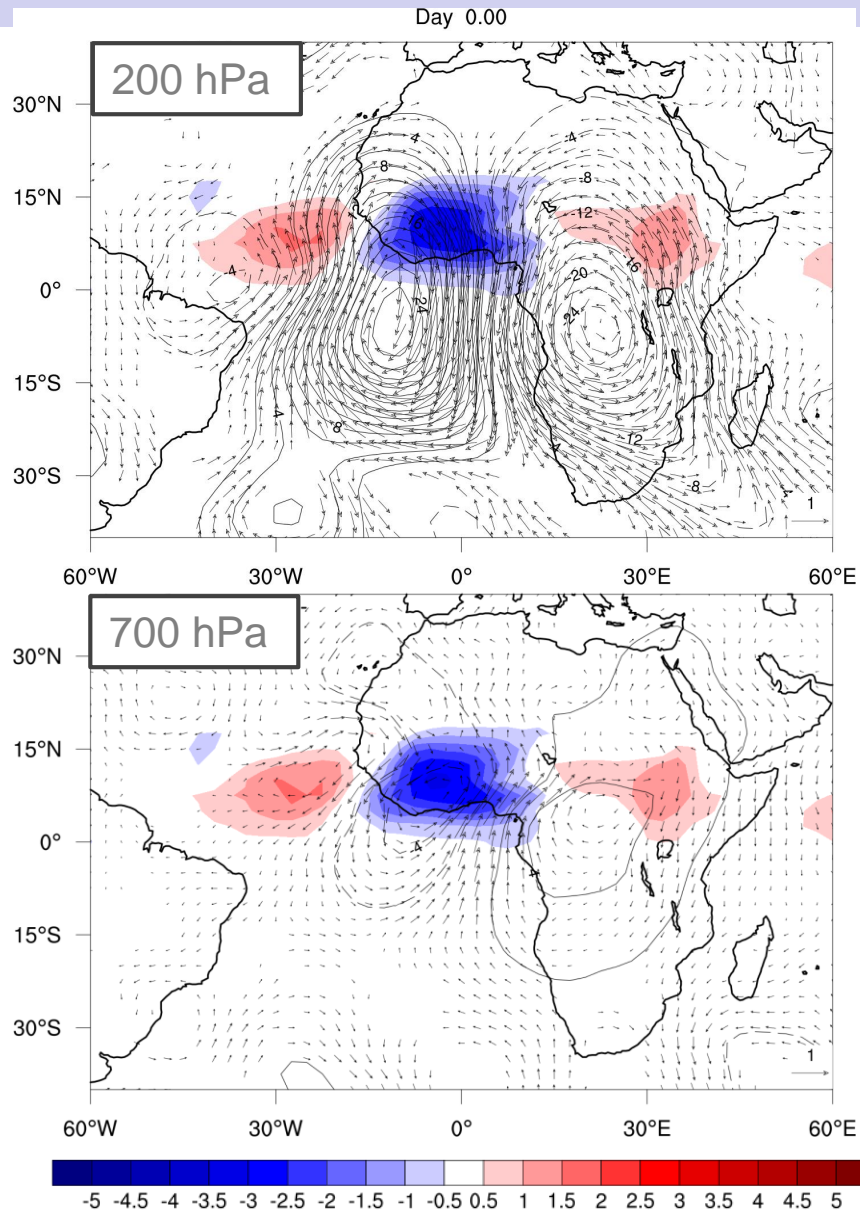


Kiladis et al. (2016)

T_b (shadings, K), 200-hPa wind (m s^{-1}) and streamfunction (contours, $2 \times 10^5 \text{ m}^2 \text{ s}^{-2}$)

A coherent MRG structure in both convective and kinematic fields

Vertical Structure of v200 EOF

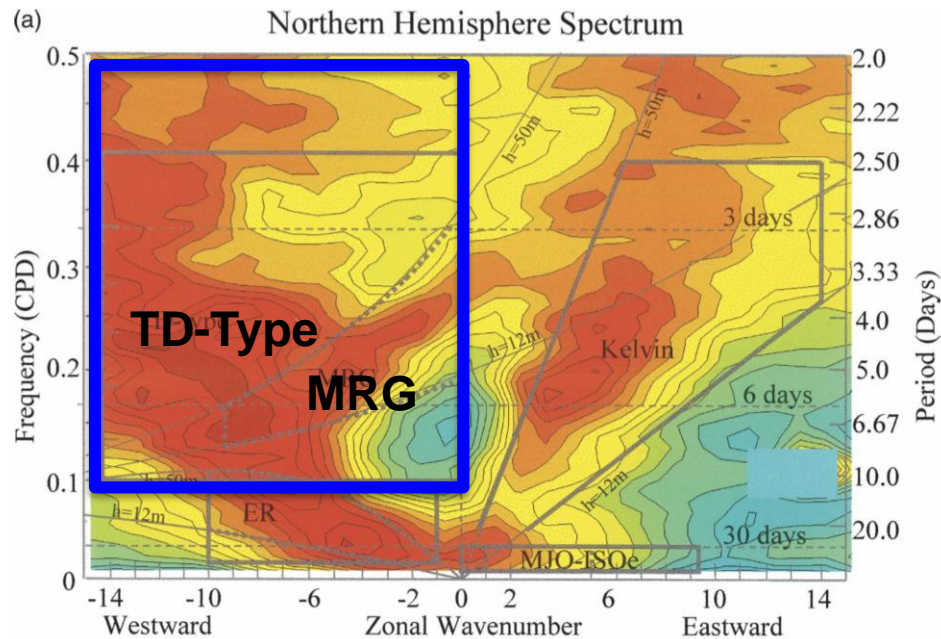


- A hint of AEW structure is seen at the mid-lower levels
- Upper-level MRGs may modulate the structure of AEW.
- Could MRGs explain some of the observed larger scale AEWs?

T_b (shadings, K), wind (m s^{-1}) and streamfunction (contours, $2 \times 10^5 \text{ m}^2 \text{ s}^{-2}$)

AEW-MRG Hybrid

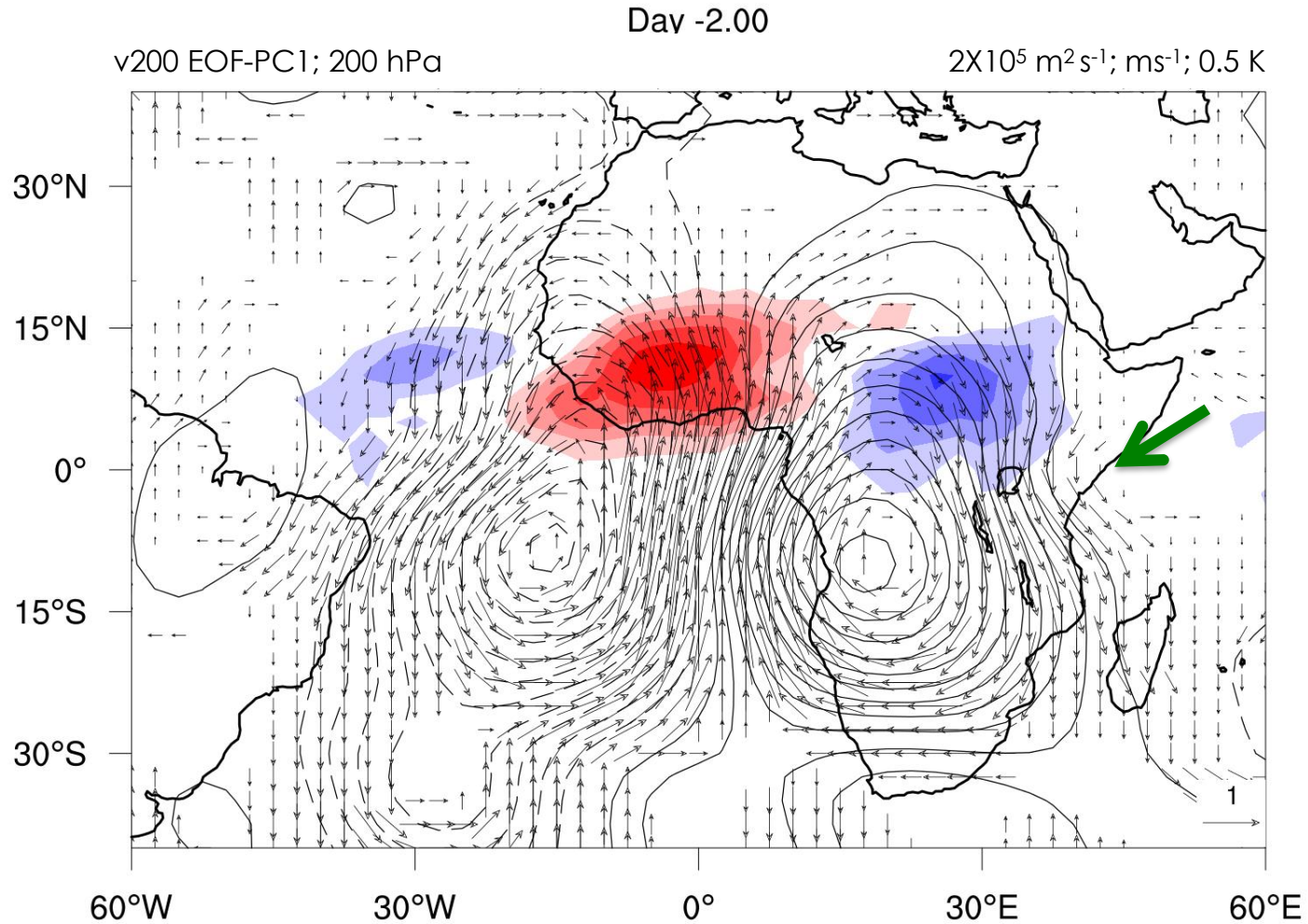
- The results highlight the coexistence of AEWs and MRGs across the Africa-Atlantic sector.



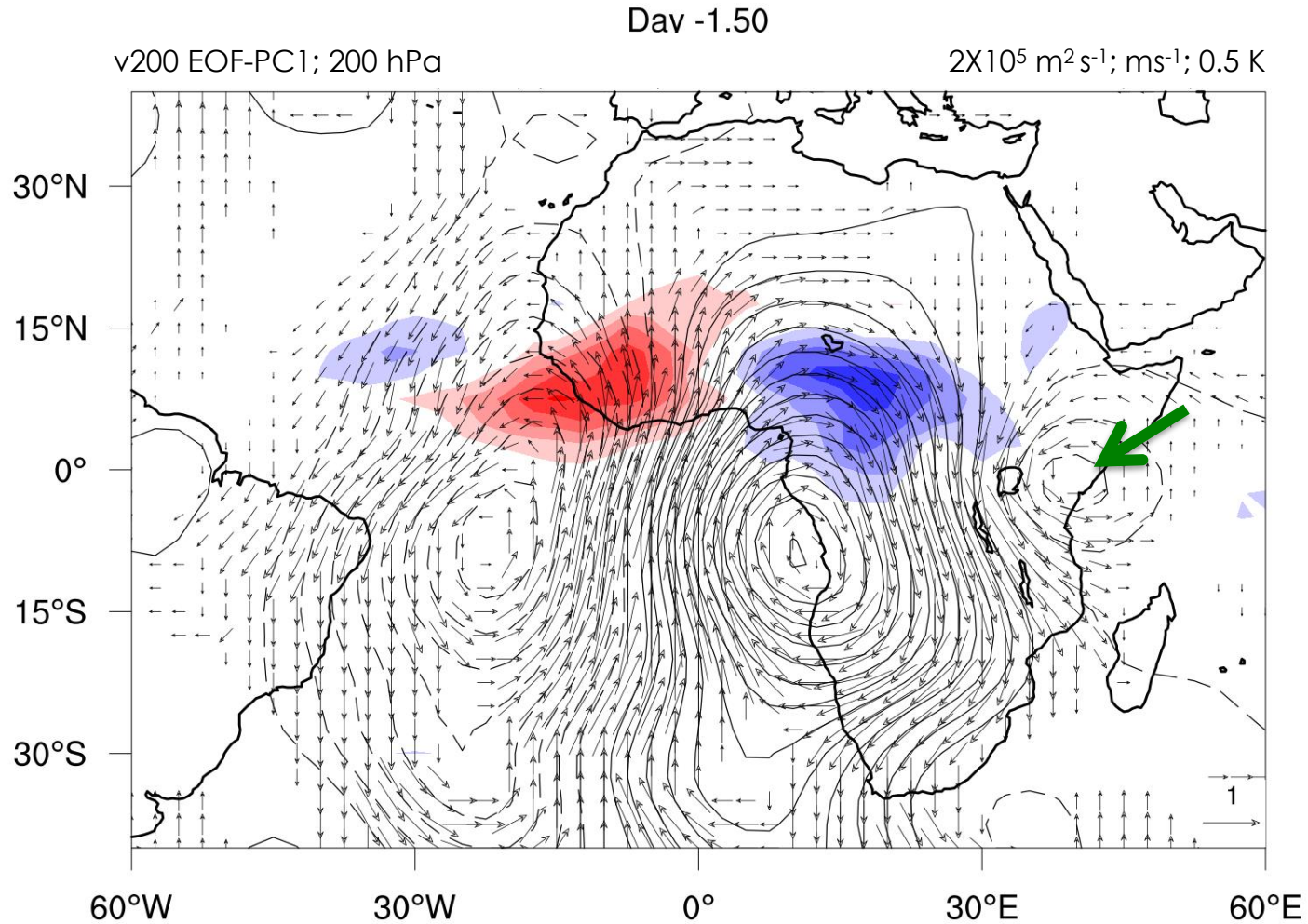
Frank and Roundy (2006)

- What is the origin of the MRG over Africa?

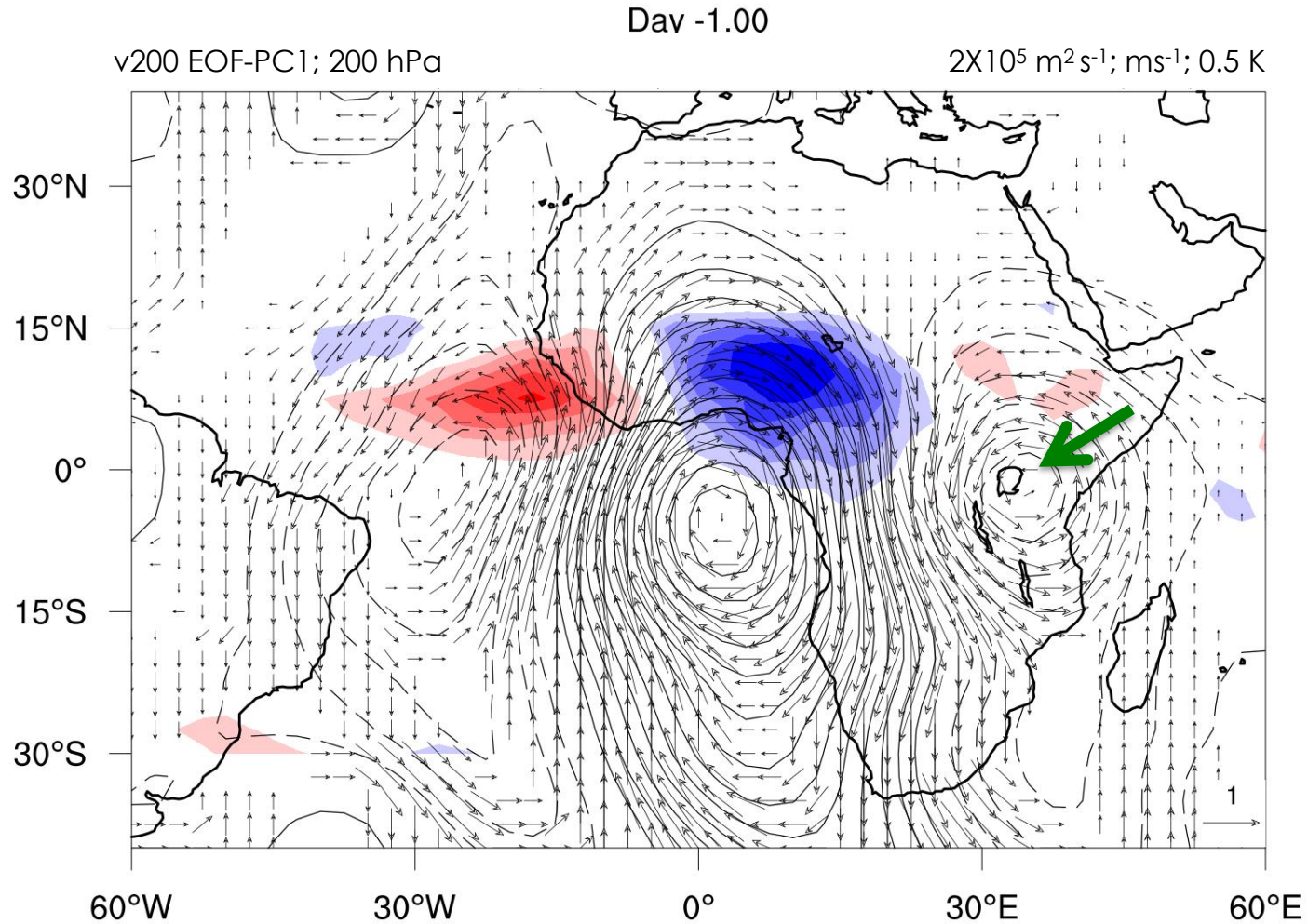
v200 EOF (upper-level MRG)



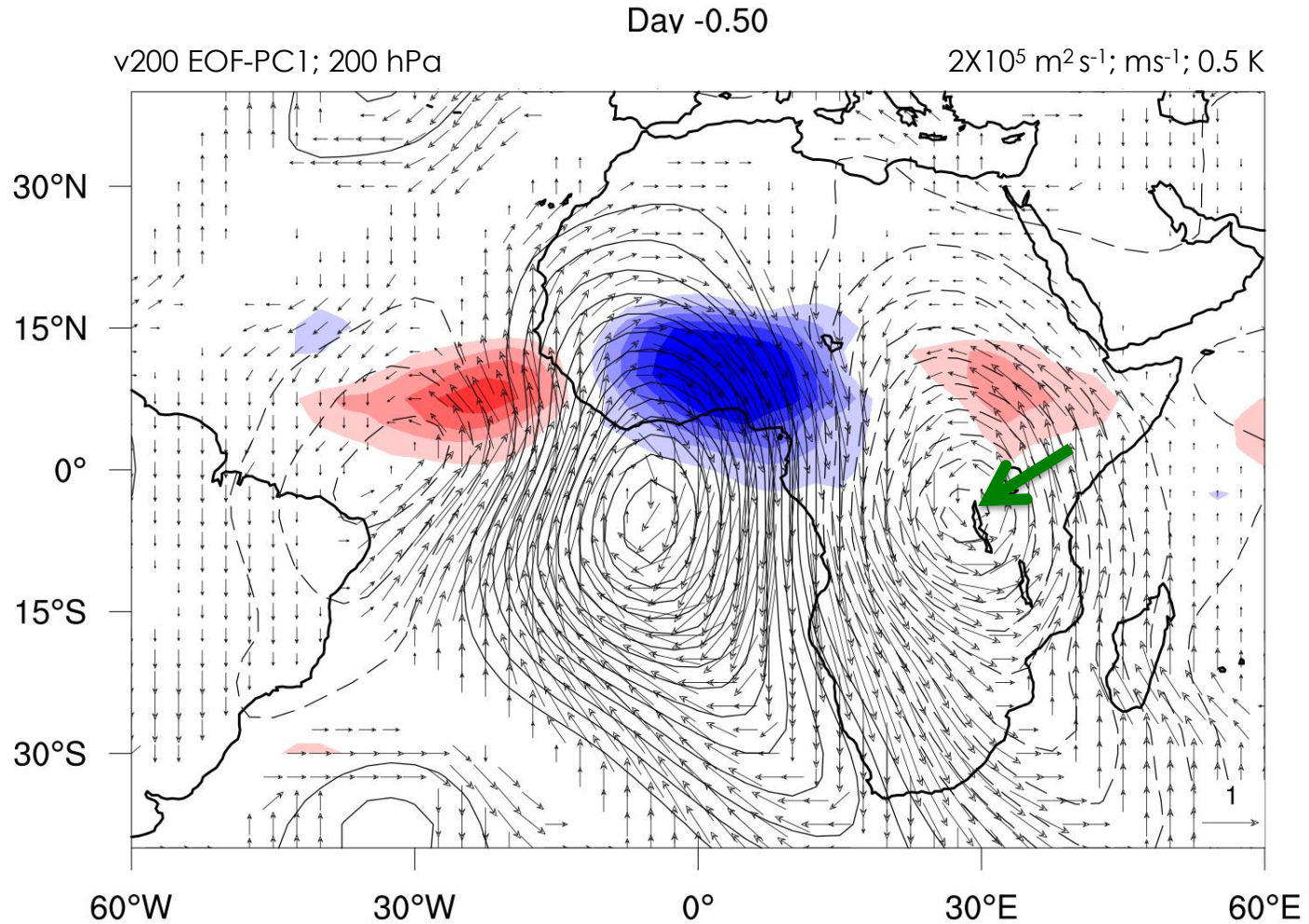
v200 EOF (upper-level MRG)



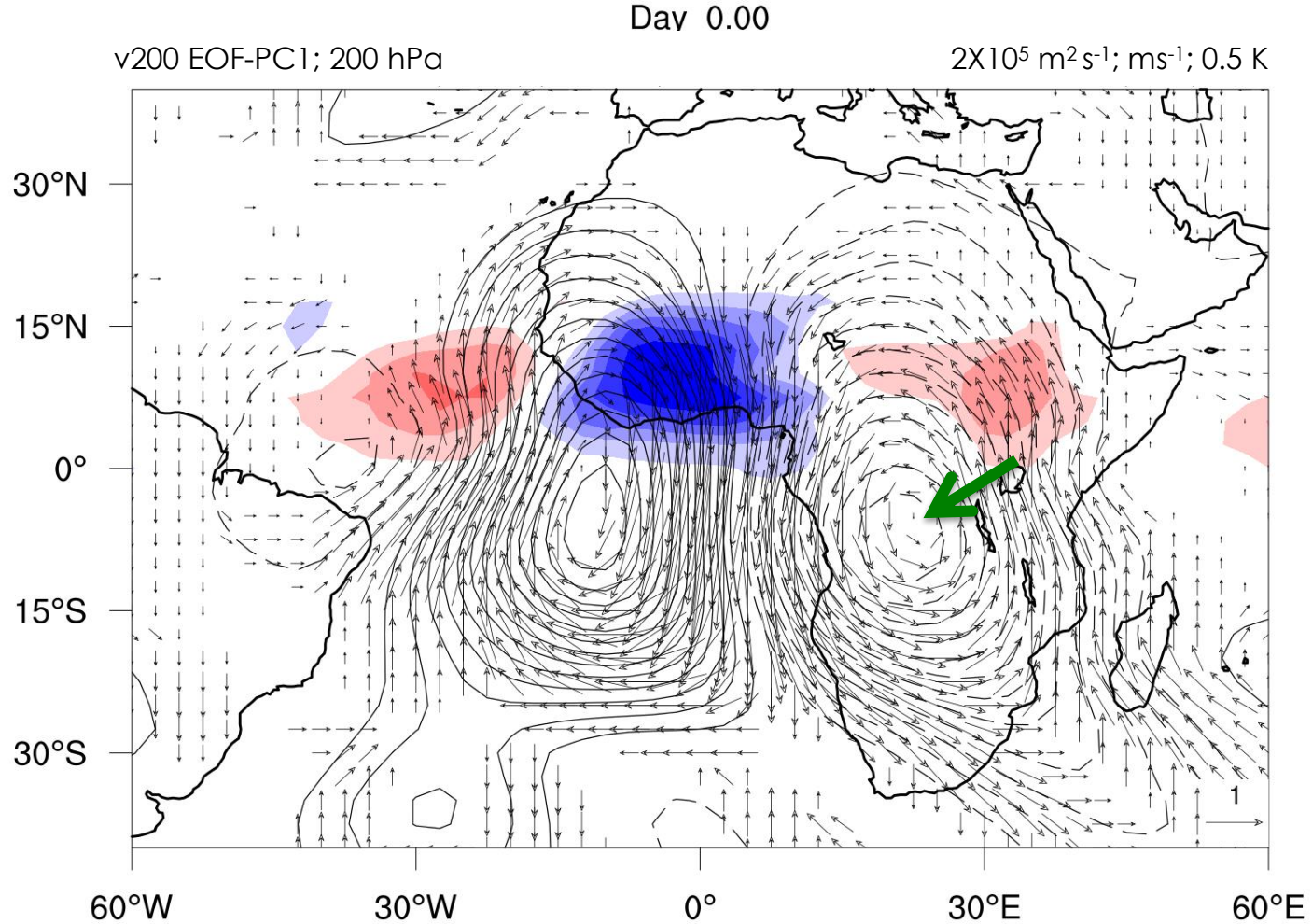
v200 EOF (upper-level MRG)



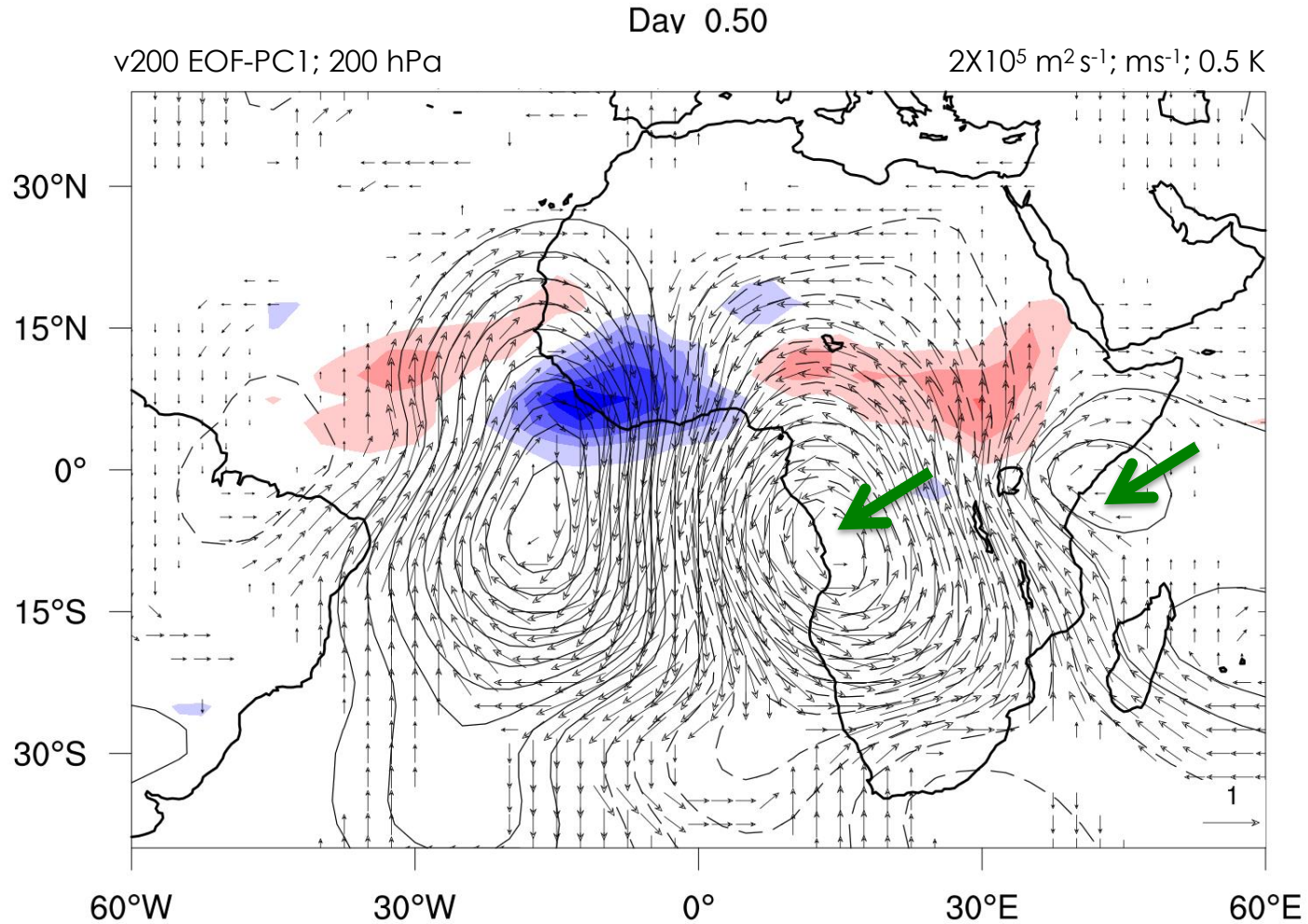
v200 EOF (upper-level MRG)



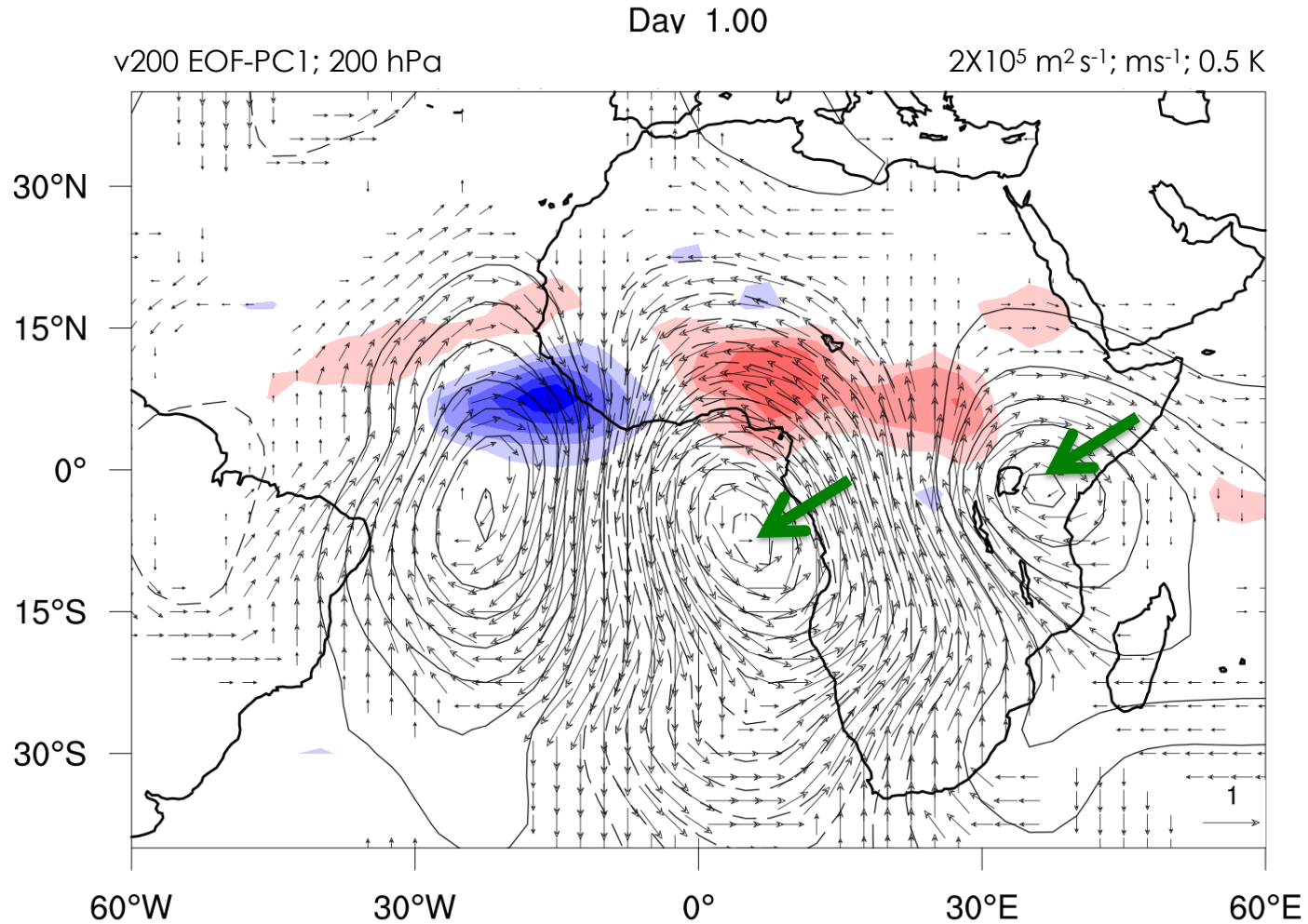
v200 EOF (upper-level MRG)



v200 EOF (upper-level MRG)



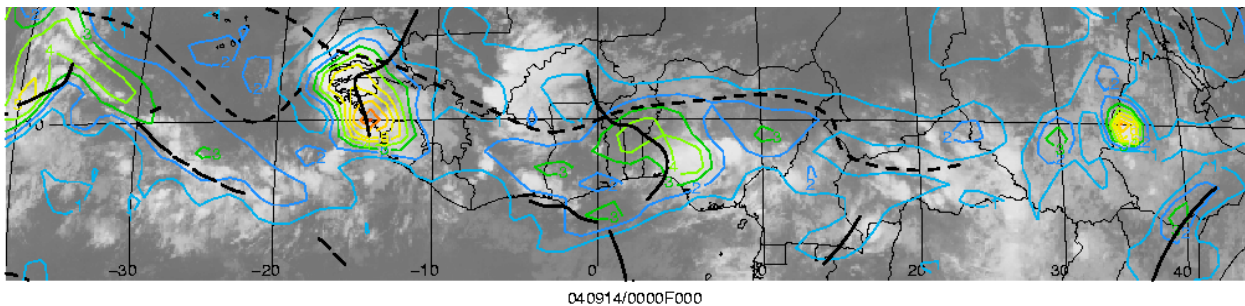
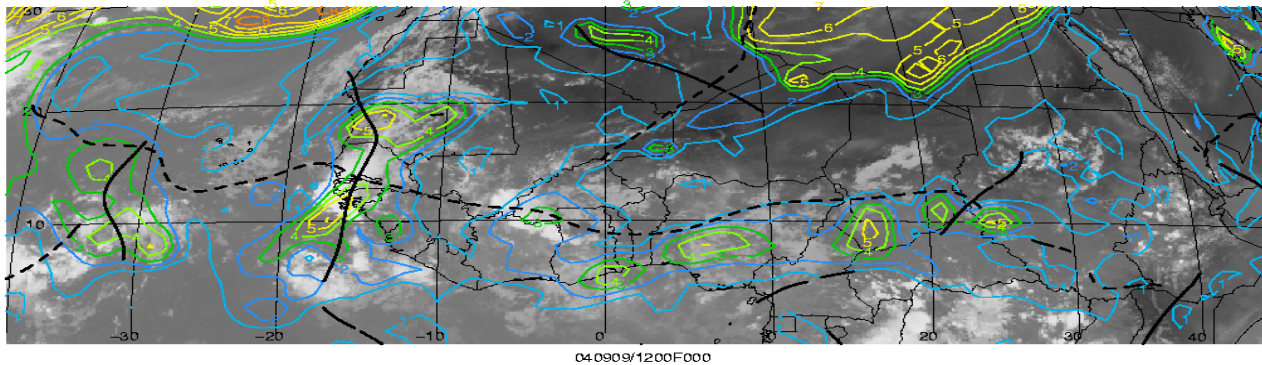
v200 EOF (upper-level MRG)



3. AEW-TC Relationship

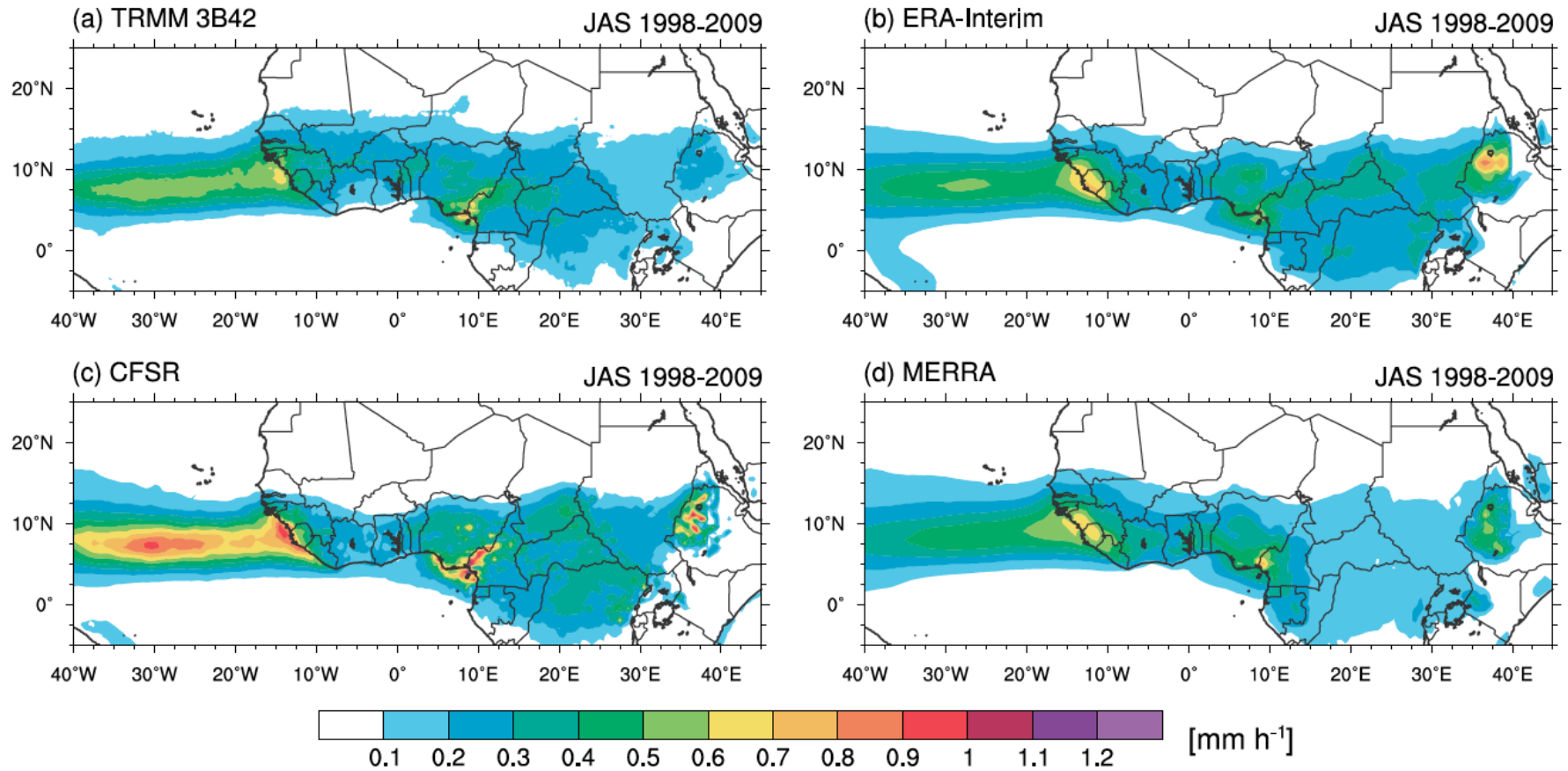
Most AEWs do not trigger Tropical Cyclones.

Most TCs develop in association with AEWs – but which one?

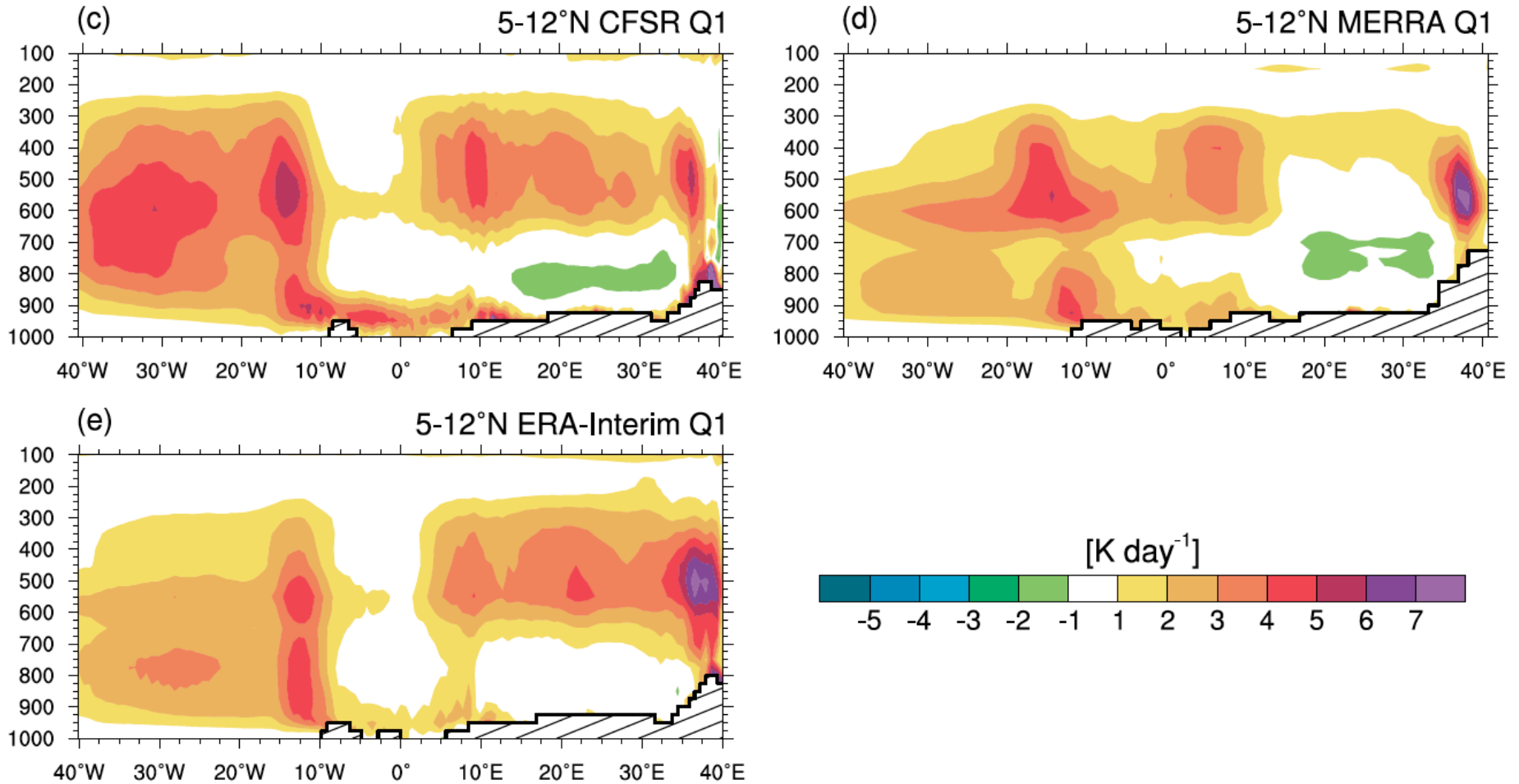


Regional Variations in African Easterly Wave Structures

Janiga and Thorncroft (2013)

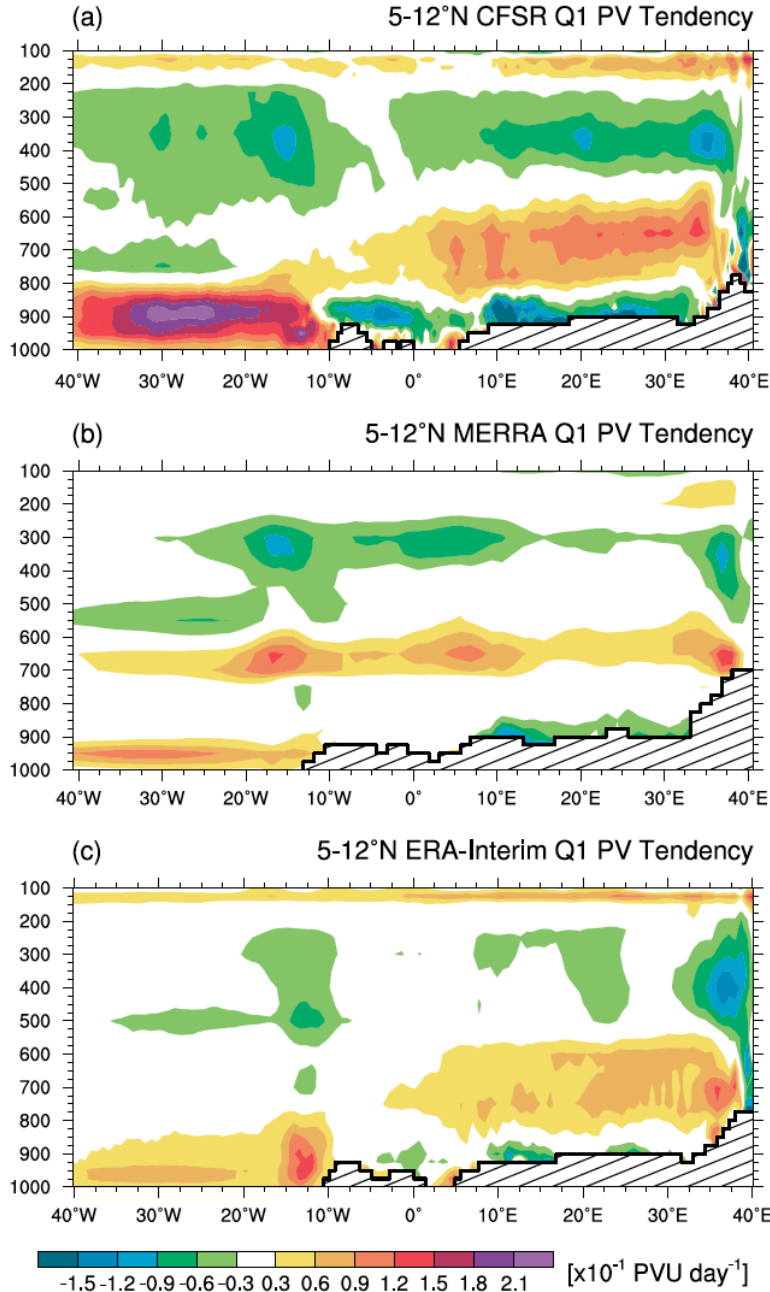


Zonal Variations in Diabatic Heating



Notable E-W variations in heating rates and profiles are seen in the reanalyses

Zonal Variations in PV Tendency



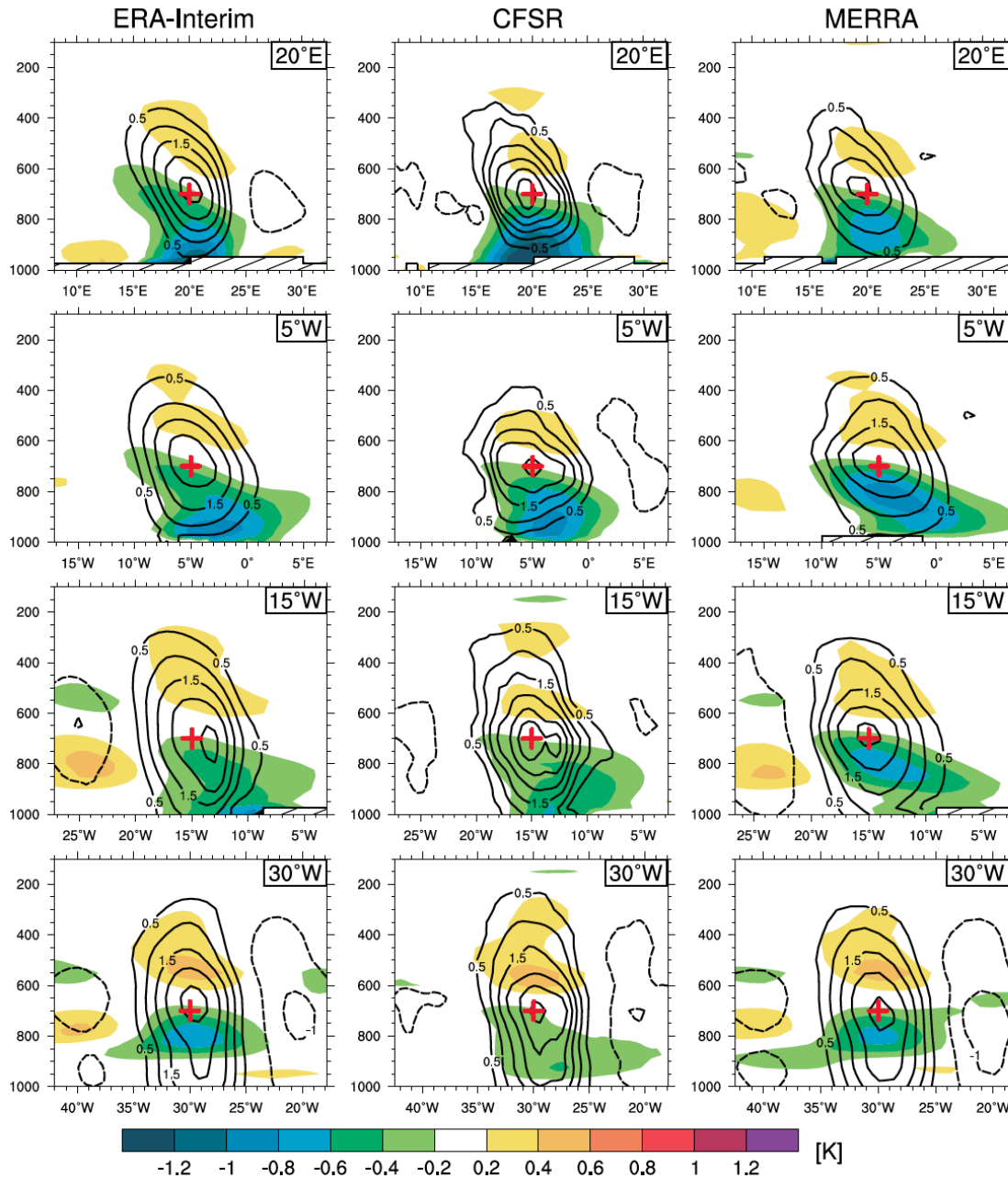
Consistent with the variability in heating rate profiles there are marked E-W variations in PV tendencies

Note following general characteristics:

- Positive mid-level PV generation between 40E and GM.
- Weaker PV tendencies between GM and coast.
- Increased positive PV tendencies at low-levels over ocean.

We expect this to impact AEW structures

Zonal Variations in AEW Structures



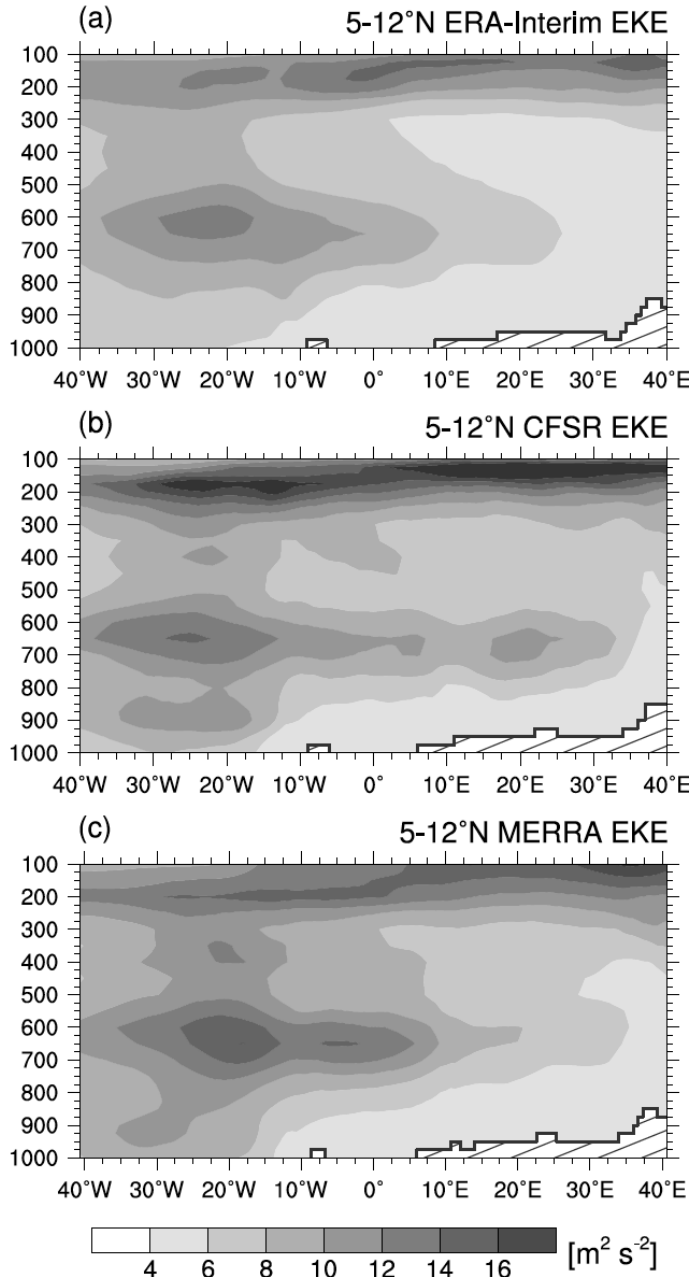
Note marked changes in AEW structure between E and W Africa and the Atlantic

Especially weakened intensity of cold core and development of low-level circulations

Variability in such processes may impact probability of downstream tropical cyclogenesis

Zonal Variations in EKE

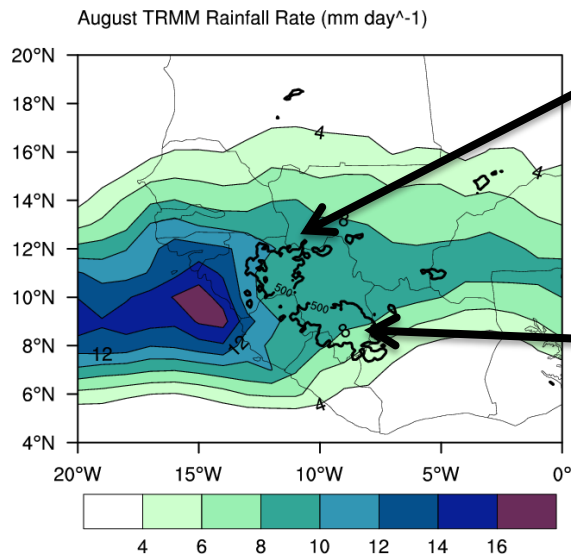
Rapid change in vertical structure occurs as AEWs reach the coastal region.



Importance of Guinea Highlands

- Marked transition takes place close to Guinea Highlands and Coastal region
- AEWs are often invigorated as they pass these regions – especially at low-levels
- May influence tropical cyclogenesis probabilities

Fouta Djallon Highlands ~914m



The Nambia Range ~460m

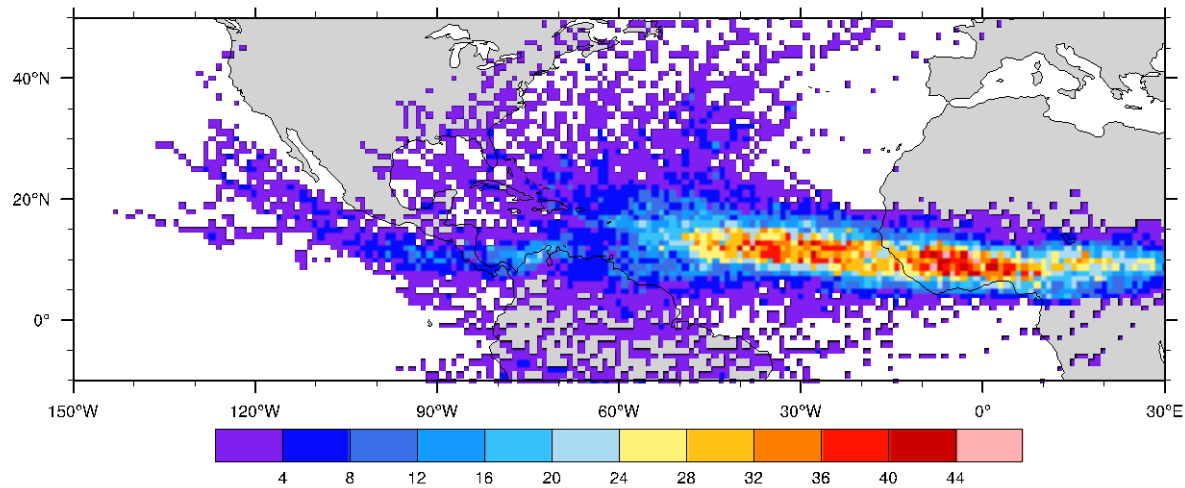
Deep convective bursts over West African coastline feedback on trough increasing vorticity for developing waves (Ross & Krishnamurti 2009,2012)

Widespread deep convection over coast more important than small intense convection (Leppert et al 2013)

Horizontal flux of moist enthalpy important for sustained MCSs moving off the coast (Arnault & Roux 2009,2010)

TPW, Precipitation, SST, 1000-600 hPa Vertical shear among best predictors for developing / non-developing systems over Atlantic (Peng et al 2012)

AEW trough tracks



Count per 0.5° grid of all waves/ storms originating from Africa tracked over 1979-2012 tracked at 700 hPa.
Developing cases classified as TD+ by 45° W

Brammer and Thorncroft 2015

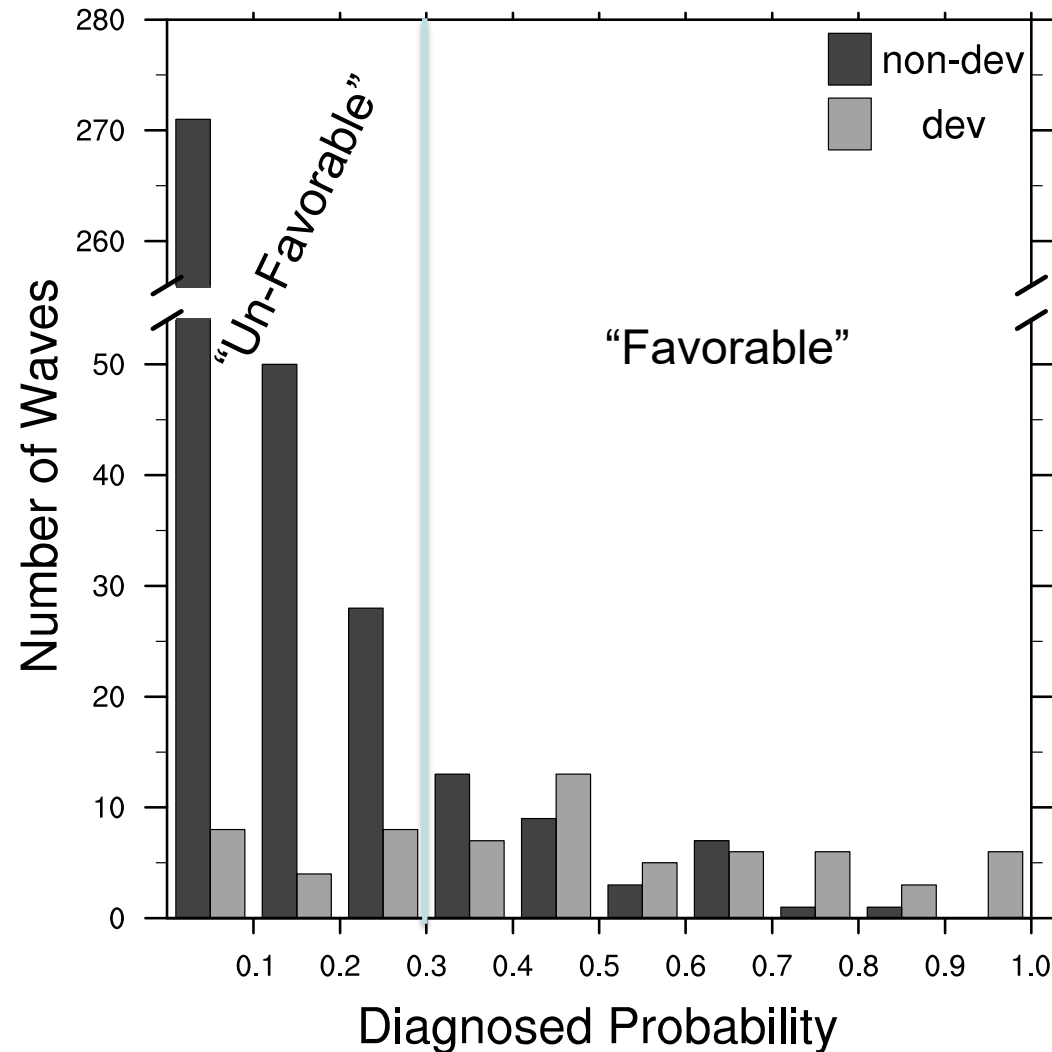
AEW Genesis Diagnostic

Statistical Predictors	Synoptic Predictors	IR predictors
<p>Julian day - 239¹²³ (Peak Day of AEWs) Latitude of system Total Phase Speed of wave Meridional Phase Speed Zonal Phase Speed 850RV 5° longitude tendency³</p>	<p>850:700 hPa Specific Humidity</p> <p>600 hPa Relative Humidity</p> <p>Relative Vorticity (RV) 850 hPa¹² RV 850:600 hPa layer average RV 600-850 hPa difference 400:200 hPa Temp Anom¹² 200 hPa Divergence 300:200 hPa Divergence² Vertical Velocity 800:300 hPa¹² Deep Vertical Shear 200-850 hPa Mid. Vertical Shear 500-850 hPa</p>	<p>Mean IR Brightness Temp</p> <p>Std. Dev. IR Minimum IR Area less than 240 K¹³ Area less than 220 K Mean IR 24 to 0 hours before coast³ Minimum IR -24:0 hr Area less than 240 K -24:0 hr Area less than 220 K -24:0 hr</p>

A logistic regression model was used to find the best combination of AEW-factors to describe the probability of genesis

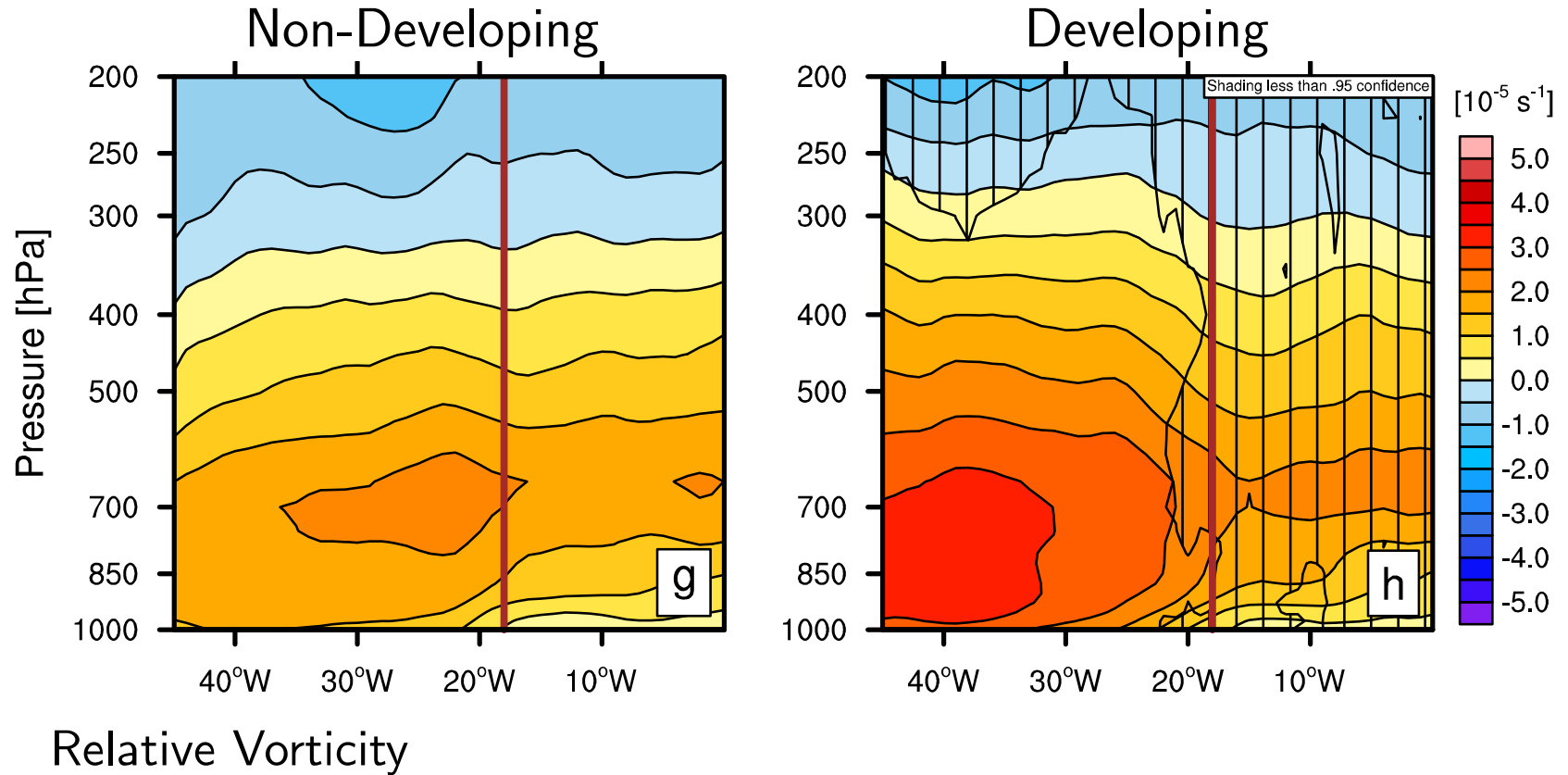
Brammer and Thorncroft 2015

Composite differences in favorable waves



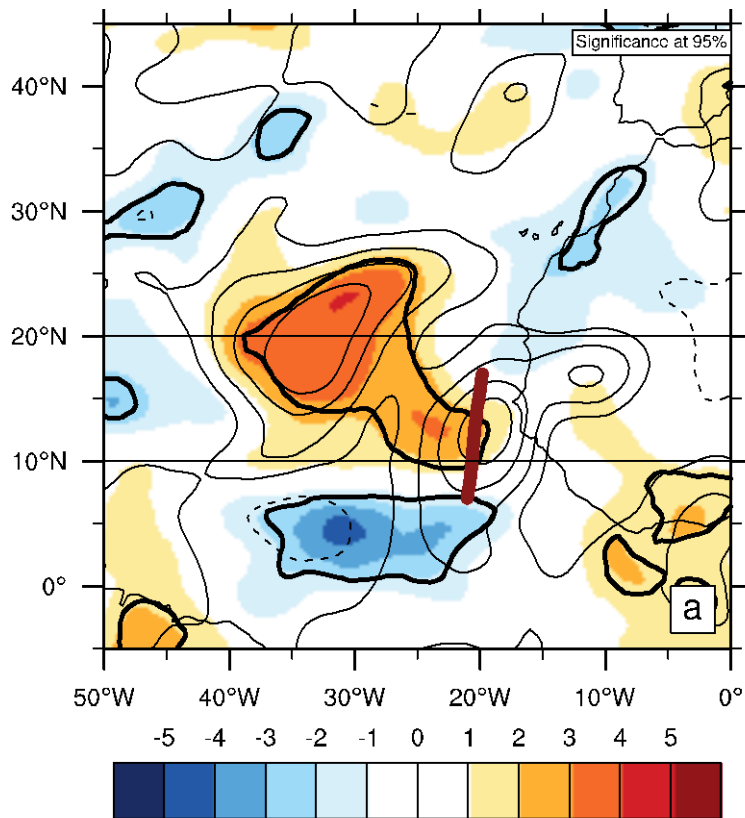
- Most non-developing waves are diagnosed as very unfavorable.
- Take the top 55, diagnostic $\sim 0.27+$

“Favourable” AEW evolution



Day 0

Developing – Non-developing AEWs

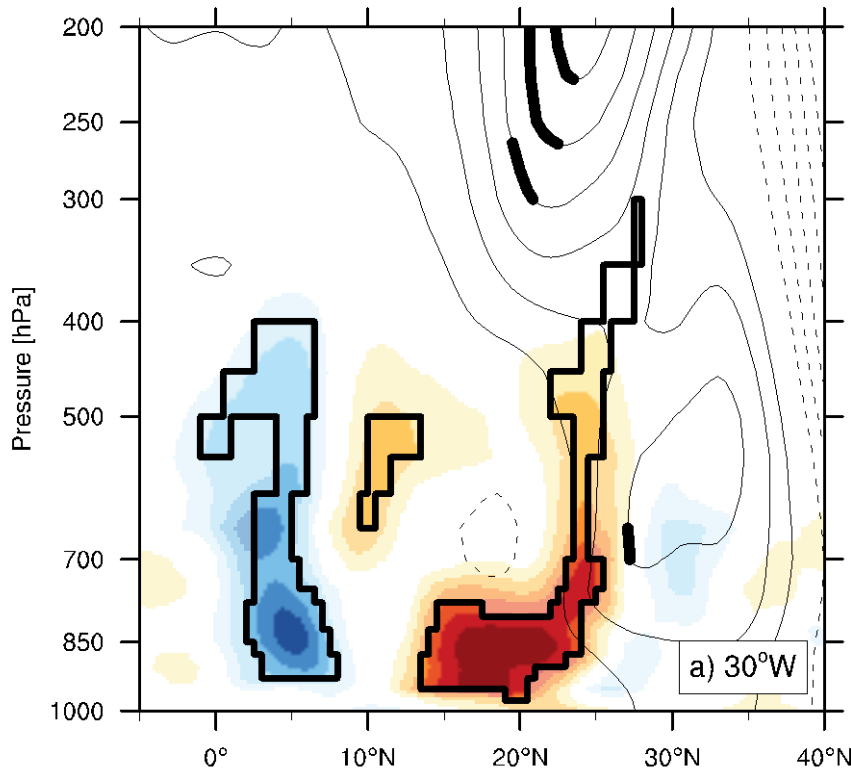


Total Precipitable Water [mm]

- Developing Waves have increased moisture to west and northwest of trough after leaving coast
- Non-developing waves have increased moisture near equator, due to horizontal tilt of trough.

Day 0

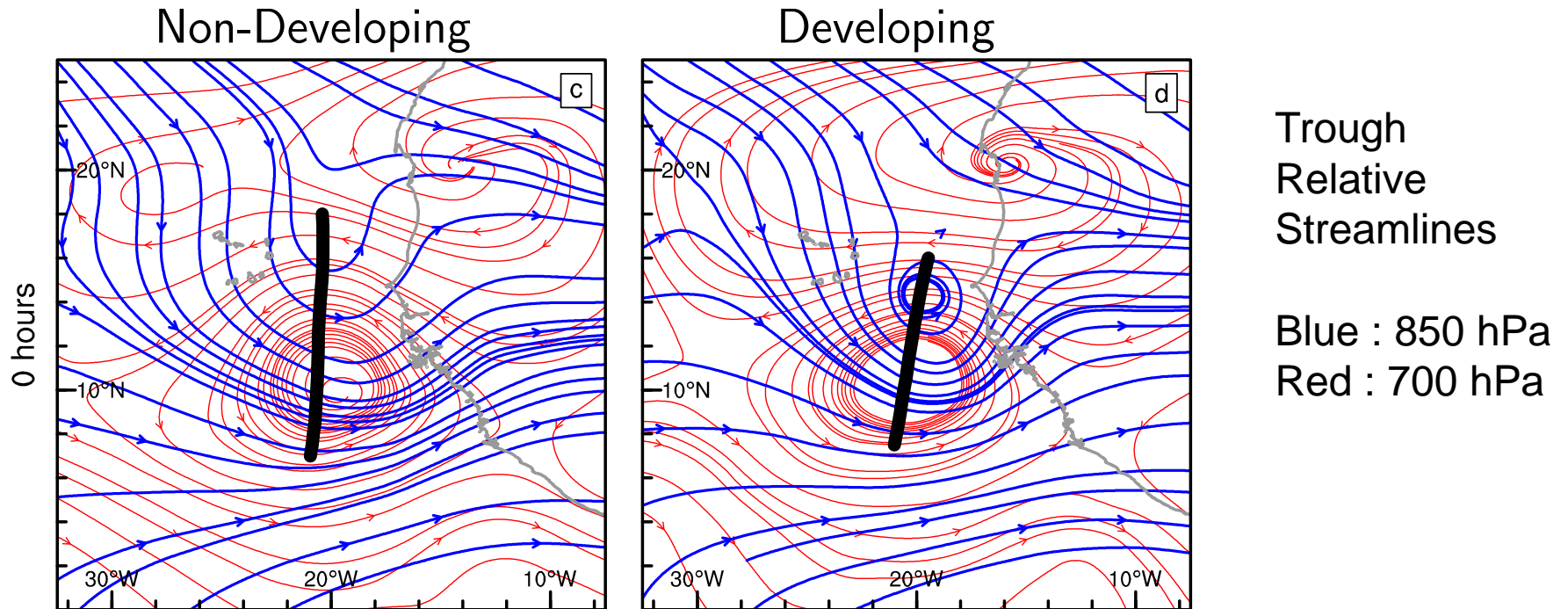
Developing – Non-developing AEWs



Latitude-height cross section of anomalous specific humidity and geopotential height along 30°W

- Moisture to northwest of trough significant at low levels (850 hPa) between 15-25°N

Relative Inflow for AEWs



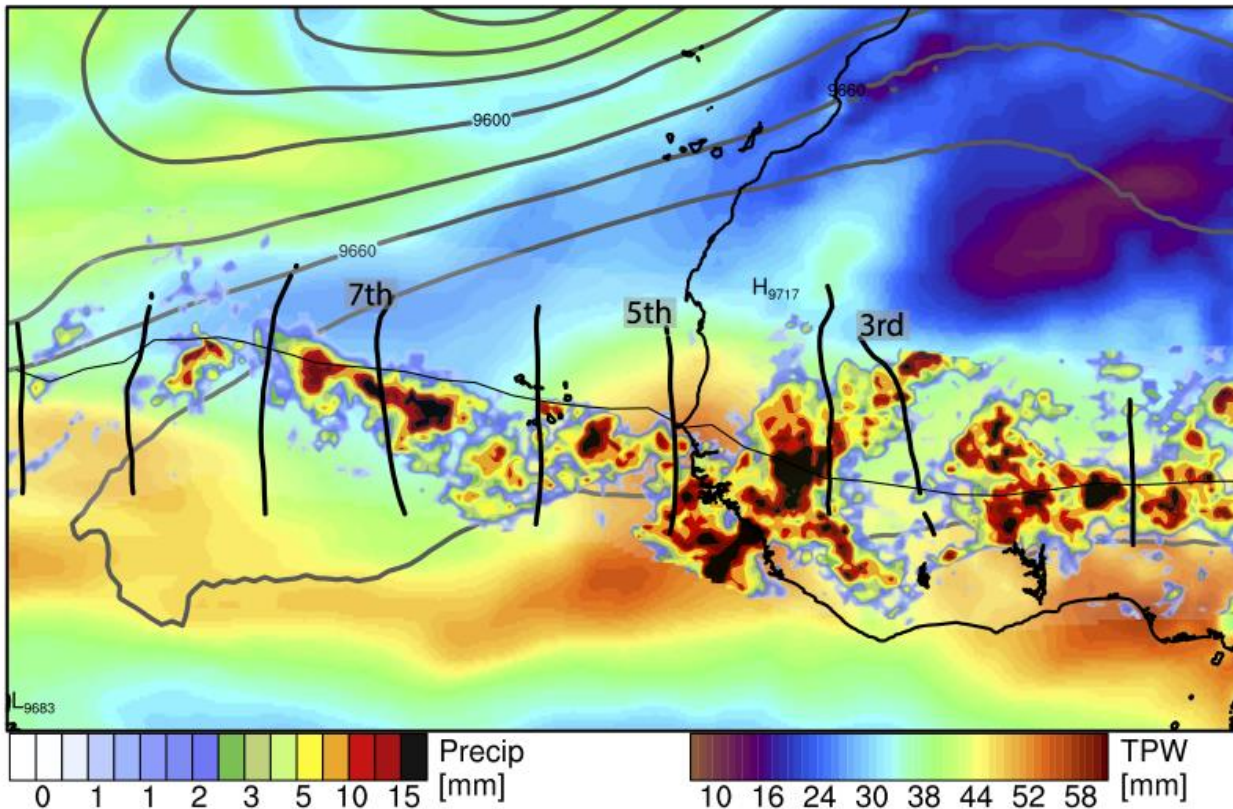
Analysis of two “Favourable” AEWs

	AL90 2014	Hurricane Leslie 2012
Coast Date	September 4th	August 26th
NHC Genesis %	50%	0 (10% 24 h later)
Days to Genesis		3.5
NW low-level	Dry	Moist
NW jet-level	Dry	Dry
AEW diagnostic	Marginal	Favourable

Analysis of two “Favourable” AEWs

	AL90 2014	Hurricane Leslie 2012
Coast Date	September 4th	August 26th
NHC Genesis %	50%	0 (10% 24 h later)
Days to Genesis		3.5
NW low-level	Dry	Moist
NW jet-level	Dry	Dry
AEW diagnostic	Marginal	Favourable

2014 Non-developing (AL90)

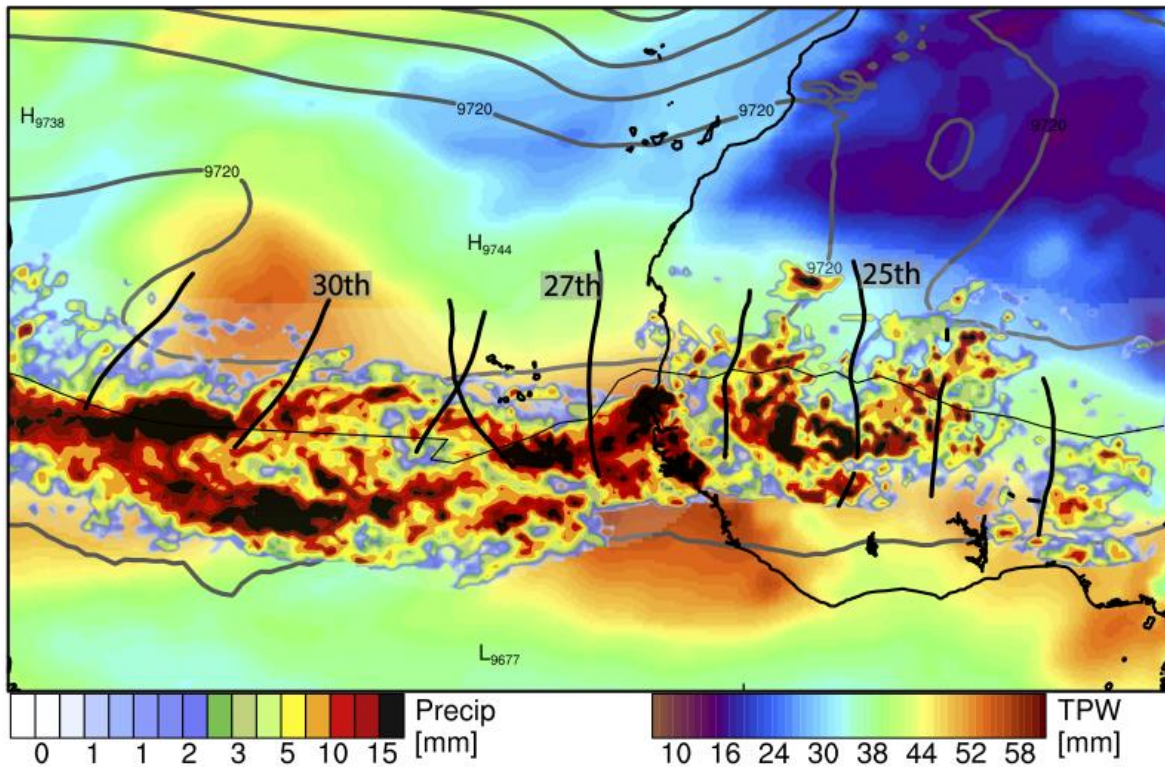


Accumulated precipitation within 750km of trough.

Trough axes every 24h

TPW and 300hPa geopotential height for 5th September 2014

2012 Pre-Leslie



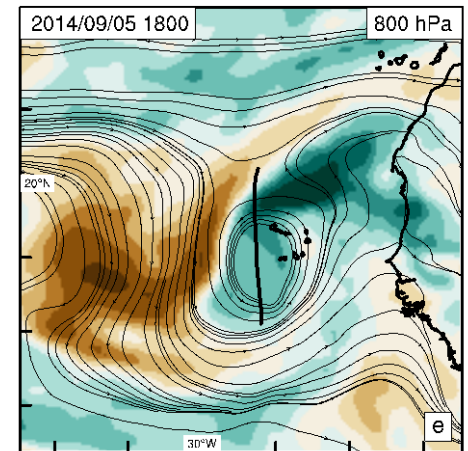
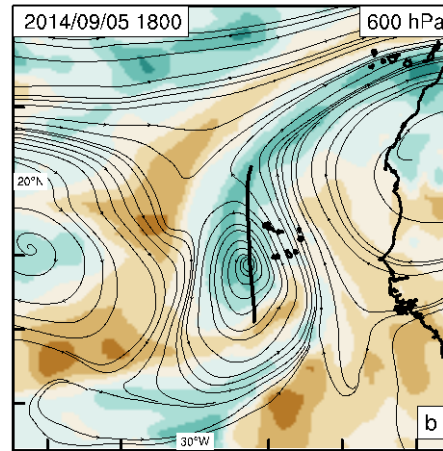
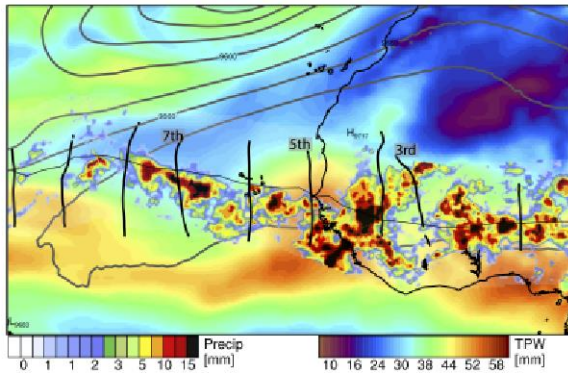
Accumulated precipitation within 750km of trough.

Trough axes every 24h

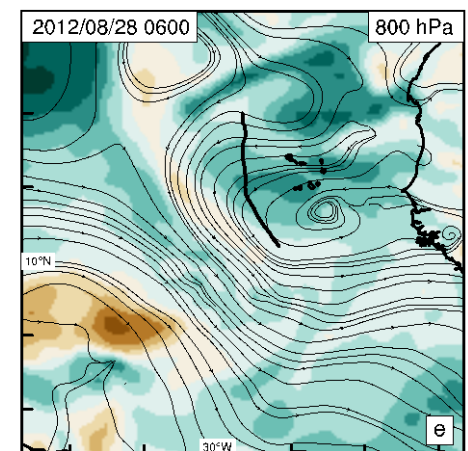
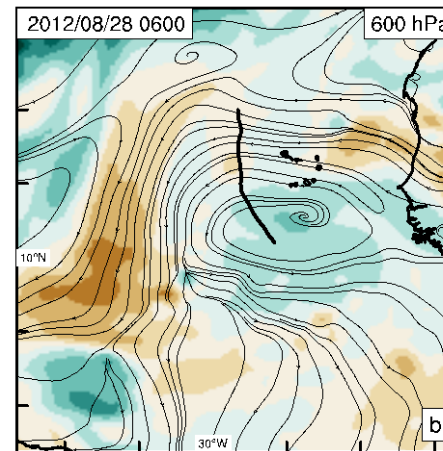
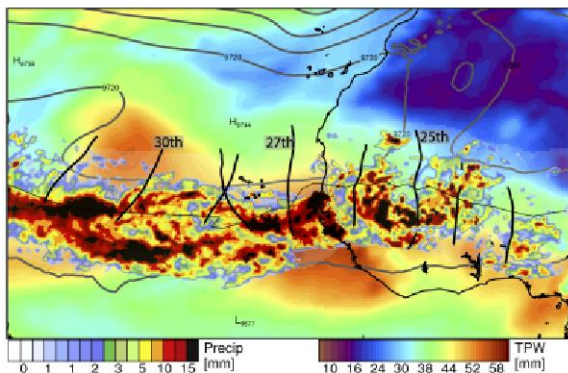
TPW and 300hPa geopotential height for 26th August 2012

AL90 /pre-Leslie comparison

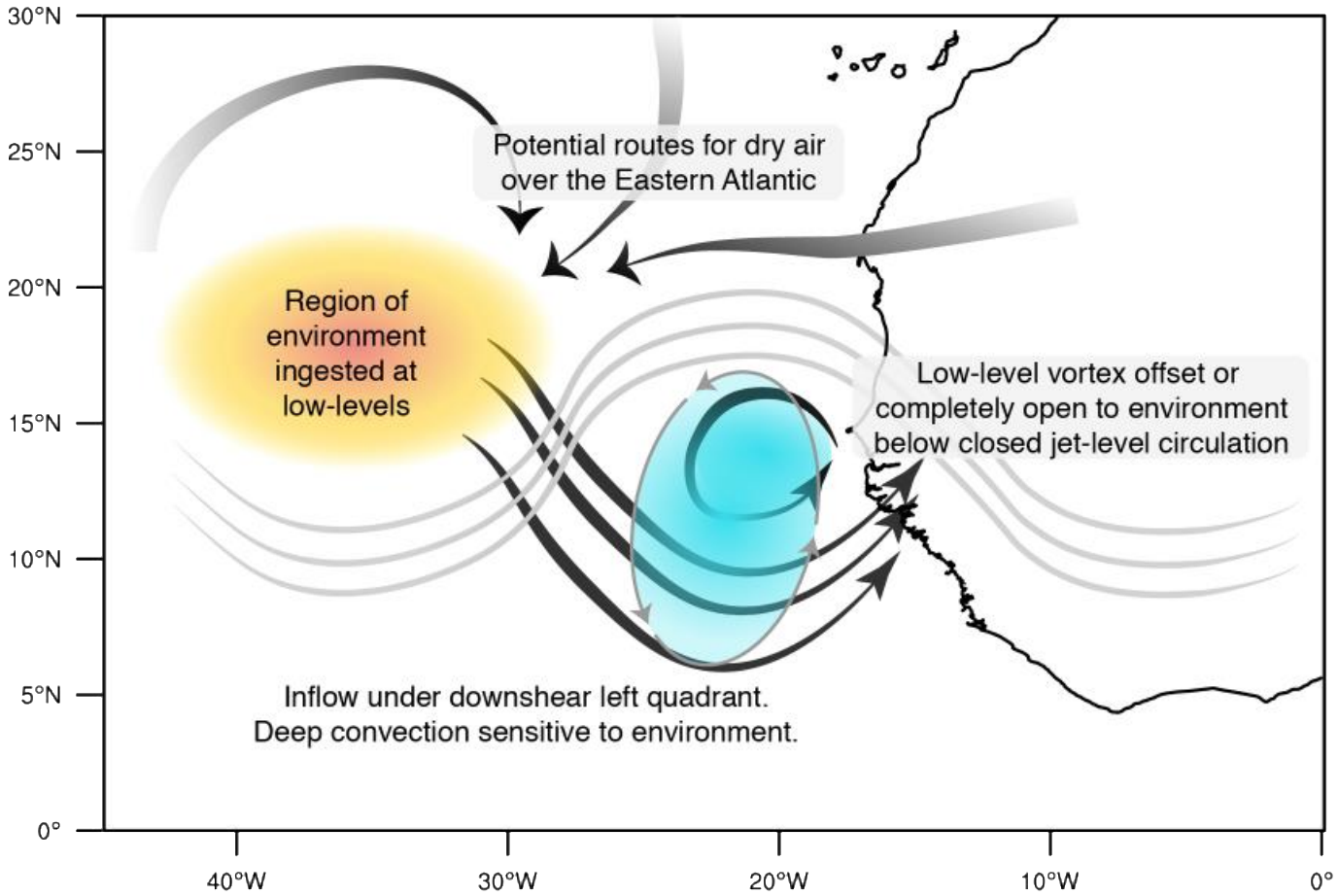
Non-Developing AL90



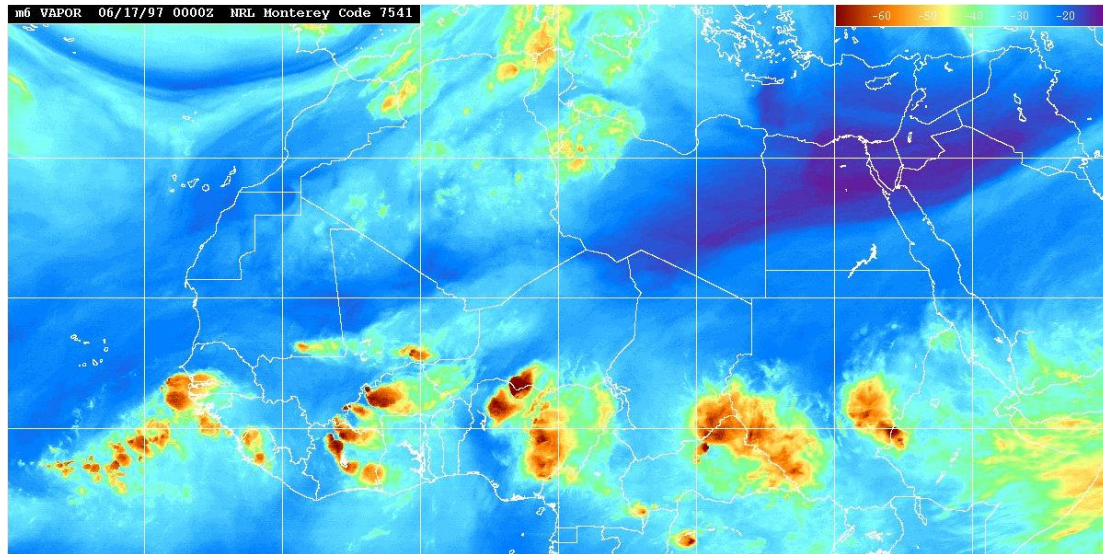
Developing pre-Leslie



Schematic

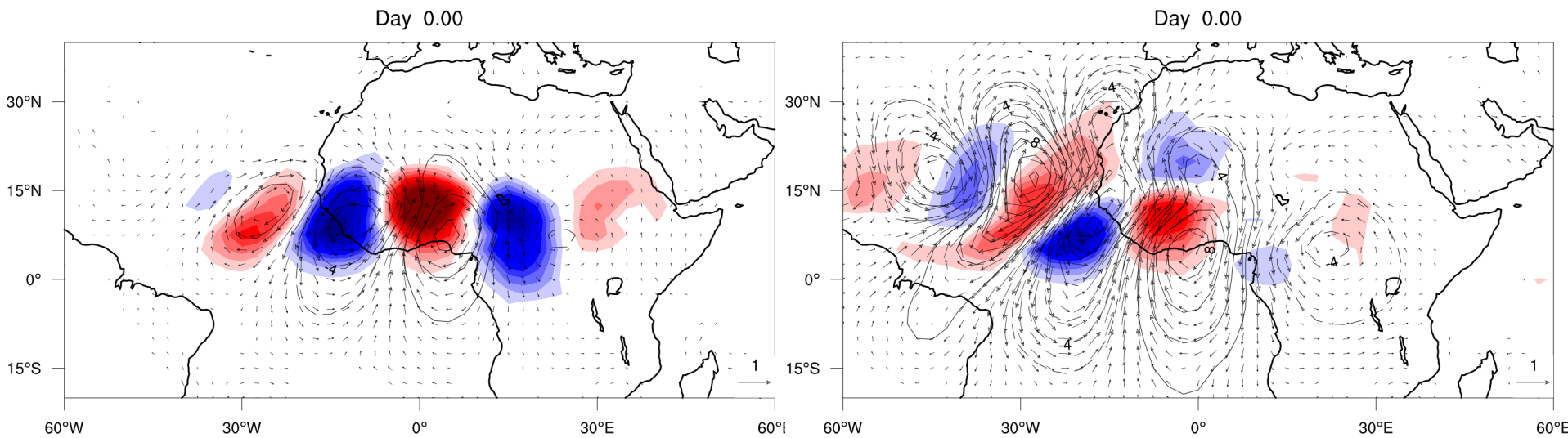


SUMMARY AND FINAL COMMENTS



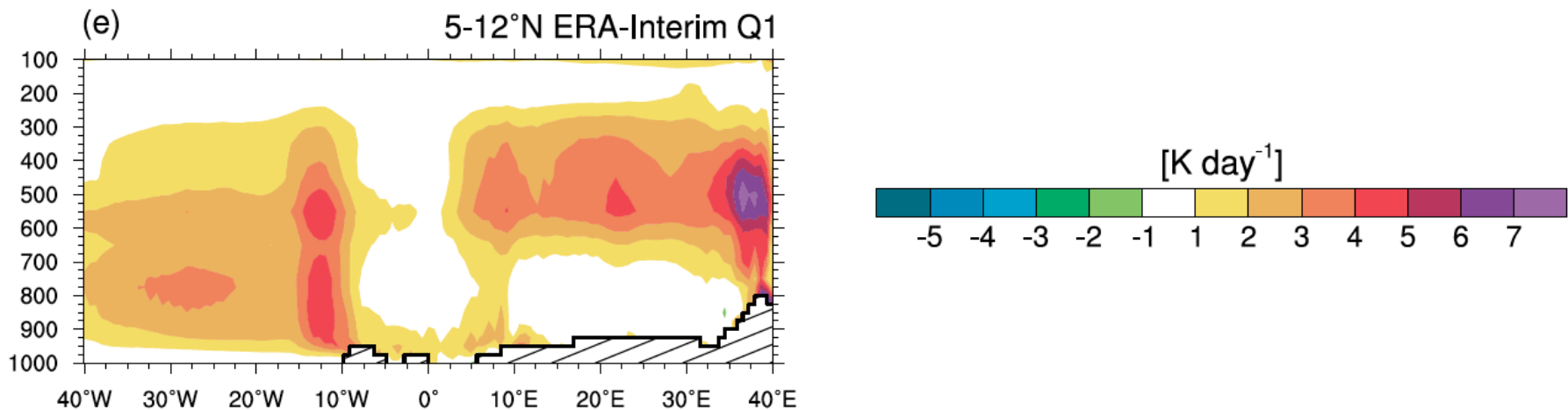
Two Types of AEW Behavior

- EOF Analysis has highlighted two types of AEW Behavior
- **AEW-Strongly Coupled with Convection:** Circulation closed coupled with convection, centered and confined around the ITCZ
- **AEW-MRG Hybrid:** broad meridional extent of the wave - interacting with Moroccan vortex and MRG
- More work needed on the origins of the MRG and MRG-AEW interactions



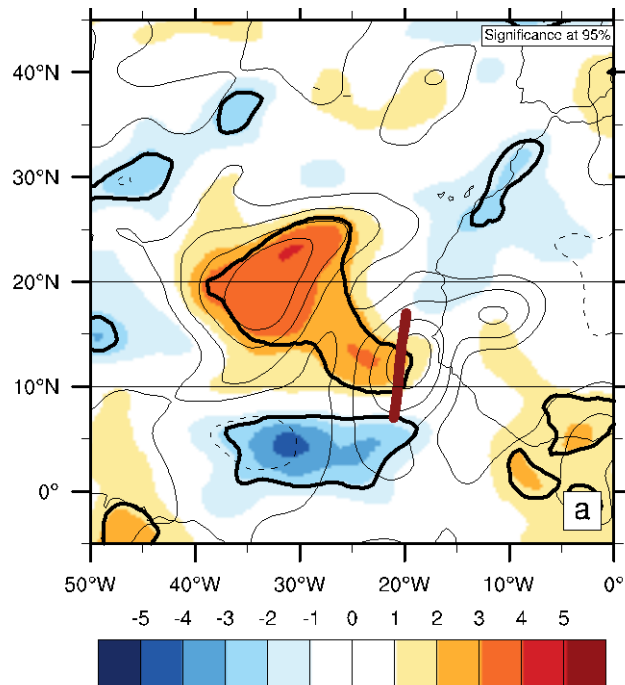
Regional Variations in AEW Structure

- There are marked variations in AEW structures as they propagate between the African continent and the ocean.
- AEWs intensify and develop low level circulations as they pass the Guinea Highlands and coastal region.
- These changes appear to be associated with changes in the type of convection and vertical profile in heating rate.
- Variability in these processes likely impacts probability of tropical cyclogenesis. But that is not the whole story!



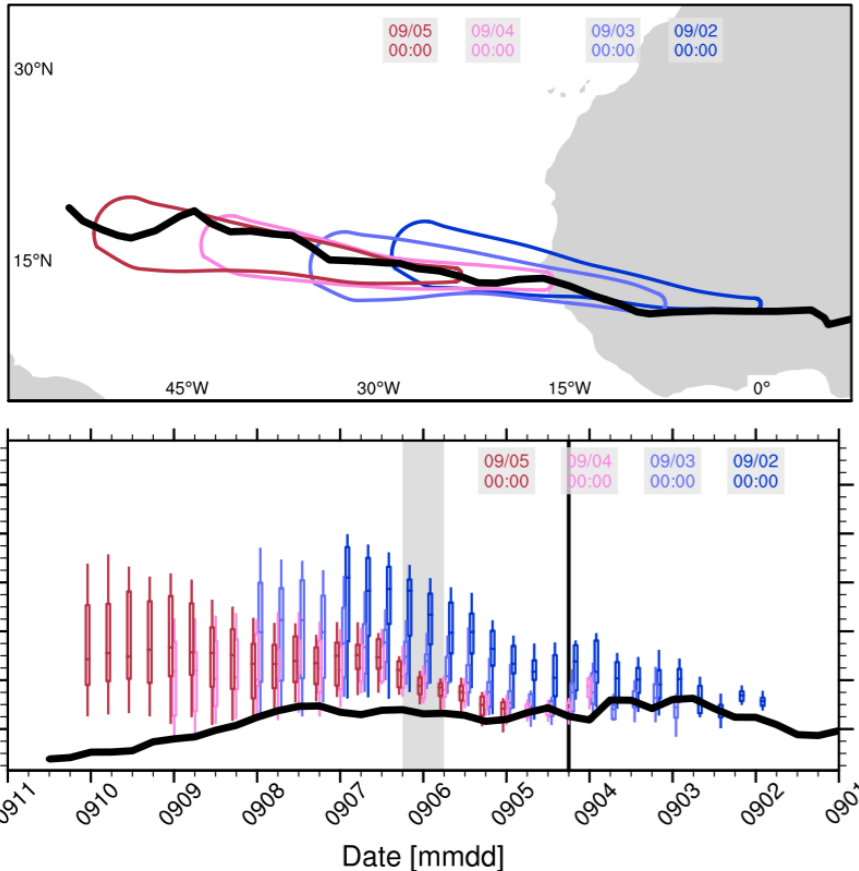
Tropical Cyclogenesis in East Atlantic

- Favorable mid-level AEW-troughs are often “open” at low-levels – due to low-level westerly flow (and a NE-relative shift of low-level vortex over the ocean).
- Non-developing favorable troughs tend to be associated with dry low-level air NW of the trough which is ingested beneath the mid-level trough.
- Source regions for the low-level dry air include Midlatitudes, Sahara and Equatorial region. More work needed on how this impacts predictability.



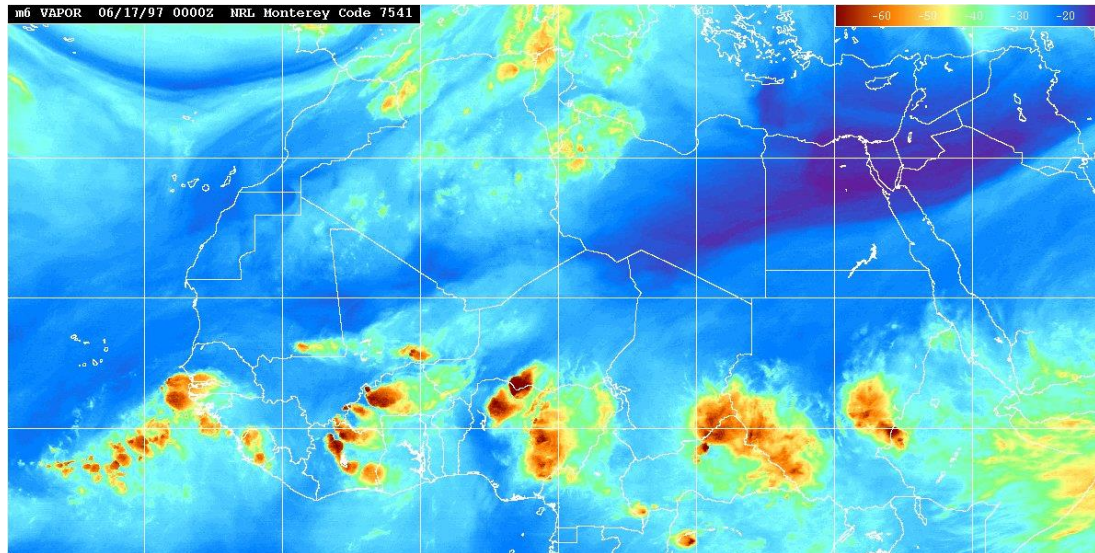
Predictability of the non-developing AL90 Case

Ensemble operation GEFS forecasts during coastal transition of AL90.



The genesis bias seen in the forecasts appears to be associated with a bias in convection close to the West African coast – that acts to strengthen and align the circulation centers, as well as moisten them. ***This impacts each forecast within the first 24 hours***. The environmental dry air becomes irrelevant in this case (c.f. Dunkerton et al, 2009).

THANK YOU!

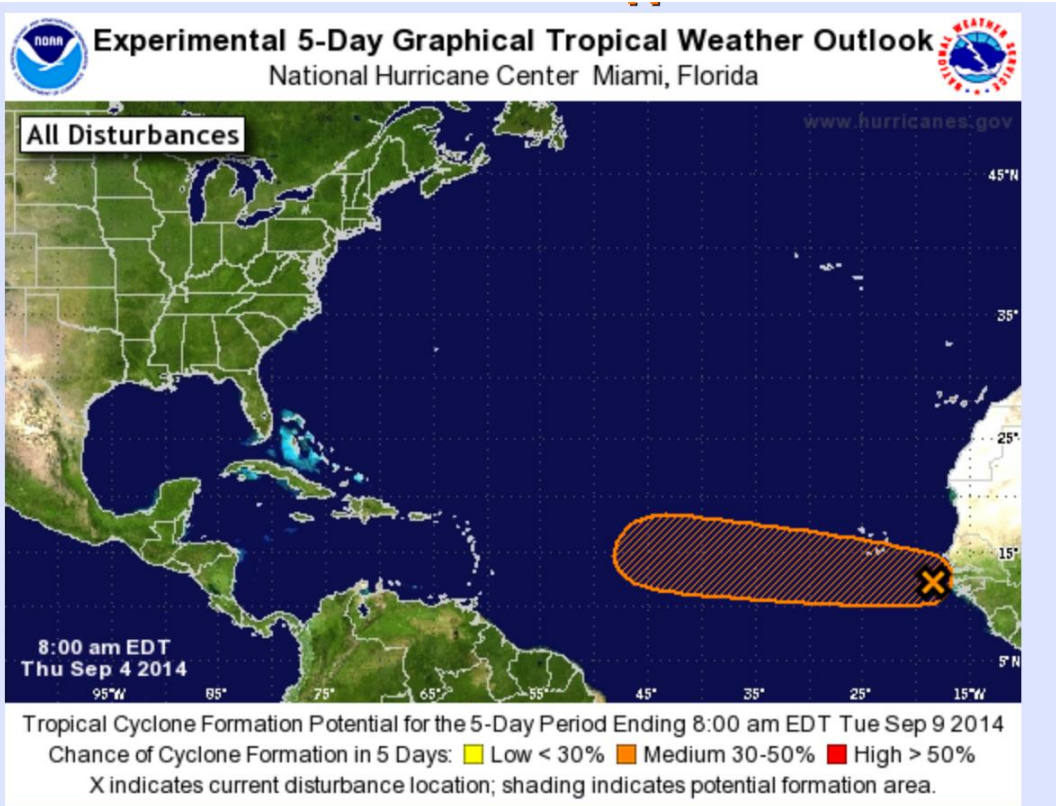


AL90: A moderate chance of development!

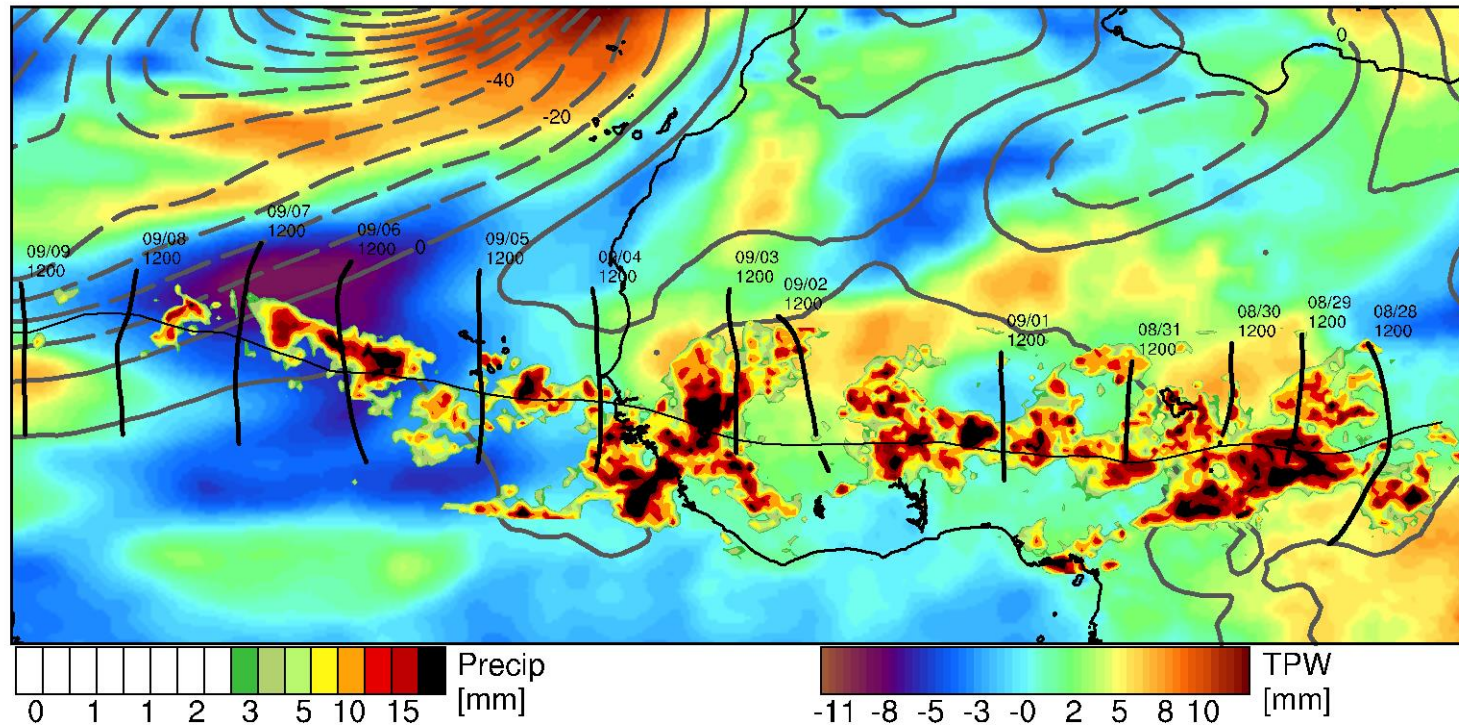
As of 8.00am EDT Thu Sep 4th 2014

A tropical wave accompanied by a broad low pressure system, is located a few hundred miles east-south-east of the Cape Verde Islands. Environmental conditions are expected to be conducive for some development of this disturbance through early next week while it moves westwards at about 15mph.

- Formation chance through 48 hours: low 10%
- Formation chance through 72 hours: medium 40%



Observations

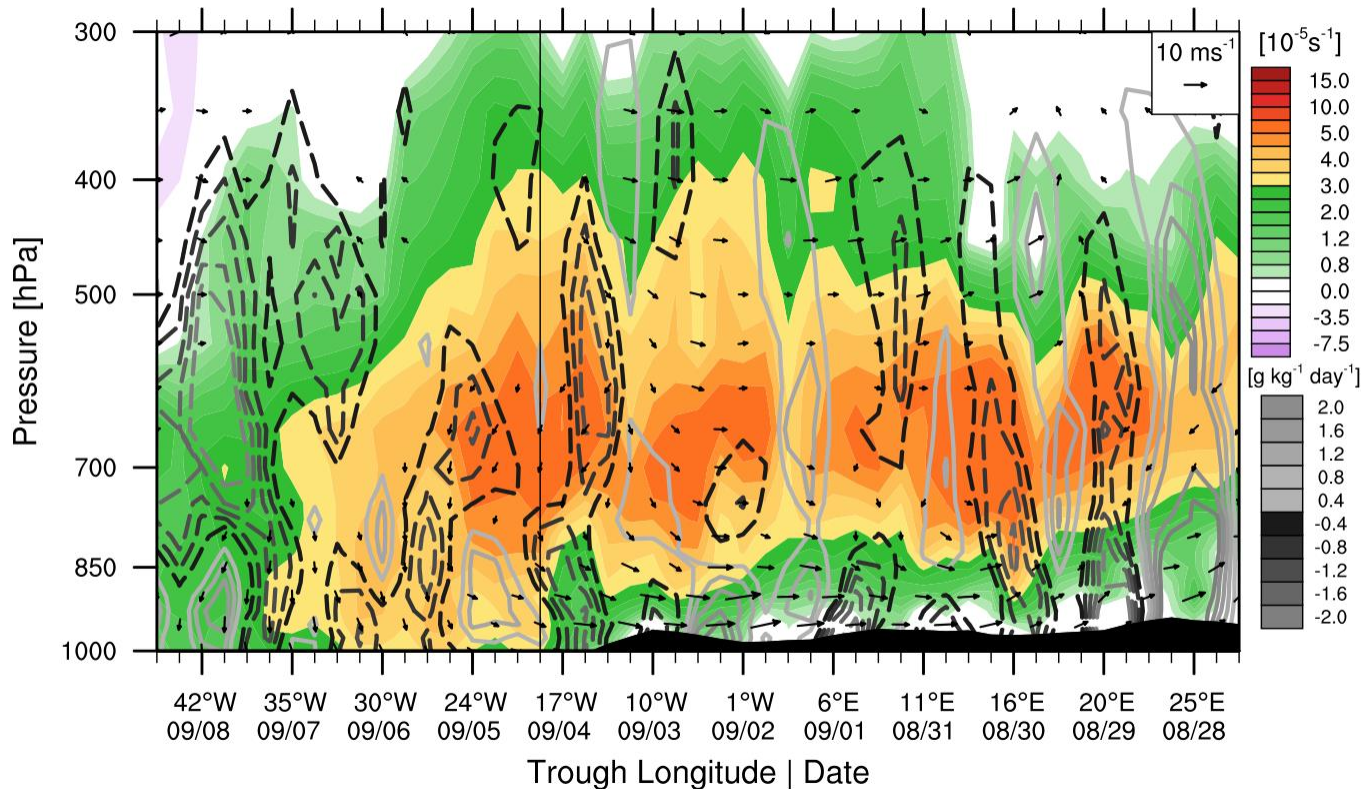


African Easterly Wave trough left the coast around 9/4/2014 when it was convectively active.

NHC posted a 40% probability of development within next 5 days.

Area of convection reduced as the trough reached a drier environment over the ocean.

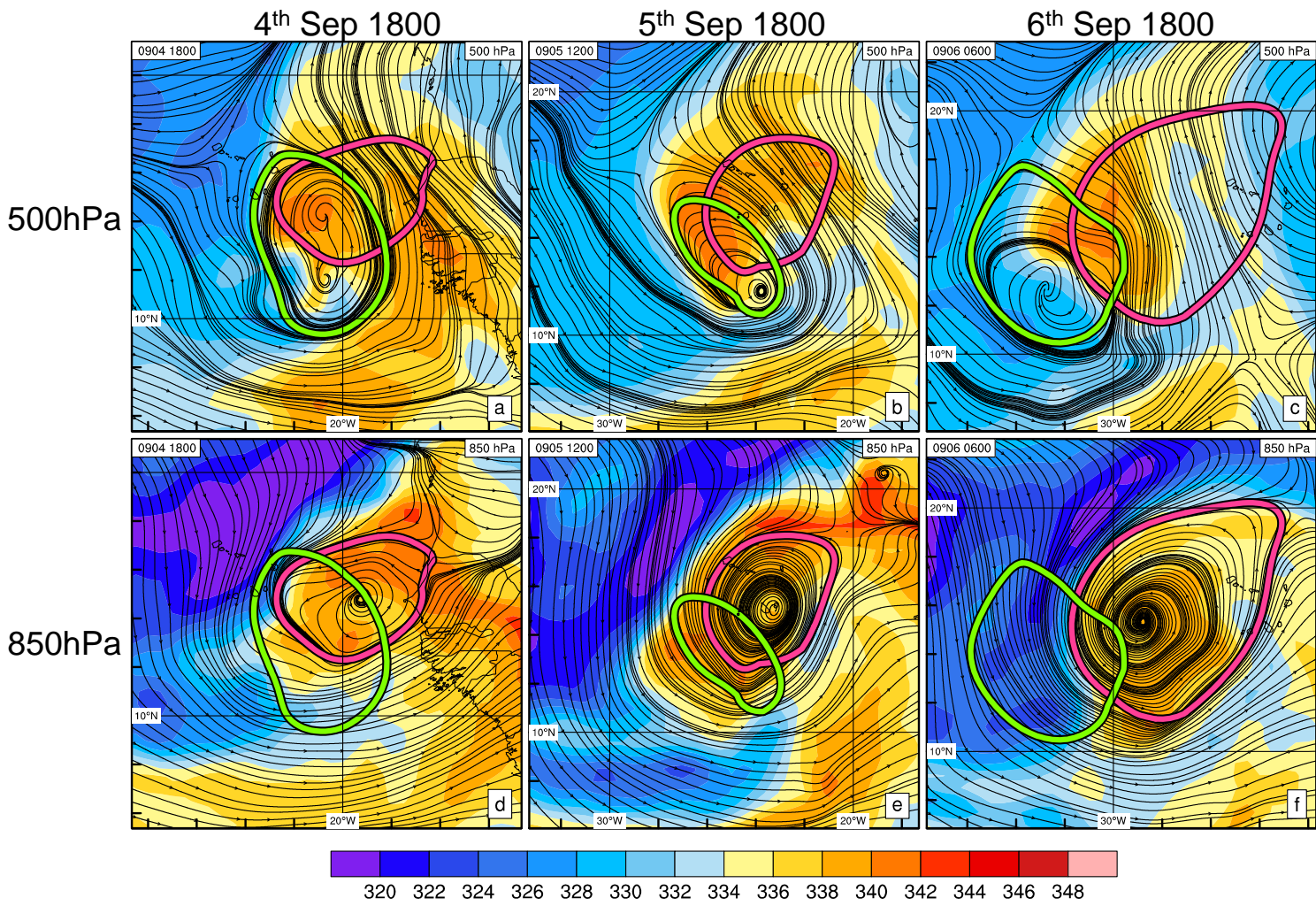
No significant development occurred.



Although there is an attempt to develop a low level circulation, the trough weakens after leaving the coast.

Trough dries after leaving the coast, although there is initial moistening at low-levels.

Vertical profile evolution for 6 hourly variables averaged over 300 km around the trough center. Relative vorticity (background shading), the 6-hourly change in specific humidity (contours) and wave relative zonal and meridional wind (vectors)



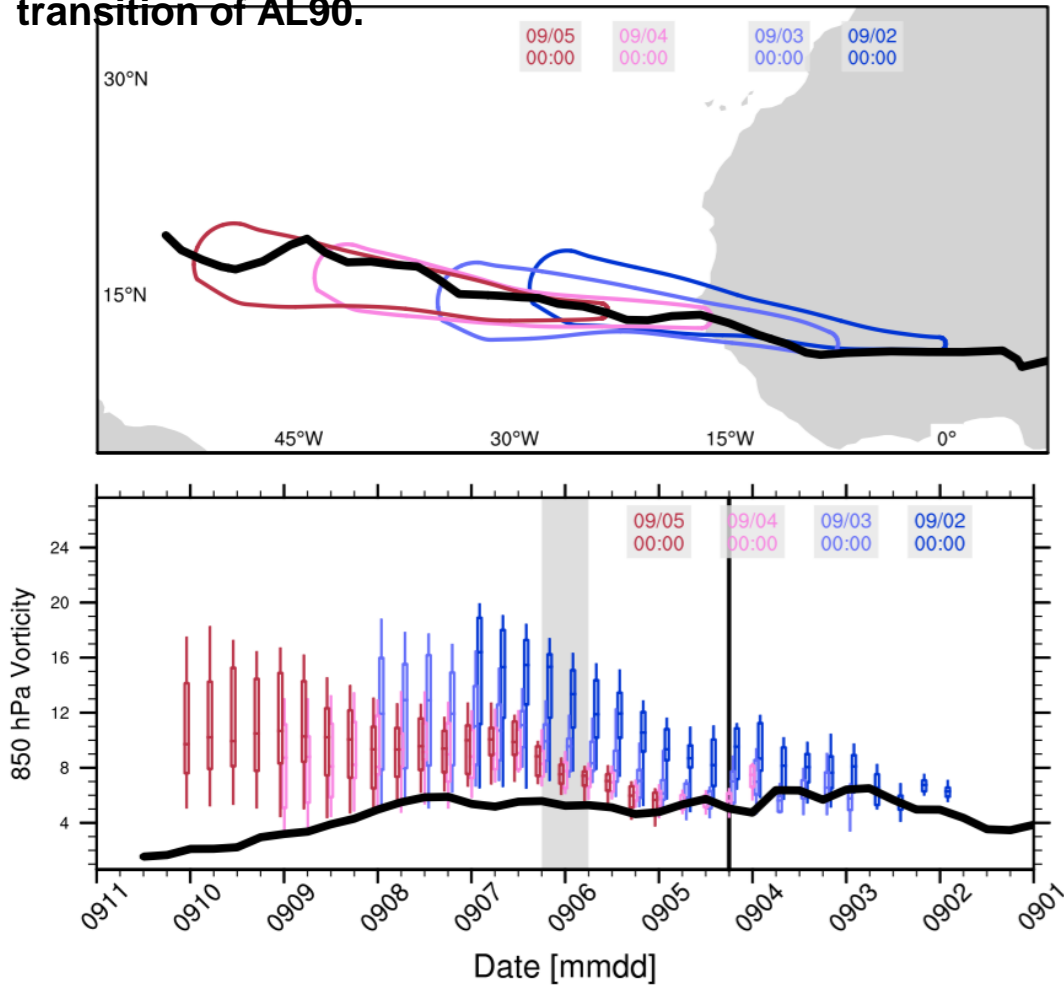
NOTES:

- Pouches tilt with time
- PPN always present within 850hPa pouch
- But limited to Western side
- Dry advection east of this enhanced due 500hPa being displaced to west
- 500hPa pouch VERY dry by the 6th
- Low-levels spins up but mid-levels do not.

500-850hPa relative streamlines with “pouches” (Dunkerton et al, 2009) and equivalent potential temperature and TRMM PPN

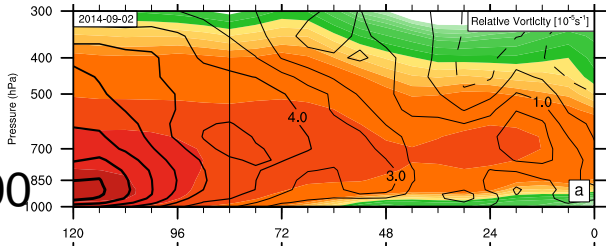
Predictability

Ensemble operation GEFS forecasts during coastal transition of AL90.

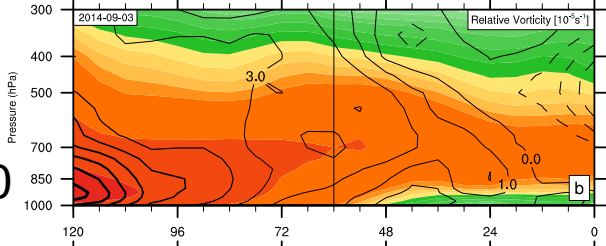


- Slight poleward bias in track overland
- Ensemble members generally over intensify for all lead times

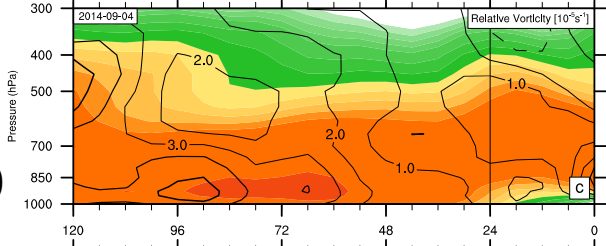
Forecast initialised on: 2nd Sep 0600



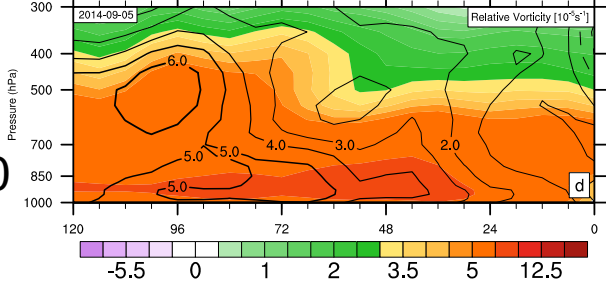
3rd Sep 0600



4th Sep 0600



5th Sep 0600



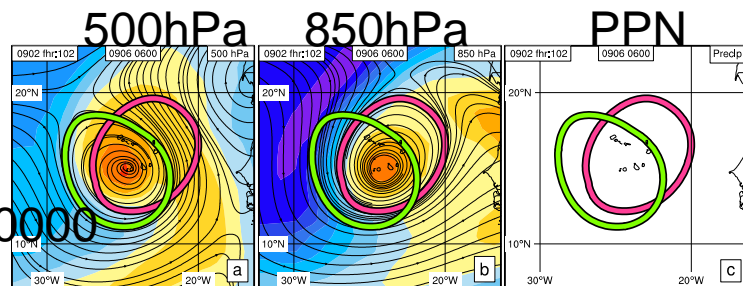
Forecast evolution of vertical profile in relative vorticity for ensemble mean (shading) and error(contoured)

Forecast hour increases from right to left

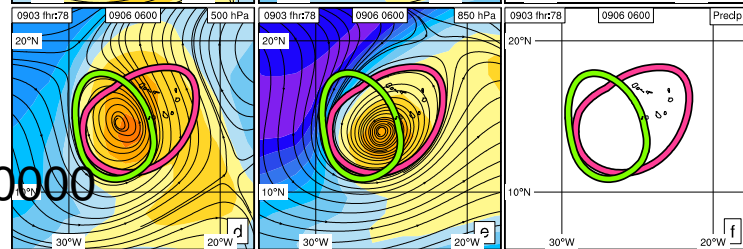
Vertical line is time of coastal transition.

All forecasts over-develop – especially the earlier ones.

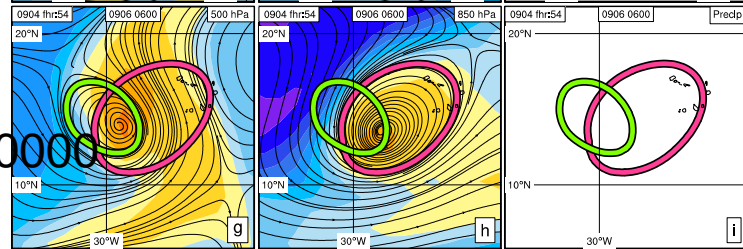
Forecast initialised on 2nd Sep 0000



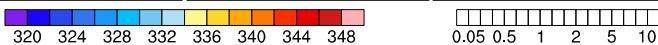
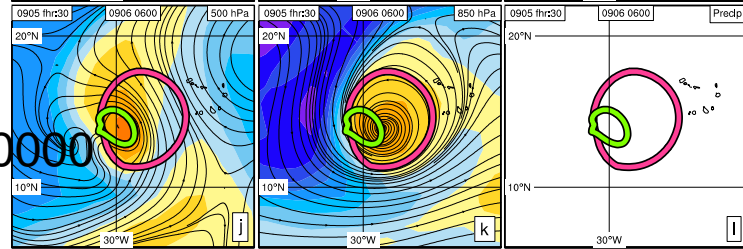
3rd Sep 0000



4th Sep 0000



5th Sep 0000

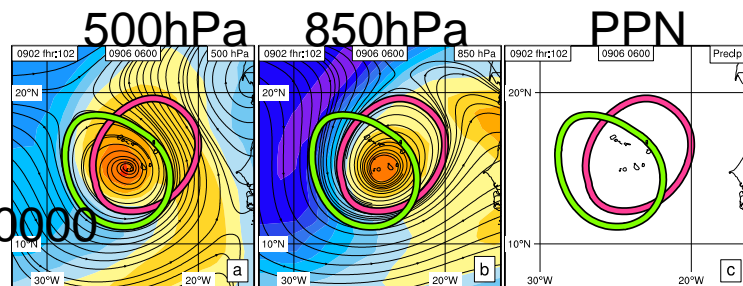


Ensemble mean forecast fields from 4 initialisation times all verifying for 6th Sep. Relative streamlines and equivalent potential temperature.

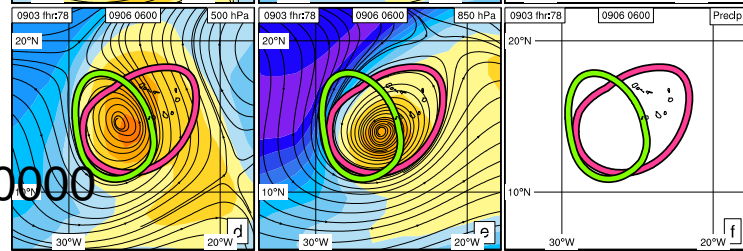
As lead time decreases forecasts behave more like observed evolution:

- Pouches become slightly more displaced from each other.
- More dry air is wrapped around the southern side of the trough.
- Areal extent of rainfall reduces (consistent with dry advection)

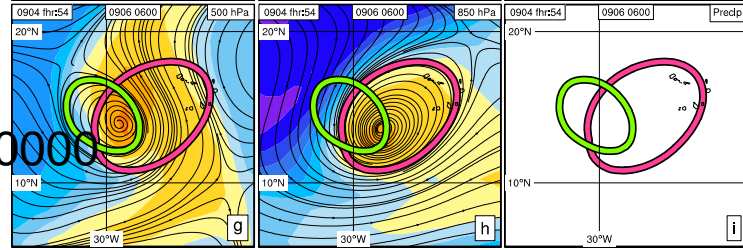
Forecast initialised on 2nd Sep 0000



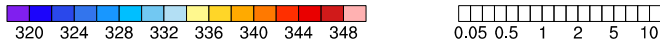
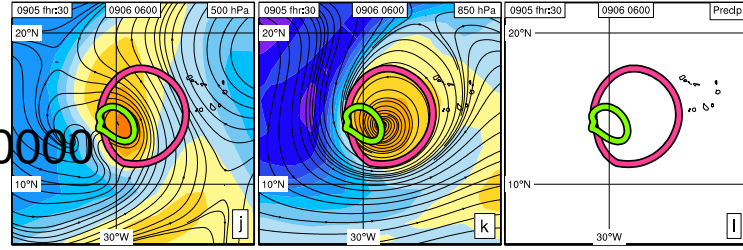
3rd Sep 0000



4th Sep 0000



5th Sep 0000



There are two competing processes:

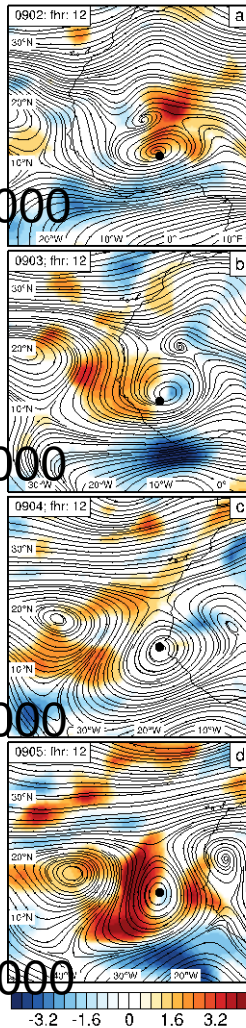
(i) Displacement of pouches leading to dry advection across each pouch – weakens convection and/or decreases its areal coverage

(ii) Intense convection in the AEW trough generates vorticity in the column (including 500hPa) that becomes resistant to the environmental shear.

It appears that a bias in the modeled rainfall favors (ii) in this case over (i) and results in over-prediction of genesis.

This bias sets in less than 24 hours into each forecast.

Forecast initialised on: 2nd Sep 0000



3rd Sep 0000

4th Sep 0000

5th Sep 0000

So what is the initial condition sensitivity to subsequent rainfall?

Over land its moist static energy north of the trough

Closer to the coastline it's the moist static energy to the north and west.

Conclusion: Errors in these regions can influence the outcome downstream

Trough-relative streamlines layer averaged between 900hPa and 700hPa. Shading shows sign and significance of 42 hour PPN sensitivity to layer average moist static energy.

Conclusions

- The lack of genesis in the East Atlantic associated with this event appears to be linked to dry advection at low and mid-levels, favored by misaligned circulation centers. The dry environment ahead of the AEW trough is important for the lack of genesis (c.f. Brammer and Thorncroft, 2015).
- The genesis bias seen in the forecasts appears to be associated with a bias in convection close to the West African coast – that acts to strengthen and align the circulation centers, as well as moisten them. ***This impacts each forecast within the first 24 hours (see next talk).*** The environmental dry air becomes irrelevant in this case (c.f. Dunkerton et al, 2009).
- Observations are suggestive of some dry (and dusty air) having entrained into the circulation center before the Global Hawk flight - ideally need more frequent flights earlier than this stage to see pathways for this apparent entrainment.
- Future work should consider a more in-depth Lagrangian analysis to assess the evolution of pouch properties (including OW).